



# UNIVERSITÀ DEGLI STUDI DI SALERNO

Dipartimento di Ingegneria Industriale

**POR Campania FSE 2014-2020 ASSE III – Ob. Sp. 14 Az. 10.5.2**  
**Avviso Pubblico “Dottorati di Ricerca con Caratterizzazione Industriale”**  
**D.D. n.155 del 17.05.2018 – CUP D44J18000310006**

Corso di Dottorato in  
“Ingegneria Industriale”  
(Ciclo XXXIV)

## **Advanced Driver Assistance Systems for Active Safety of Modern Tram**

Tutor: Prof. Vincenzo Galdi

Candidato:  
Dott. Catello Di Palma

Coordinatore: Prof. Francesco Donsì

Anno Accademico 2021-2022

Frontespizio inserito a fini di disseminazione

**Advanced Driver Assistance  
Systems for Active Safety of Modern  
Tram**

**Catello Di Palma**



# UNIVERSITY OF SALERNO



## ***DEPARTMENT OF INDUSTRIAL ENGINEERING***

*Ph.D. Course in Industrial Engineering  
Curriculum in Electronic Engineering – XXXIV Cycle*

## **Advanced Driver Assistance Systems for Active Safety of Modern Tram**

### **Supervisor**

*Prof. Vincenzo Galdi  
Dr. Luigi Fratelli*

### **Ph.D. student**

*Catello Di Palma*

### **Scientific Referees**

*Prof. Mario Pagano  
Dr. Giuseppe Graber*

### **Ph.D. Course Coordinator**

*Prof. Francesco Donsì*



*"To my children Vincenzo and Adriana"*



# Acknowledgement

The present work would not have been possible without the support of many who helped me in one way or another. I would first like to express my gratitude towards my supervisor Prof. Vincenzo Galdi, as you inspired me with vast knowledge, deep reasoning, critical thinking and the ability to address a wide range of subjects. This allowed me to explore topics unknown to me in a familiar and comfortable way. In addition, I thank Eng. Luigi Fratelli which allowed the thesis industrial application.

I am grateful to the PIS office of Hitachi Rail STS SpA that welcomed me during the experimental phase, Eng. Bruno Busco, Eng. Gennaro Maresca, Eng. Pietro Renzulli with whom I shared most of the working days.

I would like to thank Hitachi Rail STS SpA and ANM SpA for providing tram data.

My Ph.D. course coordinator Prof. Francesco Donsì, you are an exceptional teacher. You carefully guided me over the course of the Ph.D., with clarity and dedication. My sincere thanks go to the Department of Industrial Engineering (DIIn) of the University of Salerno and the Academic Board of the Ph.D. program in Industrial Engineering, for giving me the opportunity to conduct my research and providing me the resources to complete my Ph.D.

I am also grateful to my scientific referees, Prof. Mario Pagano and Eng. Giuseppe Graber, for investing their time into the examination of this thesis and its improvement with valuable suggestions.

Additional thanks go to Prof. Vito Calderaro for bringing serenity and harmony to the laboratory by ensuring that I always felt at ease.

To my many colleagues and friends at the S.I.S.T.E.M.I laboratory, especially Antonella R. Finamore, I learned a lot from you and enjoyed your company on the telephone or at lunch time, perhaps along with a coffee, and most of all our research activities.

Eng. Gregorio Barberio, with your '*vir buon*' you were my friendly mentor from the very beginning, when I asked your opinion on many transversal topics, and through every (moral, engineering, neonatal) dilemma.

Simona Parrella, Piera Stella, Giovanna Adinolfi, Felice De Luca, Andrea Fretta, I treasured your daily company where we shared thoughts and coffee, and the fact that I could always count on you.

I shall not forget about Annalisa Napoli, a hard-working “sentinel”, who shared with me countless “pressure tests”.

My dear friends to whom I owe my social life outside the Ph.D. (and therefore my sanity): Alessandro De Felice, Angelo Esposito, Giuseppe Di Ruocco.

Special thanks to my neighbours Maurizio and Giuseppina for our sunny coffee breaks on the terrace, where they lightened the days of hard lockdown at lunchtime.

I am thankful to my parents Vincenzo and Annunziata, along with my brother Michele, with their continuous and warm-hearted support to succeed in my academic achievements, which culminated in this thesis.

I am grateful to my dear grandmother Maria and a dear thought to grandfather Catello.

Final thanks to my wife Michela, for having endured the stress of these years. You gave me two fantastic children, playful and joyful, Vincenzo and Adriana, that refilled me with positivity every time I came back home.

# List of publications

- C. Di Palma, V. Galdi, V. Calderaro, “Driver Assistance System for Trams: Smart Tram in Smart Cities”, 2020 IEEE International Conference on Environment and Electrical Engineering and 2020 IEEE Industrial and Commercial Power Systems Europe, 10 June 2020, Madrid.
- C. Di Palma, V. Galdi, V. Calderaro, “Communication Infrastructure Requirements to include ADAS Technologies in New Generation Trams”, WCRR-22, Birmingham. (**UNDER REVIEW**)
- C. Di Palma, V. Galdi, V. Calderaro, “Integration of ADAS technologies in on-board communication systems for Smart Tram”, Melecon-2022, Palermo. (**UNDER REVIEW**)
- C. Di Palma, V. Galdi, V. Calderaro, P. De Fazio, L. Carrarini, G. Rizzano, “Weigh-In-Motion based on FBG sensors for Smart Road Applications”, Calgary2022, Birmingham. (**UNDER REVIEW**)



# Table of contents

Acknowledgement.....	7
Table of contents .....	I
List of figures .....	III
List of tables.....	V
Abstract .....	1
Introduction.....	5
Chapter I.....	7
Mobility in the cities: transport demand and safety hazard.....	7
I.1 Urban passenger transport demand.....	7
I.1.1 CO2 Emissions from mobility in the cities .....	10
I.1.2 Road traffic fatalities.....	12
I.2 Safety hazard in trams: context analysis .....	14
I.2.1 Common types of safety hazards .....	16
I.2.2 Risk assessment for active safety of tram .....	19
I.3 Objective of thesis .....	21
Chapter II .....	23
Advanced Driver Assistance Systems (ADASs).....	23
II.1 Overview of the state of the art in ADASs .....	23
II.1.1 Forward Collision Warning systems .....	24
II.1.2 Autonomous Emergency Braking systems .....	25
II.1.3 Adaptive cruise control systems .....	26
II.1.4 Traffic Sign Recognition systems.....	27
II.1.5 Lane Keeping Assistance System.....	29
II.1.6 Driver Status Monitoring systems .....	30
II.2 Environmental-Recognition Sensors for ADAS.....	31
II.2.1 RADAR Sensor .....	31
II.2.2 Camera Sensor .....	33
II.2.3 LiDAR Sensor .....	34

II.2.4 Ultrasonic Sensors .....	35
II.2.5 V2X Communication System .....	36
II.3 Levels of Driving Automation: a SAE standard.....	36
II.4 Sensor Fusion and Perception Technology.....	39
Chapter III .....	43
ADAS for trams: spread analysis and technological porting .....	43
III.1 Automatic Train Control Systems .....	45
III.1.1 Grades of Automation (GoA) .....	48
III.2 ADAS functionality for trams .....	49
III.3 Grades of Automation improved for trams using T-ADAS .....	54
III.3.1 Model's structure.....	54
III.4 ADAS sensors for the tram.....	56
III.4.1 The remote sensing requirements for the tram .....	57
III.5 T-ADAS: between future and revamping.....	61
Chapter IV .....	63
Distance to Collision Estimation (DCE) model for T-ADAS .....	63
IV.1 Forward vehicle collision warning systems .....	63
IV.2 Railway braking models.....	66
IV.2.1 Requirements for trams and light rail vehicles.....	72
IV.3 Proposed braking model.....	75
IV.3.1 Proposed methodology .....	76
IV.3.2 Model's structure.....	77
IV.3.3 DCE model formulation .....	78
IV.3.4 Theoretical performance of the model .....	86
IV.4 Case study .....	90
IV.4.1 Real acquisition of braking distance .....	93
IV.5 Analysis of braking distance results.....	95
IV.5.1 Driver reaction error definition .....	95
Chapter V .....	99
T-ADAS implementation: a holistic approach for a next generation Tram .	99
V.1 In-vehicle networking infrastructure .....	99
V.1.1 Network standard requirements.....	101
V.1.2 TCMS functional zone.....	102
V.2 Proposed implementation approach for ECN.....	103
V.3 Proposed implementation approach for MVB.....	106
Conclusions .....	109
References .....	111
List of Acronyms.....	119
List of Symbols .....	123

# List of figures

Figure I.1 <i>Urban transport demand by mode</i> .....	8
Figure I.2 <i>Transport land-use feedback cycle</i> .....	10
Figure I.3 <i>CO2 emissions in cities by mode of transport</i> .....	11
Figure I.4 <i>Road fatalities in the EU</i> .....	12
Figure I.5 <i>Road fatalities in Italy</i> .....	13
Figure I.6 <i>Tram accidents in Italy</i> .....	13
Figure I.7 <i>Global ADAS Market by geography</i> .....	14
Figure I.8 <i>The framework of assessment for tram active safety</i> .....	20
Figure I.9 <i>A forward collision case for tram</i> .....	20
Figure II.1 <i>ADAS roadmap for applications and technologies</i> .....	24
Figure II.2 <i>Schematic representation of an ACC system</i> .....	27
Figure II.3 <i>Block diagram of TSDR system</i> .....	28
Figure II.4 <i>LKA typical function</i> .....	29
Figure II.5 <i>Virtual lane recognition in LKA</i> .....	30
Figure II.6 <i>Head and eye direction monitoring</i> .....	31
Figure II.7 <i>Typical automotive millimetre-wave RADAR</i> .....	32
Figure II.8 <i>Basic waveform of FMCW radar</i> .....	32
Figure II.9 <i>Stereo camera</i> .....	34
Figure II.10 <i>Operating schemes: (a) Rotating 2D LiDAR, (b) rotating 3D LiDAR, (c) solid state 3D LiDAR</i> .....	35
Figure II.11 <i>SAE J3016 levels of driving automation</i> .....	37
Figure II.12 <i>Market penetration of ADAS vehicle</i> .....	39
Figure II.13 <i>Features comparison of the principal sensors</i> .....	41
Figure II.14 <i>Typical sensor fusion architecture</i> .....	41
Figure III.1 <i>LRT and tram system opening per half-decade, 1985-2019</i> .....	44
Figure III.2 <i>Automatic Train Control</i> .....	46
Figure III.3 <i>Structure of Automatic Train Control system</i> .....	47
Figure III.4 <i>Operation of the ATO system: (a) train speed control, (b) train stopping</i> .....	47
Figure III.5 <i>Grade of Automation (GoA) classification</i> .....	49
Figure III.6 <i>From assisted driving to autonomous driving: comparison between LoAs and GoAs</i> .....	51
Figure III.7 <i>Automatic emergency braking protocol for trams</i> .....	53
Figure III.8 <i>Longitudinal dynamic control for tram</i> .....	54

Figure III.9 ADAS spread to tram: T-ADAS.....	57
Figure III.10 Layout of camera-radar sensor pair .....	58
Figure III.11 Car–vehicle dangerous simulation scenario.....	59
Figure III.12 Tram–vehicle dangerous simulation scenario .....	60
Figure III.13 T-ADAS sensors performances .....	61
Figure IV.1 Schematic of the forward collision process .....	64
Figure IV.2 Stopping distance for Pedelucq formula.....	67
Figure IV.3 SCMT protection curve .....	68
Figure IV.4 Coefficient of adhesion as a function of speed.....	71
Figure IV.5 Stopping distance for Semi-empirical braking model for wet and dry rail.....	71
Figure IV.6 Braking process detail .....	75
Figure IV.7 Flowchart of the proposed model .....	78
Figure IV.8 Adhesion and friction coefficients.....	83
Figure IV.9 Braking distance in the proposed model.....	84
Figure IV.10 Safety band definition in driving task .....	85
Figure IV.11 Theoretical braking performance comparison on dry and wet tramways in the plains.....	88
Figure IV.12 Theoretical braking performance comparison on slope and dry tramways .....	89
Figure IV.13 Theoretical braking performance comparison on curve and dry tramways .....	90
Figure IV.14 Connection to the RS485 data line in the valance. ....	90
Figure IV.15 Monitoring of parameters in real time.....	91
Figure IV.16 Layout of Sirio tram Napoli .....	92
Figure IV.17 Real braking performance comparison on wet tramways .....	94
Figure IV.18 Real braking performance comparison on dry tramways.....	94
Figure IV.19 Misjudgement in real braking, comparison with DCE .....	96
Figure V.1 TCN architecture: Train Backbone and Consist Network .....	100
Figure V.2 Concept of functional zones .....	102
Figure V.3 Functional zone implementation example.....	103
Figure V.4 ECN architecture for T-ASAS concentrate integration .....	105
Figure V.5 ECN architecture for T-ASAS concentrate integration .....	106
Figure V.6 MVB architecture for T-ASAS concentrate integration .....	107

# List of tables

Table I.1 <i>Italian accident in 2018 involving tram</i> .....	15
Table I.2 <i>Annual statistics of emergency brake events at Luas, Dublin</i> .....	16
Table I.3 <i>Potential interaction points</i> .....	17
Table I.4 <i>Possible accidents for various situations</i> .....	18
Table II.1 <i>Comparison of the commonly employed sensors in self-driving cars</i> .....	40
Table III.1 <i>Automation comparison for automotive and railway</i> .....	50
Table III.2 <i>Spread analysis for ADAS functionalities on tram</i> .....	52
Table III.3 <i>GoAs improvement for trams</i> .....	55
Table III.4 <i>Porting of sensors on tram to achieve the GoA 2.3 level</i> .....	56
Table III.5 <i>Main revamping trams</i> .....	61
Table IV.1 <i>Coefficient <math>\phi(v_0)</math> as a function of speed for Pedelucq formula</i>	67
Table IV.2 <i>Types of emergency braking</i> .....	73
Table IV.3 <i>Theoretical operational performances</i> .....	74
Table IV.4 <i>Gauge values and radius of curvature</i> .....	80
Table IV.5 <i>Values of the coefficient <math>k</math> for surface vehicles</i> .....	81
Table IV.6 <i>Main features of Neaples tram network</i> .....	91
Table IV.7 <i>Technical information of SIRIO tram Napoli</i> .....	93
Table IV.8 <i>Evaluation metrics of the DCE and the EN 13452-1</i> .....	95
Table V.1 <i>Comparison for train bus technology</i> .....	101
Table V.2 <i>Sensor's characteristics of the T-ADAS system</i> .....	104



# Abstract

Mobility in smart cities is becoming smart as well, promoting on one hand transport modes based on zero-emission electrical technologies and, on the other, providing vehicles with technological solutions that support the drivers in driving operations. The two objectives that this strategy aims to achieve are both environmental sustainability and the reduction of deaths from road accidents. In 2019 only, road accidents in the European Union summed up to 22.660 fatalities and 120.000 people seriously injured. However, the trend of accidents is decreasing every year and looking to the past, the decrease coincides with the market penetration of Advanced Driver Assistance Systems (ADASs).

Nowadays, almost all manufacturers offer cars with level 3 of driving automation (SAE 3 levels) and many prototypes of self-driving vehicles are developing and circulating on our roads. From a medium-term perspective, all vehicles running in the smart city will be equipped with autonomous driving technology or advanced driving aids, including public transport vehicles, such as buses.

Therefore, the winning keys for mobility in the cities of the near future are electrified transport solutions with assisted driving and the tram is the ideal candidate for this revolution of green and safe mobility.

Trams are the combination of two worlds: railways and the road environment. In fact, unlike the other rail transport systems, use the same road infrastructure as cars, motorbikes, bikes but also pedestrians and will soon find themselves interacting with vehicles with increasingly higher autonomous driving levels. It is clear, therefore, that even for trams, the time is ripe to accommodate driving support systems. Indeed, the tram is experiencing a new spring today, due to its green nature that makes it a candidate for sustainable city mobility, and it will be the next candidate to host ADAS technologies. In this compound, tram manufacturers are moving towards the use and integration of automotive technologies and solutions, already available with a high level of maturity and reliability, based on Sensor Fusion and Perception Platforms. In fact, those technologies are today widespread in the automotive: in fact, vehicle collision warning systems have been studied by many researchers, and many approaches related to technologies and problem formulation have been developed and a lot of commercial solutions

today are available. Among the ADAS, FCW-AEB (Forward Collision Warning - Autonomous Emergency Braking) systems represents the one with the highest percentage of crash avoidance effectiveness: FCW alone, low-speed AEB, and FCW with AEB reduced rear-end striking crash involvement rates by 27%, 43%, and 50%, respectively.

However, due to the very different braking distances, a careful analysis of the tram braking dynamics to identify the most suitable technological solution is necessary.

The purpose of this thesis is to provide a contribution to the implementation of a driving assistance system designed for the tram, here called T-ADAS (Tram Advanced Driver Assistance System), both by analysing the technological aspects, and by developing a model for Estimation of the Distance to Collision (DCE – Distance to Collision Estimation) fitted for the tram.

In the thesis, the key elements of technological porting and the choice of functionalities for a T-ADAS system according to the Degrees of Automation indicated with GoAs (Grades of Automation) are initially investigated and defined. The degrees/levels of automation in automotive and railway systems are presented and compared to each other. Then, according to the implication level of a remote sensing system in each tram driving task, new GoAs for tram are proposed. These systems are designed to help the tram driver cope with potential hazards by having defensive driving. Therefore, the proposed GoAs correlated to ADAS will be useful to understand how this automation acts the action of the tram driver, and the safety of the entire transport system.

The problem of braking for the tram is then analysed to define quantitative requirements for the design and validation of the Forward Collision Warning and Autonomous Emergency Braking systems that will have to guarantee compatible responses with the dynamics of trams, which are very different from that of a car.

For this purpose, the proposed DCE model, which uses tram and tramway data (mass, power, grip, slope, radius of curvature) and real-time data (speed, weather conditions, and GPS) will allow the calculation of the safety braking distance.

The main difference between the model proposed and those of the literature and/or of the commercial ones, is mainly related to the vehicle dynamic. Therefore, in the proposed approach, instead of considering only the deceleration and speed data to calculate the stopping distance, we consider many other important factors that tune this calculation to the real one.

The robustness of the model was verified by comparing the values obtained with the theoretical and real values recorded on the tram, the latter obtained from a test campaign carried out on vehicles manufactured by Hitachi Rail STS SpA in collaboration with an Italian transportation company (ANM – Azienda Napoletana Mobilità SpA) that operates trams and public transportation in the city of Naples.

The T-ADAS system is integrated into the vehicle logic by considering the driver's actions through the manipulator. When the designated braking action is not performed correctly, the system will adapt the braking curve to model one.

In the final part, the implementation of the T-ADAS in the on-board network of the tram will be provided and the evaluation of the data traffic is performed. In fact, the newest railway network infrastructures based on Ethernet bus technologies can facilitate the integration of the T-ADAS systems with the Train Control Management System (TCMS), providing larger bandwidth and more flexible networks making this technology immediately transferable to railway systems such as the tram.

Throughout the entire work of the thesis, the acquisition of the real braking data of the case study and the implementation approach was carried out with ANM and Hitachi Rail STS SpA respectively, to which the author is grateful for the support and contribution offered.



# Introduction

Road accidents causes can mostly be connected to driver distraction or misjudgement of potential danger (Cioran, 2015). For this reason, the development and implementation of vehicle safety systems have grown, especially in the last decades. The first active safety systems, known as Driver Assistance Systems (DAS), were introduced with the Anti-lock Braking System (ABS) and the Electronic Stability Control (ESC) in the 1970s, and have contributed to reduce the number of road fatalities (Gietelink, 2007). Thanks to the technologies advances, the automotive industry increases to adopt sensors and microcontroller in order to perceive environment inputs and to autonomous intervenes on the driving activity. Advanced Driver Assistance Systems (ADAS) are the evolution of the DAS and nowadays are emerging as fundamental to improve road safety.

ADAS are a first step towards Autonomous Vehicles (AV) and as these systems are becoming more complex and safety critical, it is important to analyze the test methods used to validate them.

If so much has been done for the automotive sector Autonomous driving, in the rail industry is in its infancy.

The research activity on autonomous driving systems for trams, derived from the “Research to INspire the Future - REINForce” project in collaboration with the Engineering Department of the University of Salerno and Hitachi Rail STS S.p.A., was an opportunity to investigate the applicability of autonomous driving technologies developed by the automotive industry to the rail domain, and demonstrate what capabilities a future autonomous tram may offer. In many respects, autonomous driving for trams is very similar to autonomous driving for cars, they operate in similar environments where they interact with other road users such as cars, pedestrians, and cyclists, and they must obey similar traffic rules and signals.

Some aspects of the problem are simplified by the rail-bound nature of the vehicles, there are limited areas that need to be mapped, path planning is not required, and the possible locations of the vehicle are heavily restricted. However, the rail-bound nature also makes the problem of avoiding obstacles considerably more challenging. Not only are trams unable to steer in order to avoid potential collisions, they also cannot decelerate as fast as cars, both due to physical limitations and the risk of injuring unsecured passengers.

---

More specifically, the thesis is arranged in:

- Chapter I focuses on the two key aspects that motivated the research: the growing demand for mobility and road safety. An overview is provided on the demand for public transport on a global level first and, in particular, on Europe then, which appears to be the largest investor in ADAS technologies. The specific types of road accidents involving the tram are also explained.
- Chapter II refers to the state of the art on ADAS. Starts with an overview of the ADAS functionalities, classification, and current legislation. The characteristics of the sensors and the importance of sensors fusion are highlighted.
- Chapter III reports the degrees of automation in the railway sector. They are compared with the SAE definitions that are used by the automotive sector for the automation of cars. The analysis of the comparison led us to propose a potential increase in the Grades of Automation (GoAs) starting from the analysis of the technological and functional porting of the ADAS to the tram.
- Chapter IV show a novel model to calculate safety distance for collision avoidance for tram, based on laws of motion, which takes into account the specific parameters of the tram and tramway.
- Chapter V describes the implementation of the T-ADAS systems in the on-board Passenger Information Systems (PIS) and diagnostic tram network in a logic both for modern and revamped trams.

The Ph.D. dissertation closes with conclusions that outline the contribution of the work described, resuming the main achievements of the study and proposing a direction for future research that might address yet unresolved issues.

# Chapter I

## Mobility in the cities: transport demand and safety hazard

Economic and social transformations have rapidly increased mobility demand leading to a growth in car use, which has been aggravated by urban sprawl and new commuting needs: by 2030, most of the world's population will be concentrated in cities and this trend is destined to consolidate in the future. City planners are increasingly aware of the need to maintain a balance between facilitating mobility, essential for cities' economic and social vitality, and managing or mitigating its negative effects. Therefore, in urban areas, addressing the negative externalities of transport, including congestion, road accidents and pollution, is considered an essential challenge of modern times. Among these externalities, the European Union considers that congestion needs urgent attention, given the expected growth in transport demand and the associated economic cost, which amounts roughly 1% of annual European Gross Domestic Product (GDP) (EU Commission, 2018). The future will bring a transportation landscape in which cars, buses, pedestrians, bicycles, freight, and rail will be woven into a connected network to save time and resources, producing lower emissions and congestion, and promoting efficient land use and improved safety.

This chapter presents a brief overview of the current mobility demand and future forecasts, with an analysis on the safety and pollution contexts highlighting the importance of an ecological vehicle such as the tram.

### **I.1 Urban passenger transport demand**

One of the most certain global evolutions of the coming decades will be the process of urbanization, especially in developing countries. It will change all aspects of urban life and make the organization of efficient transport in cities a challenge. In 2050, 66% of the population will live in urban areas, up from 54% in 2014, and the cities will continue to concentrate more and more the wealth: while today cities above 300.000 inhabitants represent 31% of the world population and 50% of the world GDP, in the 2050 they will grow to 37% and 56% respectively.

All this obviously determines an expected grow of the mobility demand: in the baseline scenario, it is 95% higher in 2050 than in 2015, reaching more than 50.000 billion passenger-kilometres in that year, Figure I.1

The increase in urban mobility will take place overwhelmingly in developing countries, where the process of urbanization is strongest. While the population of cities in OECD countries only marginally increases, Asian cities, for instance, double in size will represent 20% of the world population in 2050. Compared with 2015, the mobility by car will only grow 32% by 2050 in OECD countries, against +185% in non-OECD countries, going to congest infrastructures that are already congested today.

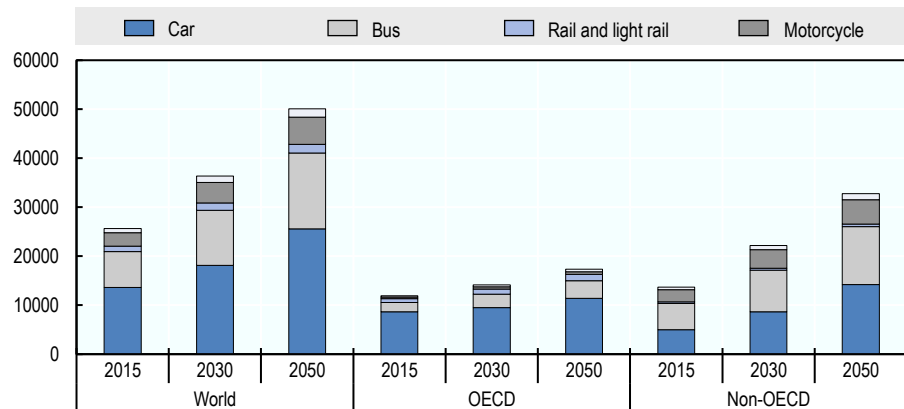


**Figure I.1** *Urban transport demand by mode*

To tackle this, many policy instruments target the negative effects of car use in urban areas, highlighting the advantages of electrified public mobility such as the tram (Ajanovic, 2021). This means that the baseline scenario, which mimics the current evolution of transport policies, is already quite restrictive for urban transport in some areas. Indeed, the growth rate of urban mobility by public transport in this scenario is 105%, slightly higher than the urban mobility by private modes (90%).

If public policies can influence demand and induce some behavioural changes, the effects of such changes are likely to remain small. Any effort to provoke a modal shift will struggle to make a real impact because the growth in demand for private cars is stronger. With 30 million additional cars arriving on the roads each year, changing modal shift by 1% remains a significant challenge. The intensity of economic growth in developing regions, and of the increase in transport demand that comes with it, constitutes a groundswell against which current policies can appear derisory, especially when the effects are measured on a global scale.

However, as highlighted in (Moghaddam, 2017) and (Litman, 2021), the scenario analysis of passenger transport in cities shows that strict policies targeting Land Use (LU) planning, development of public transport and economic instruments have the capacity to directly influence demand and behaviour.

On top of being an additional source of CO<sub>2</sub> mitigation, these measures help reduce congestion and can improve air quality. As well explained in (Chen, 2017), three fundamental scenarios are to be considered for the estimates both on the mobility demand and on the CO<sub>2</sub> emissions:

- **Baseline**, in the baseline scenario, no additional measure aiming at influencing travel demand and reducing CO<sub>2</sub> emissions is implemented during the 2015-50 period. This scenario constitutes a business-as-usual reference for travel demand and CO<sub>2</sub> emissions in the urban transport sector against which to measure the efficiency of additional policies and compare alternative scenarios. It assumes that the future trends of car ownership, road supply, public transport supply, pricing structure and urban area growth will follow the trajectories of the past.
- **Robust Governance (ROG)**, this scenario assumes that local governments play an active role and adopt pricing and regulatory policies to slow down the ownership and use of personal vehicles from 2020 onwards. Existing literature has proved the effectiveness of rigorous pricing strategies.
- **Integrated Land Use and Transport Planning (LUT)**, this scenario in addition to the policies introduced in the ROG, assumes stronger prioritisation for sustainable urban transport development and a joint land-use policy. As land use and transport planning decisions interact, it is widely acknowledged that better coordination and integration are a prerequisite for sustainable development (OECD, 2017). In contrast to the ROG scenario, the LUT scenario anticipates higher supply of public transport, extensive deployment of mass transit and restrictions on urban sprawl in cities.

The impact of public transport on Land-Use (and in general their interaction as the Transport Infrastructure Networks -TINs) depends on a considerable extent on exogenous factors which can influence their supply, as shown in Figure I.2. Major advances in TIN technology, such as the emergence of light rail or the tramways, have been declared as a major driving force of LU change (Xie, 2011). Infrastructure investments and transport policies influence the supply, but also the usage of TINs. Transport policies result directly in the investment in and the improvement of major TINs.

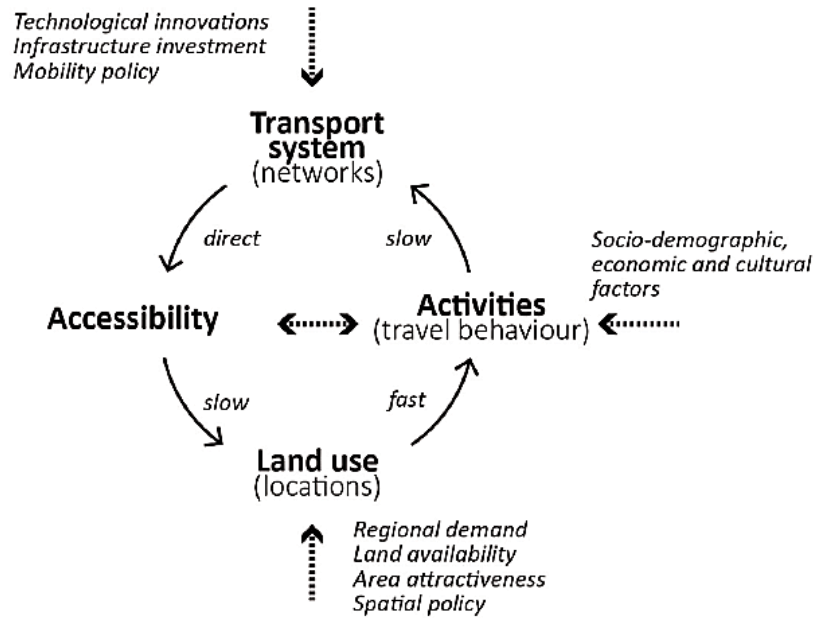
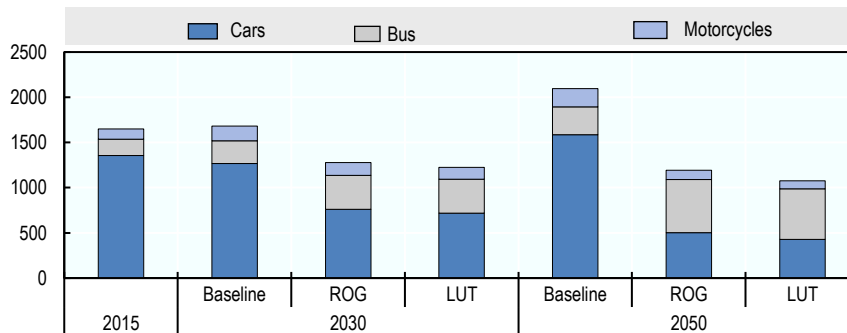


Figure I.2 Transport land-use feedback cycle

### 1.1.1 CO<sub>2</sub> Emissions from mobility in the cities

Emissions from transport in the cities have received a lot of attention because of the large impact that local pollutants can have on health. The quality of the outdoor air is a more immediate concern to the inhabitants of cities than CO<sub>2</sub> emissions and has become the subject of much debate and policies. The policies range from direct and indirect restrictions in car usage to efficiency standards for new cars. However, the climate change impact of urban transport cannot be neglected.

As Figure I.3 shows, in the baseline scenario, the level of total CO<sub>2</sub> emissions in large cities in 2050 is 26% (419 Mt) higher than in 2015. Global emissions do not change between 2015 and 2030, due to the large fuel efficiency gains expected during the decade to come, and the low economic growth for the years up to 2020. However, emissions grow again from 2030 onwards based on the assumptions related to vehicle technology and fuel efficiency as described in the IEA's Mobility Model (Gorner, 2018). The world average fuel efficiency for on-road passenger light duty vehicles improves by 29% from 2015 to 2030 but only 14% from 2030 to 2050. This pace of technology improvement is not enough to offset the growing mobility demand between 2030 and 2050.



**Figure I.3** *CO<sub>2</sub> emissions in cities by mode of transport*

Policy interventions, especially rigorous car pricing policies, lower transit fares and higher vehicle technology improvements introduced in the ROG scenario could intensely mitigate CO<sub>2</sub> emissions from the urban passenger transportation sector. With solely the policy measures from ROG, the avoided CO<sub>2</sub> emission could reach 397 Mt in 2030 and 886 Mt in 2050 compared with the baseline. The additional policies introduced in LUT scenario would further reduce the CO<sub>2</sub> emissions by 48 Mt in 2030 and 104 Mt in 2050. Under the most effective policy scenario LUT, the global CO<sub>2</sub> emissions level from the urban transport sector would be 26% lower in 2030 and 35% lower in 2050 compared with 2015 levels.

Private cars are the main contributor of CO<sub>2</sub> emissions in cities, representing around 82% of all emissions in 2015 and around 75% in 2030 and 2050. With the implementation of the policy measures of the ROG and LUT scenario, the contribution of cars decreases to 40% in 2050.

Bus and motorcycle emissions represent 11% and 7% respectively of all emissions in cities in the base year, going up to 15% and 10% in 2030 and remaining stable until 2050, in the baseline scenario. In the ROG and LUT scenarios, the contribution of buses in total emissions increase both because of the additional public transport supply in these scenarios and because of the lower level of emissions from cars. Buses emit as much as cars in the ROG scenario in 2050; in the LUT scenario, buses even become the main contributor of CO<sub>2</sub> emissions in 2050. CO<sub>2</sub> emissions from urban rail are null in this model, as only tank-to-wheel CO<sub>2</sub> emissions are considered and urban rail as a tram is assumed to be fully electric: tramway systems are considered green solutions to decrease Greenhouse Gas (GhG) emissions. According to the EU25 Electricity calculation model, the travel emission for a passenger car is 45 g CO<sub>2</sub>/km, 15 g CO<sub>2</sub>/km for a bus, and 5.45 g CO<sub>2</sub>/km for a tram (HengirmenTercan, 2021). Vice versa, a life-cycle analysis would increase the CO<sub>2</sub> emissions from urban rail, especially in India and Africa where the IEA projects that electricity production will remain carbon intensive through 2050.

### 1.1.2 Road traffic fatalities

The pandemic crisis due to COVID-19 has altered the trends and estimates of data regarding the global situation of accidents and road deaths. In this work we will consider as the latest reference data those relating to 2019. As clearly reported (ITF, 2019) the causes of death from road accidents in 2019 are ranked in tenth place globally with about 1.2 million victims. In accordance with the ROG and LUT policies described in the previous paragraph, which also contain safety aspects related to the management of the growing demand for mobility, these numbers are decreasing. By focusing on the European scenario, where these policies are most widely applied, there is a strongly decreasing trend in road fatalities.

In 2019, in fact, an estimated 22800 road traffic fatalities were recorded in the 27 EU Member States. This represents almost 7000 fewer fatalities compared with 2010, a decrease of 23%. Compared with 2018, the number fell by 2%. While the underlying trend remains downward, progress has slowed in most countries since 2013 and the EU target of halving the number of road deaths by 2020 (relative to the 2010 baseline) will not be met, as shown Figure I.4.

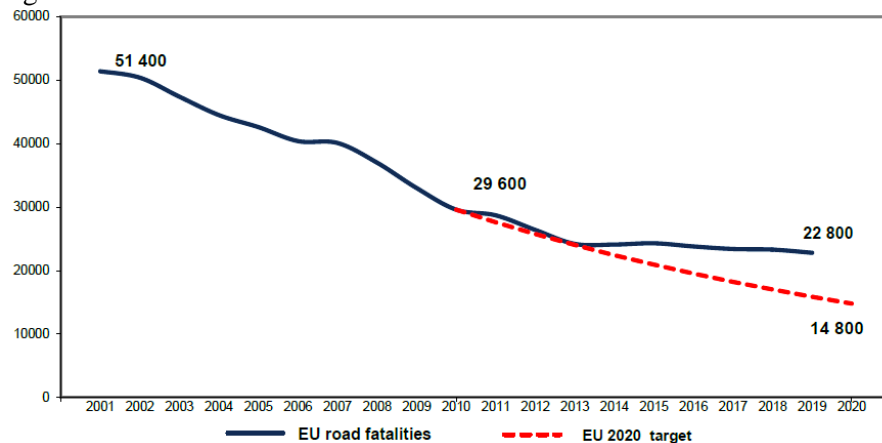


**Figure I.4** Road fatalities in the EU

The Italian situation follows the European trend. Here too the target set in 2020 was missed with a stabilization of the trend compared to the previous two years. As reported in (ACI - Istat, 2020), there are strong signs of an increase in soft mobility, with an increase in e-bike sales and the spread of other forms of micro-mobility that contribute to the number of accidents.

Chapter 1 – Mobility in the cities: transport demand and safety hazard

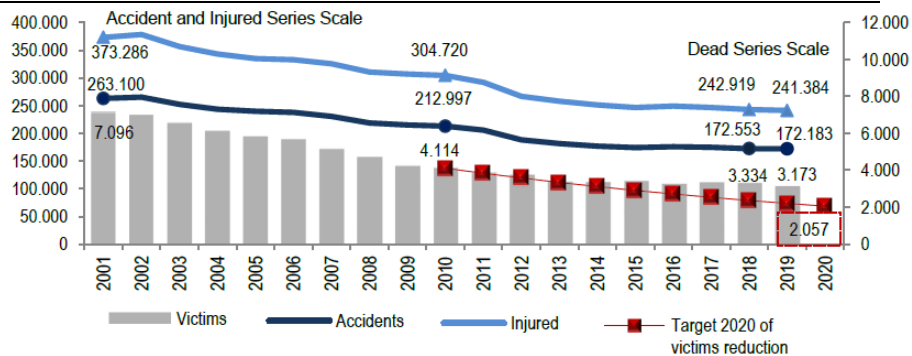


**Figure I.5** Road fatalities in Italy

With focus on the Italian scenario for the same period of observation, it is possible to note that the trend of accidents involving the tram has dropped by about 70%, as show Figure I.6. The contribution lies in the investments for the increase of reserved lanes and the replacement of the fleet with more modern means.

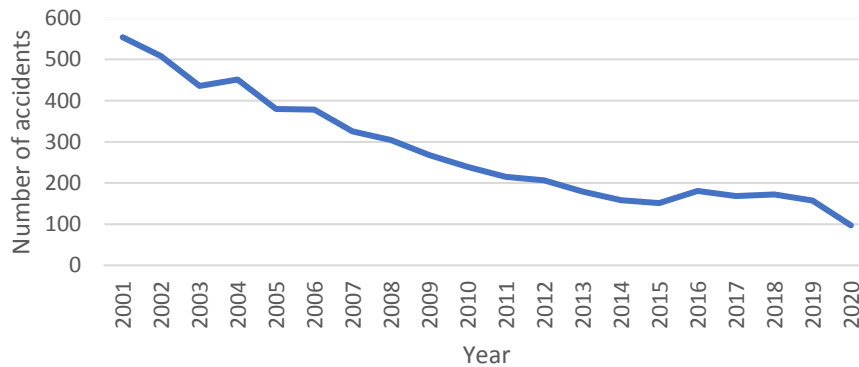


**Figure I.6** Tram accidents in Italy

European policies, more than in other parts of the world, have identified ADAS as the winning key for reducing road accidents. As shown in the Figure I.7, the penetration of ADAS in the market is destined to grow in the near future and Europe is its largest investor. Increased adoption of ADAS will drive the future growth of the automotive sector. The age of autonomous cars due to the recent advancements in technology and tech-savvy modern demands for drivers as well as passengers will be the main driving factor. Although Autonomous Driving applications are still in their early days, they eventually become the main feature of differentiating automotive brands (Choi, 2016). Also, they will become one of the most important revenue sources for major car manufacturers.

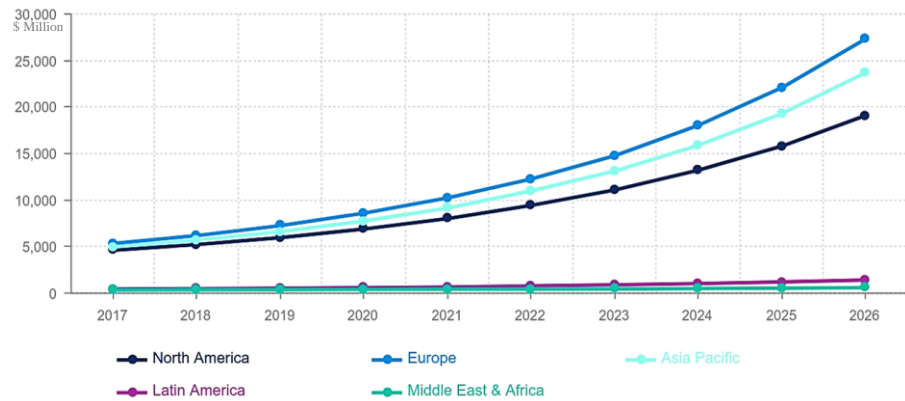


**Figure I.7** Global ADAS Market by geography

These same technologies enable the creation of fully AV, which have now also become a significant focus of research and development to high-tech players like Tesla, Microsoft, Apple, and Google. Many semiconductor companies, such as STMicroelectronics, are also participating in the automotive sector-now offering autonomous driving products or developing them.

With advancements in Artificial Intelligence (AI) of things, Internet of Things (IoT) and with ever-growing dependence, the demand for cars is no longer limited to electric vehicles. ADAS software will become the driving factor for the future of the automotive industry.

ADAS software will become the driving force for the future of the automotive industry and beyond. New scenarios are expected for the application of ADAS systems to public transport where there are already applications for assisted driving for buses (Ye, 2021). The evaluation of migrating these systems to a natural green vehicle such as the tram would make it possible to improve in terms of safety this vehicle which shares the same road infrastructure with other vehicles (cars, bicycles, motorcycles, etc.), thus attracting development policies more thrust as well as restoration of old vehicles and abandoned or disused sections.

As we will see later, in order to be able to better evaluate the portability of ADAS systems towards the tram sector, we will explain in the next paragraph which safety risks affect the tramway systems.

## I.2 Safety hazard in trams: context analysis

The use of tramways into an urban area so that they can operate safely and efficiently while interacting with other public space users is one the most important challenges to improve the development of this transport vehicle and to plan principles on urban rail infrastructure design.

For this purpose, it is extremely useful to know where the main accidents involving the tram take place. For example, ISTAT, the Italian National Institute of Statistics, in the 2018 annual report on Italian road accidents (Istat, 2019) highlights how most accidents involving trams occur at intersections and straights due to greater interaction of cars, motorcycles and pedestrians, with tramway. More recent data have no meaning due to the COVID.19 pandemic which has significantly reduced travel.

**Table I.1** *Italian accident in 2018 involving tram*

<b>Accident place</b>	<b>Percentage occurrence</b>
Crossroad	56%
Roundabout	3%
Level crossing	1%
Straight	37%
Curve	2%
Gallery	1%

To find the best adapted and safest system for optimising interactions between tramways and other users of urban space, is for public transport operators and authorities one of the means to improve the level of service, and thus help to grow the modal shift in favour of public transport (COST , 2015).

The methodological approach led to separate discussions in two parts: the first one dealing with data collection, processing and evaluation tools, and accident scenarios, whereas the second one is dedicated to the choice of sensor technology to be used to cover the scene under investigation in all possible conditions.

There are three different parts of the tramway system that influence safety: the vehicle, the infrastructure, and the operation management. The infrastructure is the basis of main issues, but is also the most expensive part of the system and it is very hard to change once the system has been built. On the other hand, the operation management can solve some problems generated by a poor infrastructure design, but this ability is limited and not every infrastructure problem can be solved in this way. In this thesis, we will understand safety as precautions to be taken to reduce the level of risk related to foreseeable accidents or injuries, such as the design and installation of an ADAS for trams (which will be called here T-ADAS).

Keep in mind that improving tramway safety will play a part in improving road safety in general and for vulnerable users in particular. Tram drivers are trained in defensive driving techniques and are constantly vigilant of pedestrians and cyclists, and brake to prevent a collision. Evidence suggests that these emergency brake applications are often made because of acts by third parties, e.g. the road vehicle driver, pedestrians and cyclists. A useful indicator of a precursor to an incident (near-miss) is the number of emergency brake applications tram drivers must make (COST , 2015). However,

communication with the driver is needed to avoid the possible negative implications of recording Emergency Brake (EB). For example, if the driver is concerned that a sanction might be imposed on him, the number of EB applications might decrease, compromising safety. The numbers of EB applications by Luas (Dublin) drivers is shown in Table I.2.

**Table I.2** *Annual statistics of emergency brake events at Luas, Dublin*

Emergency brake origin	2005	2006	2007	2008	2009	2010	2011	2012	2013
EB applications by driver	940	747	540	435	350	374	478	414	446

In 2013, road vehicles were the cause of 38%, pedestrians 27%, and cyclists 4% of all EB. The number of EB is an indication of dangerous situations that can often lead to accidents.

### ***1.2.1 Common types of safety hazards***

The ADAS system could mitigate the number of EB by providing driving support. Safety events, mainly accidents but also incidents relevant to safety, can be classified according to a variety of factors, such as location, modes involved or time of occurrence. In the Table I.4, the reader is invited to answer each of the above questions. Each column is independent so the table should not be read row by row. The red line is a possible reading example. The table is intended both for analysing specific safety events and for use during a broader analysis of a network. The classification does not include all internal accidents that can happen to trams because the focus is on interactions between trams and other street users.

Another classification can be made by the causes of accidents where a third party was responsible. Based on this approach, accidents can be divided into four main groups: including vehicles, cyclists, pedestrians, or trams. Different street users imply various hazards; therefore, in each of those groups different causes of road events can be considered. Causes of accidents, where a vehicle which could include a tram in some cases, is the responsible party: disrespect of traffic light, non-permitted turn (left or right), visibility problems, non-awareness of tram presence, traffic-light regulation problem.

Causes of accidents, where cyclists or pedestrians are the responsible party: disrespect of traffic light, crossing outside the pedestrian crossing, non-awareness of tram presence.

Once this distinction was made, we define potential interaction points, as well as the potential conflicting users for every one of them.

**Table I.3** *Potential interaction points*

Interaction point ID	selection		
	pedestrians	cars	cyclists
Road junctions (cars and cyclists) with tramway		<b>X</b>	<b>X</b>
Road junctions (cars and cyclists) with a left turn		<b>X</b>	<b>X</b>
Roundabouts		<b>X</b>	<b>X</b>
Tramway segregation along the street (lanes and sidewalks)	<b>X</b>	<b>X</b>	<b>X</b>
Tramway perception on mixed streets (cars and cyclists)		<b>X</b>	<b>X</b>
Tramway perception on pedestrian areas	<b>X</b>		
Pedestrians level crossings	<b>X</b>		<b>X</b>
Cyclists in segregated areas			<b>X</b>
Stops and its accesses	<b>X</b>	<b>X</b>	<b>X</b>
Interchange areas	<b>X</b>	<b>X</b>	<b>X</b>
Traffic (road & pedestrians) signals	<b>X</b>	<b>X</b>	<b>X</b>
Line signs and signals (for tram drivers)	<b>X</b>	<b>X</b>	<b>X</b>

**Table I.4** Possible accidents for various situations

WHAT?	WHERE?	WHEN?	WHO?	HOW?	WHY? (DIRECT CAUSE)	WHY? (ROOT CAUSE)
Near miss	Tram stop	Peak hour	Tram Vs. Bus	Parking manoeuvres	Infrastructure problem	Infrastructure design
Collision with other motor-vehicle	Running sections (excluding junctions)	Off-peak hour on weekday (daytime)	Tram Vs. Private car	Prohibited or unexpected movement	Disregard for traffic rules or unsafe driving	Human factor (pedestrian)
Collision with pedestrian	Roundabouts	Weekend or holiday (daytime)	Tram Vs. Heavy road vehicle	Vehicles travelling same direction, same lane	Weather conditions	Human factor (private vehicle driver)
Collision with bike user	Signal controlled junction	Night-time	Tram Vs. Bike	Vehicles travelling same direction, different lane	Vehicle problem	Bad maintenance (vehicle, infrastructure)
Collision with object (inc. parked car)	Uncontrolled junctions	During a special event	Tram Vs. Pedestrian	Vehicles travelling different direction (no left turn)	Drugs or alcohol	Inadequate training of tram driver
No collision but injuries	Pedestrian or cycle crossing	Other	Other	Road vehicle turning left	Security issues (deliberately caused)	Unclear or unsafe operational procedures
Other	Depot or other reserved area	-	-	One vehicle stopped or parked	No apparent cause or other	Other
-	-	-	-	People waiting, entering or exiting tram	-	-
-	-	-	-	People crossing the tram line or walking over the tram line	-	-
-	-	-	-	Other	-	-

In any case, the tramway should be clearly identified in the urban context so that all street users are aware of it. Therefore, a junction or roundabout that has a tramway traversing it should be readily recognised as such by other road users.

### ***1.2.2 Risk assessment for active safety of tram***

Generally, the safety technologies of tram systems can be categorized in passive safety and active safety. The passive safety mainly aimed on improving the quality of tram body, like enhancing the strength and refining the structure of the tram, etc. The active safety refers on active detection of surrounding environment, safety risk assessment in running, timely braking technologies etc. Obviously, passive safety protection methods can only reduce the damage after the accidents but cannot prevent the occurrence of accidents itself. Therefore, T-ADAS for active safety protection methods of tram becoming a crucial issue and acquire much more attention.

The safety assessment methods can be stochastic based algorithms and deterministic ones. The stochastic algorithms evaluate the risk by calculating the probability distribution of the collision between the running tram and the different targets (obstacles). This type of assessments can describe the interaction between multiple targets, thus can be applied in complex scenarios and different safety systems. However, the stochastic algorithms usually use Monte Carlo sampling methods, which cause a large amount of calculations. Moreover, it is a posteriori analysis. Thus, the stochastic based assessment method is still being studied yet and cannot provide a real-time control strategy for the active safety of tram. The deterministic algorithms usually consider several kinds of specific scenarios, which can assess the current risk degree by some parameters such as collision time, braking distance, etc.

The proposed assessment active safety framework in this paper based on the characteristics of the braking behaviour of the trams in the real world, as a real-time risk assessment method, can provide a basic function for the avoiding Forward Collision (FC) strategies in the modern or revamped tram.

As shown in Figure I.6, through analysing the status of movement objects in the surrounding environment and considering the dynamic characteristic of the tram, we can get the safety assessment model for the collision avoidance.

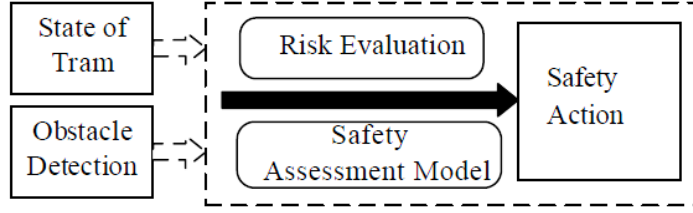


**Figure I.8** The framework of assessment for tram active safety

As seen on the potential risks in the driving environment of the tram we can summarize that they can occur while driving, the potential dangers of tram running possible have four cases, such as the forward collision, the rear-end collision, the lateral collision and overspeed. Thus, the quantification of the risk can be utilized by quantize these four types of dangers, by what we can get the model of safety assessment.

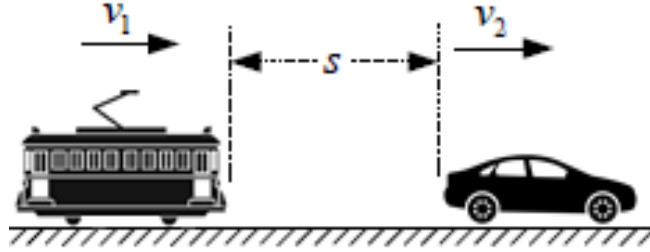


**Figure I.9** A forward collision case for tram

In this work we will focus on the parameters of a forward collision avoidance system, whose dynamics are shown in the Figure I.7: the unidirectional object (forward object) in front of the tram, with  $s$  is the current distance between the tram and the forward object,  $v_1$  and  $v_2$  represent the current speed of the tram and the forward object, respectively. When  $v_1 > v_2$ , collision may occur.

$$R_f = \begin{cases} (s, v_1, v_2, a_b, h_1, h_1), & \frac{v_x^2}{2a_{b1}} + \Delta < s \\ 0, & \frac{v_x^2}{2a_{b1}} + \Delta < s \end{cases} \quad (I.1)$$

$$v_x = \begin{cases} v_1, & v_2 \geq 0 \\ v_1 - v_2, & v_2 < 0 \end{cases} \quad (I.2)$$

$R_f$  is the risk estimation function for potential hazard can be interpreted as function of following parameters,  $a_b$  indicates the maximum deceleration with

the real-time state of the tram. The  $h_1$  and  $h_2$  are the hazard indexes of tram and forward object respectively, which represent the damage degrees of them when a forward collision occurs, and depends on unit mass, braking capacity, relative velocity, and acceleration, etc.  $\Delta$  is the extra margin of braking in safety.

### I.3 Objective of thesis

The aim of this work is to provide a methodological contribution to transfer of ADAS systems to public transport vehicles such as the tram, through a model-based calculation of the stopping distance that considers the key physical parameters of the tram and tramway, allowing ad hoc parameterization of the ADAS to make the FCW and AEB functions more reliable.

The proposed approach is composed of two phases: the first is the evaluation of which ADAS functionalities can be adapted to the tram vehicle; the second concerns the calculation of the stopping distance of the tram which defines the operability characteristics of the FCW-AEB system.

The thesis is organized as follows: after a brief review of the state of the art of the main ADAS functionalities, are described the automatisms concerning the unmanned and highly automatic driving system in high-speed railway and metro, based on the Automatic Train Protection (ATP) system to ensure the running safety.

After examining the technological porting of the automotive ADAS towards the tram and proposing an increase in the Automation Degrees (GoAs), the Distance to Collision Estimation (DCE) model was presented, which calculates the safety distance starting from the stopping distance increased by guard bands. In the final part we will see how the T-ADAS system can be integrated into the on-board network of the tram to exchange information on the TCMS and the PIS buses.

The basic idea developed in this thesis arises from the observation of the open and complex running environment of tram that is much like the cars. Recent years, driverless cars were rapidly developed and received much more attention. Though there are lots of studies in driverless cars, lots of them cannot be direct used in tram. Compared with cars, the tram body is much heavier and longer, the tram's running inertia is bigger, braking is critical, and nonlinear dynamic model of tram is more complex. Furthermore, the fixed rail track leads the active avoidance function of tram so weak which only can control the speed. Thus, the active safety methods in driverless cars cannot play well in tram context.

The model has been used to calculate braking distance for a specific tram (Sirio™ model), compared then with literature one and real values of braking

Chapter 1 – Mobility in the cities: transport demand and safety hazard  

---

acquisition on tramway in the city of Naples. The thesis ends with the  
integration analysis of the T-ADAS in the on-board communication network.

# Chapter II

## Advanced Driver Assistance Systems (ADASs)

The previous chapter has shown the scope of this thesis, which is further explored in this chapter. The goal of this chapter is to outline quantitative requirements of Advanced Driver Assistance Systems to better define the examination of technological porting to the tram.

This chapter starts with a brief overview of the state of the art of the ADASs. Then, once the different ADASs functionalities and models are explained, the related environmental sensors are described. Furthermore, as the sensors are the key components of the self-driving vehicles, the fusion of the information from the sensors and their proper interpretation followed by control of the vehicle has the central point in the autonomous driving.

### II.1 Overview of the state of the art in ADASs

In the field of automotive safety, Advanced Driver Assistance Systems, designed to help the driver in its driver process, are receiving growing attention. Although the introduction of ADAS has contributed decreasing car accidents, the number of accidents is still high, due to the growing amount of traffic in cities and driving inattention due to the use/misuse of smartphones.

European Commission, national governments and vehicle manufactures have over the years promoted several projects and programs with the common goal of reducing the number of fatalities and injuries in road traffic accidents (Bishop, 2005), raising the effort of researchers and companies to improve this new technology to minimize even more the number of accidents.

Until today, several attempts concerning the classification and overview of ADAS field have been made (Adomat, 2003). Very often ADAS are classified according to the human machine interface they provide, like the provision of information about the state of the environment (driver information systems),

the provision of a warning message (driver warning systems), or the capability of executing an action (control intervention systems). When road safety features are examined, the distinct phases in the accident process (pre-crash, crash, post-crash) are often used for the classification of the driver-assistance systems. When the kinematical control of the vehicle is attempted, these systems are classified in lateral or longitudinal control ones, according to the support they give to the guidance of the vehicle. Other classification are less user and vehicle oriented and more impact oriented as in (Rendon, 2010), where the systems are classified according to high and low road safety and traffic efficiency impact.

Figure II-1 provides an overview of the various types of ADASs and their future deployment paths. This roadmap distinguishes between systems for longitudinal and lateral assistance, and their gradual integration towards fully autonomous driving.

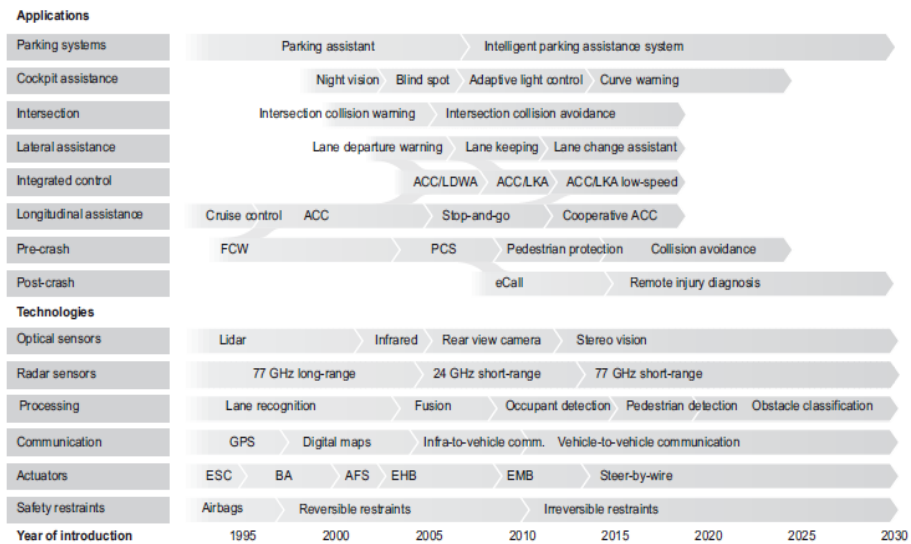


**Figure II.1** ADAS roadmap for applications and technologies

Since this field of research is very broad, this chapter only gives a summary of the ADAS control algorithms and technologies that are relevant for this thesis. The state-of-the-art overview is restricted to systems for longitudinal assistance, since these are quite generic from a functional point of view and are expected to have a significant safety potential (Rendon, 2010).

### II.1.1 Forward Collision Warning systems

The Forward Collision Warning (FCW) system is among the first active safety systems to be implemented on cars that warns a driver in the event of imminent frontal collision.

FCW provides drivers with a warning before a collision with a vehicle or a pedestrian, and collision risk information is presented mainly via sound and vibration. Thus, the positive function of the technology fitting to the development intention of FCW was the prevention of rear-end crashes. The results of traffic accident data analysis recognize this system as the most effective for preventing rear-end collisions (Baek, 2020). Typical FCW systems are based on sensors measurements from RADAR and LIDAR. More recently, as shown in (HAN, 2016), there are also camera-based and sensor fusion-based applications.

As will be explored in Chapter IV, this system mainly works with the measurement of Time To Collision (TTC). Other parameters can instead be evaluated such as the distance to the target, the deceleration, and the probability of collision.

In (Ammoun, 2009), a crossroad scenario with two vehicles equipped with GPS and Vehicle to Vehicle (V2V) communication systems, where the trajectory prediction is performed with a Kalman filter and TTC, is used for the collision risk indicator. A rear-end collision warning model based on a neural network approach is presented in (Xiang, 2014), where participating vehicles are assumed to be moving in the same lane.

### ***II.1.2 Autonomous Emergency Braking systems***

The goal of Autonomous Emergency Braking (AEB) is to avoid or mitigate collisions due to a driver's lack of attention or misjudgement. Some automatic braking systems can prevent collisions at all, but most are designed to reduce vehicle speed before crashing into the front of the car.

This can be achieved by identifying potential collisions with objects and vehicles ahead through two main sensors.

The AEB system based on commercial RADAR is discussed in (Kim, 2016) and has been widely used in many other AEB research studies. Another widely used AEB sensor in the commercial car is LIDAR (Wallner, 2014), the research shows that the laser scanner sensor can measure the distance needed for braking and slowing down the vehicle. The AEB can successfully work with the long braking distance from 3.3 m to 31.7 m.

Although the working of AEB can vary depending on the vehicle manufacturer, it can be summed in four steps, which describe the general procedure (Cioran, 2015):

- Identify critical situations: AEB determines hazardous situations by using data provided by environmental sensors, such as cameras, RADAR or LIDAR, combined with information about vehicle states.
- Prepare the braking system and warn the driver: after a critical situation is recognized, the AEB pre-fills the brake circuit with fluid, making contact the linings with the discs. In this way, the system is ready to apply full braking about 30 ms earlier, either if requested by

the driver or automatically, significantly shortening braking distances. Moreover, the FCW system warns the driver that a collision might occur by a combination of both visual and auditory signals.

- Soft braking: if the driver does not respond to warnings and the object ahead is still present, the AEB will apply light braking to make him more aware of the possible danger, with a deceleration request up to  $4 \text{ m/s}^2$ .
- Hard autonomous braking: if the driver fails to react to the warnings provided, and an unavoidable accident is established due to the position and speed of the ahead vehicle, an emergency brake is activated up to  $-10 \text{ m/s}^2$ . Taking the control of the driving actuators of the vehicle, AEB applies emergency braking at maximum force to avoid, or at least mitigate, the imminent collision, reducing the impact speed and aiming to minimize passenger's wounds.

### ***II.1.3 Adaptive cruise control systems***

The Adaptive Cruise Control (ACC) is a driver assistance system that seeks to combine safe following distance with speed regulation. ACC is the evolution of the Cruise Control (CC), which was first introduced by Mitsubishi in 1995 (Bhatia, 2003). When there is no preceding vehicle in sight, an ACC-equipped vehicle maintains a constant speed set by the driver, just as in a conventional cruise control system. When a preceding vehicle is detected, by using of own vehicle states parameters and RADAR sensors data, ACC determines the ahead vehicle's velocity and, acting on throttle/brake, it regulates own vehicle's speed to keep a safe distance between the two vehicles. For driver comfort, when regulating speed or following distance, the control system is normally limited to using significantly less than the vehicle's maximal deceleration and acceleration capacity. For this reason, ACC is not an active safety system.

The main Adaptive Cruise Control benefits are to:

- Improve traffic flow and driving comfort maintaining accurate safety distances based on instantaneous speed.
- Reduce fuel consumption and trip time.
- Use lower acceleration and deceleration rates than standard non-equipped vehicles, reducing safety-critical situations.

As illustrated in Figure II.2, the control objective of the ACC is to reach the same speed as the preceding vehicle at a desired safe distance  $x_{ref}$ .

The ACC is designed to respond like an attentive human driver, in order to regulate both the spacing error  $e_s = x_{ref} - x_s$  and the speed tracking error  $e_v = v_{ref} - v_r$  to zero.

The ACC cruise control velocity function ensures that the speed  $v_{ref}$  set by the driver is maintained, by applying an acceleration  $a_{ref}$  given by a simple proportional controller law:

$$a_{ref} = k_{cc}(v_{ref} - v_2)$$

where  $k_{cc} > 0$  is the proportional gain for the velocity error  $v_{ref} - v_2$ .

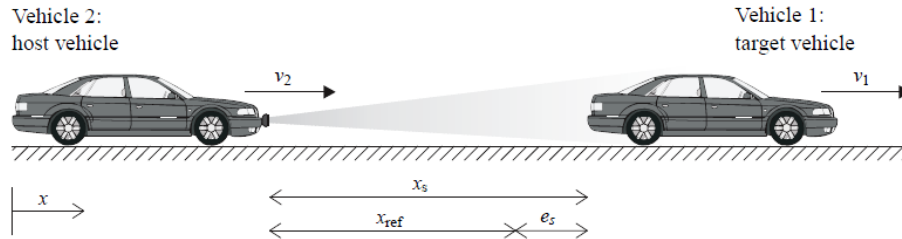


**Figure II.2** Schematic representation of an ACC system

Standard ACC is turned off automatically when the vehicle velocity drops below 30 km/h (Land Rover, 2018) and cannot detect stationary objects or pedestrians.

An extension of the ACC is the Cooperative Adaptive Cruise Control (CACC), which implements communication V2V, and can extend its environmental information including data coming from other vehicles. The advantage of CACC, compared to ACC, is that it has an increased control bandwidth and reliability allowing to maintain a smaller time headway, to reduce system peaks or jerks, and to improve traffic flow and safety (Gietelink, 2007).

The most recent technology is the Predictive Cruise Control (PCC), which uses the GPS to track the vehicle and to perform the best driving conditions over the next kilometers with the aim of fuel-saving and emission reduction. This can be achieved driving as long as possible in the highest gear and, consequently, in the optimal rpm range. Thanks to PCC, fuel consumption and CO<sub>2</sub> emissions can be reduced by almost 4%, specifically over hilly roads (Kavurucu, 2017).

In conclusion, the ACC is a ‘comfort’ functionality as it can reduce the workload of the driver during his driving task.

### **II.1.4 Traffic Sign Recognition systems**

The automatic Traffic Sign Detection and Recognition (TSDR) system is very important research in the development of ADAS, which is designed to provide drivers with vital information that would be difficult or impossible to come by through any other means (Guo, 2018). Investigations on vision based TSDR have received substantial interest in the research community, mainly motivated by three functionalities: detection, tracking and classification. The road traffic images are captured by cameras and/or LIDAR installed on the cars, and the traffic sign detection aims to extract the Region of Interest (RoI) of traffic sign from the current road traffic images. However, in the daily natural conditions, the changes of light, the complex backgrounds and the

aging of signs have caused many difficulties in accurately identifying traffic signs (Cao, 2019).



**Figure II.3** Block diagram of TSDR system

A good TSR correctly classifies a given image patch within a pre-formed set of traffic sign classes while making as few false recognitions as possible.

For this purpose, many contributions are available in the literature to improve the detection and recognition phases.

In (Wang, 2014) is proposed a red bitmap method to detect traffic signs. Firstly, color segmentation of the detected images is performed, and then shape detection of the region of interest (ROI) based on edge information is conducted. This method achieved good detection results but was only applicable to red circular traffic signs, which had some limitations. In (Hechri, 2015) is used the template matching method to match the traffic signs. By setting the sliding window of the same size as the traffic signs, the useless parts of non-traffic signs in the current road scenes were removed. However, considering that the signals have different shapes and sizes in the countries in the world, many studies are being carried out.

Traffic sign classification method based on extreme learning machine is described in (Sun, 2014), which is a supervised learning algorithm related to feedforward neural network. The algorithm classified traffic signs according to the calculation results by selecting a certain proportion of features and obtained high recognition accuracy. In (Qian, 2015) trained the traffic sign data by using the regional depth Convolutional Neural Network (CNN) and the collected Chinese traffic sign dataset for identification test, which achieved a high accurate recognition rate.

Many digital image filtering techniques as proposed in (Sun, 2019), improve the accuracy of the signal detection and classification steps, and, thus, the real-time performance.

Image enhancement is the basic operation method of image pre-processing. Image enhancement technology is to make unclear messages from the image clear to obtain the important messages from the image. In image enhancement technology, the most commonly used methods to eliminate noise in images are mean filtering and median filtering. Mean filtering is a linear filtering algorithm, which gives the target pixel a template, which contains the pixels around it, and replaces the original pixel value with the average of the pixels in the template. The mean filtering formula is:

$$g(x, y) = \frac{1}{m} \sum f(x, y) \quad (I.1)$$

where  $g(x, y)$  is the gray value of the processed image at this point,  $f(x, y)$  is the current pixel to be processed, and  $m$  is sum of all pixels containing the current pixel in the template.

### ***II.1.5 Lane Keeping Assistance System***

As a typical function of advanced driving assistance systems, Lane-Keeping Assistance systems (LKAs) aim to prevent unintended lane departures by detecting lane markings and steering the vehicle.

The lane detection system is a vision-based system based on a lane-departure procedure, which is a driver assistance system (Liu, 2008). The lane detection system includes a camera and an image processing unit. The camera provides the image which includes the information of the lane marking and the lane characteristic, and the image processing algorithm is used to recognize the lane marking. By means of adopting the road geometry model, the deviation to lane boundary will be calculated.

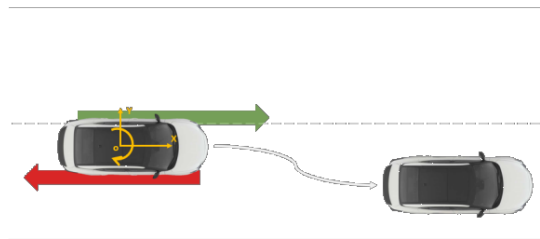


**Figure II.4** *LKA typical function*

Many works of literature proposed lateral control algorithms to obtain better path tracking performance.

As an example, Volvo (Volvo, 2021) describes the principle of its LKA solution based on a camera, which reads the side lines of the road or lane, and if the car is about to cross a side-line then LKA will actively steer the car back into the lane with a slight steering torque in the steering wheel. If the car reaches or crosses a side-line, LKA will also alert the driver with vibration in the steering wheel. As a clear difference to the Lane Departure Warning (LDW) system, which only alerts the driver of an unintentional lane departure (Cicchino, 2018), LKA interferes with the course of the vehicle by steering or braking some of the wheels in the situation of unintended lane departure (Scanlon, 2016). The potential safety effects of the LKA system can be impressive, but the system requires specific conditions to operate. Currently, one of the most crucial operational requirements for the LKA system is the visibility of lane markings. This is a challenge in adverse weather or on roads without proper lane markings.

However, since the driver is out of the control loop when using a fully automated LKS, the visual attention toward the forward roadway could be reduced (Llaneras, 2013). This can lead to hazardous driving situations if the lane detection capabilities of LKSs are not reliable. To address this issue, in (Son, 2015) is proposed the concept of predictive virtual lanes for normal lane-keeping operation when the lane detection module is momentarily unavailable. In (Saito, 2016) is designed a dual control scheme to perform safety control and identification of the driver's state simultaneously.

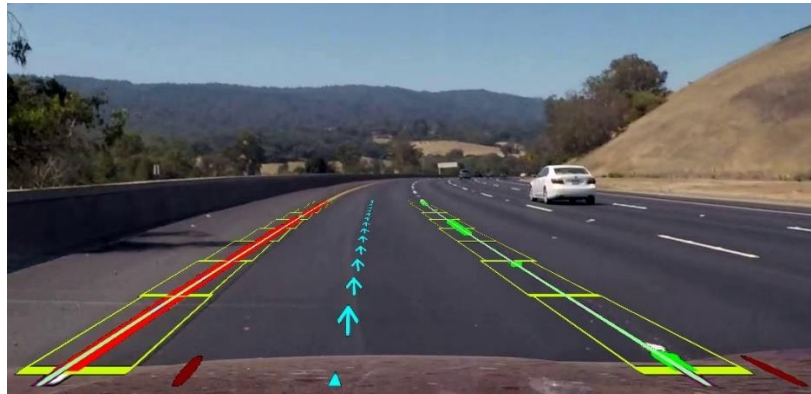


**Figure II.5** *Virtual lane recognition in LKA*

### ***II.1.6 Driver Status Monitoring systems***

To reduce the occurrence of serious traffic accidents caused by driver inability due to fatigue and drowsiness, and to protect drivers from fatal accidents, increasing attention is being paid to Driver Status Monitoring systems (DSMs) equipped with vision sensors, Steering Angle Sensors (SASs), and physiological sensors (Kim, 2019).

The driver's physiologic signals during driving are characteristic features closely related to recognizing distraction or drowsiness. The driver monitoring system using physiological measurement provides high accuracy and can be implemented in real-time (Li, 2017). Despite those merits, commercializing the system is difficult because the equipment to collect the data of physiologic signals is usually huge, expensive, and intrusive (Kong, 2015). Therefore, most DSM systems are camera based.

At present, the most commonly used non-contact physiological parameters measurement methods are:

- doppler measurement based on micro or millimetre wave (Greneker, 1997)
- laser doppler measurement (Ulyanov, 1993)
- infrared imaging measurement (Garbey, 2007)

- Imaging Photoplethysmography (IPPG).

These elements are mainly recognized based on estimating head direction (yaw, pitch, and roll) and the gaze zone. Previous studies have focused on accurately estimating the type of driver’s gaze in subdivided gaze zones, and on the closing time of the eyelids as shown in Figure II-6

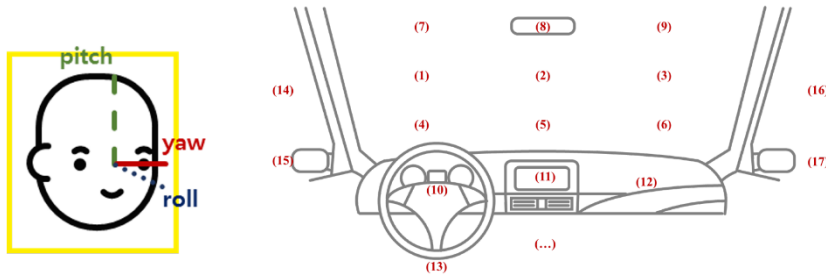


**Figure II.6** Head and eye direction monitoring

## II.2 Environmental-Recognition Sensors for ADAS

The Main sensors used for this in automobiles are RADAR, Camera, LiDAR, ultrasonic sensors, and IR sensors. A brief survey of the technical trend of ADAS sensors features will be given below.

### II.2.1 RADAR Sensor

Radar systems work in millimetre wavelengths; these are used in a wide variety of military and civil applications, such as aerial, marine, or terrestrial threat detection systems, shooting systems, and airports or meteorological systems. The ADAS for smart vehicles and the need to increase road safety have triggered the use of this type of device in the automotive. RADAR systems for intelligent vehicles work at frequencies of 24/77/79 GHz and with chirp sequence in a Frequency Modulated Continuous Wave (FMCW), known as Millimetre Wave (MMW) RADAR. The radar measures the distance between the emitter and the object by calculating the time of flight of the emitted signal and the received echo.

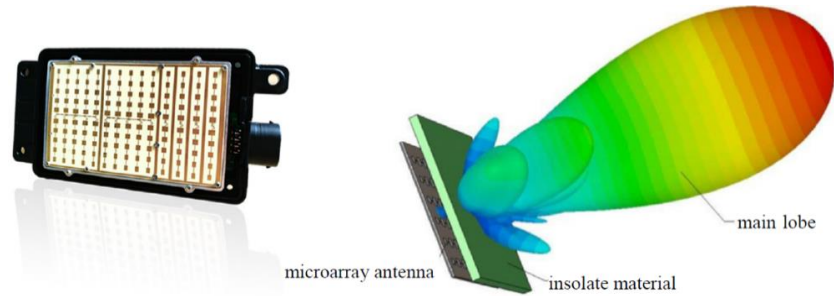


**Figure II.7** Typical automotive millimetre-wave RADAR

The radars, not only allow the detection of the distance to several targets but are also capable of accurately supplying the direction and speed of the targets. The new RADARs for vehicles use an array of micro antennas capable of generating a set of lobes that allow improvement of the range and a processing system for the detection of multiple targets.

Range millimetre-wave RADAR is applied in Blind Spot Detection (BSD), Lane Change Assistant (LCA), Rear Cross Traffic Alert (RCTA), Forward Cross Traffic Alert (FCTA) or RADAR video fusion. RADAR waves have higher penetrability because they offer good features in all weather conditions, and can accurately detect short-range targets in front, to the side, and to the rear side of vehicle. For this reason, they are used in several ADAS systems.

The basic waveform that the FMCW radar transmits and receives is the triangle waveform and it is shown in Figure II.8.

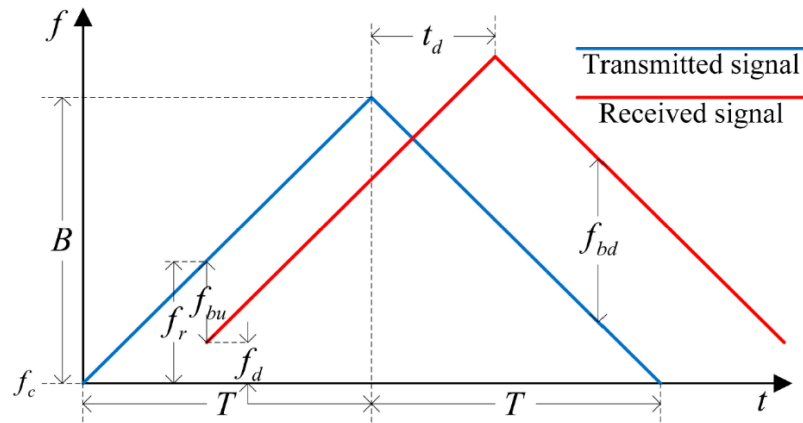


**Figure II.8** Basic waveform of FMCW radar

The waveform consists of an up-ramp and a down-ramp, and the beat frequencies available in each ramp are denoted by  $f_{bu}$  and  $f_{bd}$ . The time delay between the transmitted and the received signal is denoted by  $t_d$ , and  $f_d$  is the doppler frequency caused by the relative velocity of the target. The bandwidth

of the waveform, the period of one ramp and the carrier frequency are represented by  $B$ ,  $T$  and  $f_c$ , respectively.

RADAR can significantly improve vehicle safety performance and reduce the decision-making burden of people at the wheel. Furthermore, it can be installed besides the bumpers of the vehicle. Some disadvantages of this sensor type are the lack of precision, its reduced Field of View (FOV), and the fact that it can produce false positives due to bouncing of the emitted signal.

### ***II.2.2 Camera Sensor***

In the perception system of AV and from a point of view of the wavelength received by the device, cameras can be classified as visible (VIS) or infrared (IR). The element used by the camera to capture a scene is known as an imaging sensor and has traditionally been implemented with two technologies: Charge Coupled Device (CCD) and Complementary Metal Oxide Semiconductor (CMOS). The design of the extraction architecture of the luminosity values allows the selection and processing of Regions of RoI; furthermore, the CMOS device has a lower consumption than CCDs. These characteristics make them the most used technology for mobile devices. On the other hand, CCD technology has a high dynamic range and higher image quality in low light environments.

The differences of both technologies begin to overlap, and it is expected that in the future, CMOS technology will replace CCD. VIS cameras capture wavelengths between 400 nm to 780 nm, same as the human eye can. The visible spectrum is divided into three bands or channels: Red, Green and Blu, which will be coded separately. These devices are the most used in AV perception systems to obtain information about the surroundings of the vehicle due to their low-cost, high-quality colour information, and high resolution. The huge volume of data generated by means of the device supposes a further problem for the processing system.

The most common applications are BSD, side view control, accident recording, object identification, LCA, and signs detection. VIS cameras are highly affected by variations in lighting conditions, rain, snow, or fog conditions and for this reason are combined with RADAR and LiDAR technologies to increase its robustness. The combinations of two VIS cameras with a known focal distance allows stereoscopy vision to be performed, which adds a new channel called depth information. Cameras with these features are known as RGBD. These devices supply a 3D representation of the scene around the vehicle.

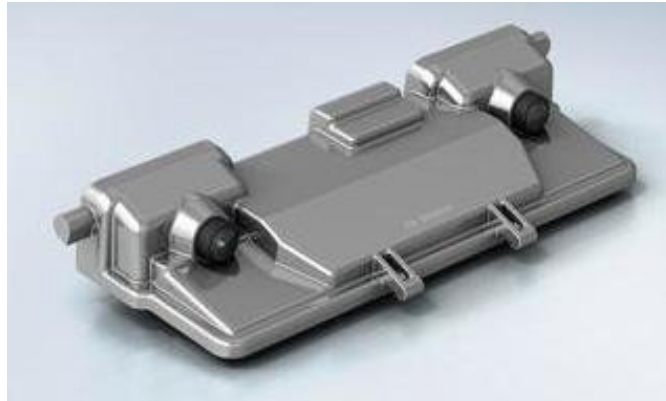


**Figure II.9** *Stereo camera*

Using a powerful lens system, the camera can record a horizontal range of 50 degrees and offers a 3D measurement range of more than 50 meters. The image sensors, which feature highly sensitive and dynamic lighting technology, can process high-contrast images.

### ***II.2.3 LiDAR Sensor***

LiDAR systems base their operation on the measurement of the time of flight of a pulsed light emitted from a laser diode until it is received by an emitter. The emissions are in infrared ranges (905 nm or 1550 nm). Emissions at 905 nm require less energy than those emitted at 1550 nm because the water in the atmosphere begins to absorb energy from 1400 nm. This initial disadvantage of power increase at 1550 nm is used by the aqueous liquid of the eye to totally filter this wavelength, making them less harmful than LiDAR at 905 nm.

Lasers used for vehicles belong to so-called first class and are safe under all conditions of normal use. LiDARs use the  $T_0$  principle to carry out the measurement of distance between emission and reception. These can be classified according to the type of information they obtain from the environment in 2D or 3D LiDARs; otherwise, it can be classified according to their construction rotary or solid-state LiDAR. The 2D LiDAR obtains information from the environment by projecting a single laser beam on a rotating mirror perpendicular to the axis of rotation. The 3D LiDAR allows to obtain a high-resolution 3D map of the environment; for that purpose, they use a set of diodes lasers mounted on a pod that rotates at high speed. The number of lasers installed in the pod determines the accuracy of the point cloud obtained in each turn. Currently we can find 3D LiDARs that integrate from 4 to 128 lasers or channels with a horizontal FOV of 360° and vertical FOV that oscillates between 20°-45° with accuracy of a few centimetres. Depending on the number of channels, 3D LiDAR are used in ACC, object

avoidance, object identification or 3D mapping. LiDAR is affected by weather conditions such as rain, snow, fog, or dusty environments due to the diffraction of light in these environments. Furthermore, they reduce their operating range detection depending on the reflectivity of the objects that are reached by the laser beams. The maximum detection capacity depending on the type of reflectivity of the material to be detected is presented in the datasheet provided by the manufacturer.

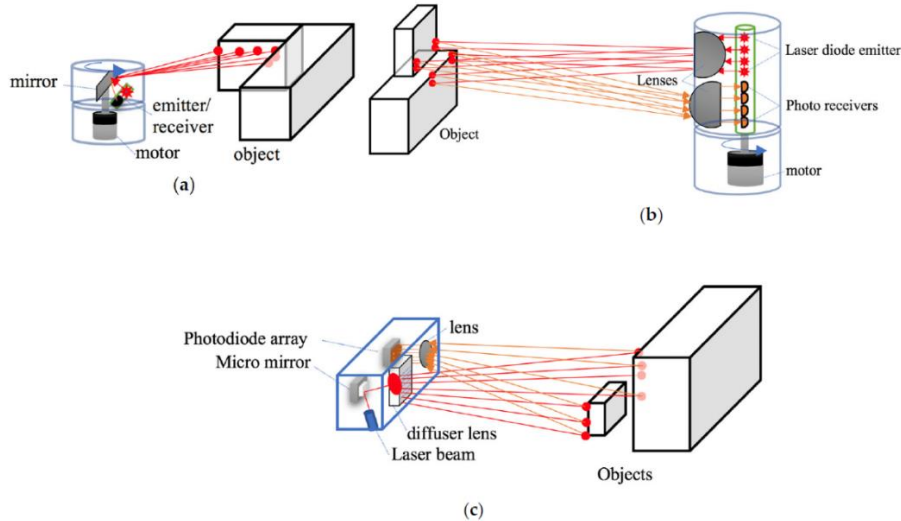


**Figure II.10** Operating schemes: (a) Rotating 2D LiDAR, (b) rotating 3D LiDAR, (c) solid state 3D LiDAR

The last kind of device based on laser measurement that has arrived in the AV world is the solid-state LiDAR. Solid state LiDAR allows a 3D representation of the scene to be obtained around the LiDAR without the use of mobile parts in the device. For that, the micro-mirror reflects the beam over a diffuser lens, which creates a vertical line that touches the objects. The light reflected is captured by a lens and is sent to a photodetector array to build the first line of a 3D matrix. The process is repeated until a point cloud of the scene is created. This feature notably increases its durability, reduces maintenance tasks, and decreases its price. Solid state has a smaller FOV than the rotary LiDAR. The trends in perception system are replacing the current rotating 3D LiDAR by a set of solid state LiDARs integrated around the vehicle.

### II.2.4 Ultrasonic Sensors

As its name indicates, ultrasonic sensors use sonic waves, in the range of 20 kHz to 40 kHz, generated by a magneto-resistive membrane, to measure the distance to an object. Its principle of operation is based on the

measurement of the time of flight  $T_0$  of the sonic wave from when it is emitted until the echo is received:

$$d = \frac{c}{2}T_0$$

where  $c$  is the wave speed in meters per second, and  $T_0$  is time of flight in seconds. These sensors are usually used in industrial environments for the measurement of height in storage of all types of raw materials. In vehicles, they are used in parking systems or as short distance measurement sensors at low speeds. These low-cost sensors produce good results when measuring distances with any material, independent of its colour, in dusty environments or in adverse weather conditions (humidity or rain). Disadvantages of these sensors include a tendency to produce false positives by bouncing, and a blind zone (blanking) in the measurements, located between the sender element of the sensor and the minimum range.

### ***II.2.5 V2X Communication System***

Smart mobility and vehicular communication open the opportunities to acquire timely information of data related to the transport system (vehicles' speed and position for the road infrastructure, intersection, traffic signal timing for vehicles, etc.) (Földes, 2016).

Vehicle to Everything (V2X) communication represents a class of communication systems that provides the vehicle with an ability to exchange information with other systems in the environment. Examples include V2V for collision avoidance, Vehicle to Infrastructure (V2I) for traffic signal timing, vehicle-to-network for real-time traffic updates, and vehicle-to-pedestrian for pedestrian signalling. State-of-the-art V2X communication is based on either Dedicated Short-Range Communications (DSRC) or cellular networks (Abboud, 2016). The IEEE 1609 family of standards for Wireless Access in Vehicular Environment (WAVE), which is developed based on the IEEE 802.11p standard, defines an architecture and a set of services and interfaces to enable DSRC-based secure V2V and V2I communication (Vivek, 2014).

### **II.3 Levels of Driving Automation: a SAE standard**

Union of Concerned Scientists (UCS) defines AV as follows: “Self-driving vehicles like cars or trucks in which human drivers are never required to take control to safely operate the vehicle” (Rosique, 2019). However, the standard way to discuss AV is to talk about “self-driving levels”, as defined by the SAE (Society of Automotive Engineers). The SAE, which is an automobile standardization agency, divided the autonomous driving capacity of a vehicle into six levels, from the vehicles without any automation to 100% autonomous driving.

SAE J3016 provides a taxonomy describing the full range of levels of driving automation in on-road motor vehicles (Williams, 2021) as shows Figure II.11. These levels help measure how advanced the technology of a certain autonomous car is (Inagaki, 2018). This has opened up numerous fields of research and development that, although end up being interconnected, correspond to very diverse areas.

<b>Automation level:</b>	<b>0</b>	<b>1</b>	<b>2</b>	<b>3</b>	<b>4</b>	<b>5</b>
<b>Description:</b>	No automation	Driver assistance	Partial automation	Conditional automation	High automation	Full automation
<b>Driver engagement:</b>	Responsible for all driving	Hands -or- feet off	Hands + feet off (partial)	Eyes off	Brain off (or driver not even present)	
<b>Driver support:</b>	none	Advanced driver-assistance systems (ADAS)			only when or if human driven	
<b>Monitors driving:</b>	Human driver			Automated system		
<b>Vehicle control:</b>	Human driver		Shared		Automated system	

**Figure II.11** SAE J3016 levels of driving automation

Let's look at these levels in more detail:

- **Level 0:** Most vehicles on the road today are Level 0: manually controlled and without any automation. The driver provides the "dynamic driving task" although there may be systems in place to help the driver. An example would be the ABS system since it technically doesn't "drive" the vehicle, it does not qualify as automation.
- **Level 1:** The driver is always essentially in control of the vehicle, but the vehicle is able to temporarily take control from the driver in order to prevent an accident or to provide some form of the support to the driver. The Level-1 automated system may include features such as ACC, AEB, Parking Assistance (PA) with automated steering, and LKA systems that will actively keep the vehicle in the lane unless the driver is purposely changing lanes. Level-1 is the most popular form of what can reasonably be considered "self-driving technology". Since Level 1 does not control the vehicle under normal circumstances, it requires the least amount of processing power of the autonomous systems.
- **Level 2:** The driver is obliged to remain vigilant in order to detect objects and events and respond if the automated system fails to do so. However, under a reasonably well-defined set of circumstances, the autonomous driving systems execute all of

the accelerating, braking, and steering activities. If a driver feels the situation is becoming unsafe, they are expected to take control of the vehicle and the automated system will deactivate immediately.

- **Level 3:** The jump from Level 2 to Level 3 is substantial from a technological perspective, but subtle if not negligible from a human perspective. Within known, limited environments, such as freeways or closed campuses, drivers can safely turn their attention away from the driving task and start reasonably doing other. Level 3 vehicles have “environmental detection” capabilities and can make informed decisions for themselves, such as accelerating past a slow-moving vehicle, but they still require human override. The driver must remain alert and ready to take control if the system is unable to execute the task.
- **Level 4:** The key difference between Level 3 and Level 4 automation is that Level 4 vehicles can intervene if things go wrong or there is a system failure. In this sense, these cars do not require human interaction in most circumstances. However, a human still has the option to manually override. The driver must enable the automated system only when it is safe to do so. When enabled, driver attention is not required, making Level 4 the first level that can genuinely be called fully autonomous in the sense that a driver or passenger would have a reasonable expectation of being able to travel from one destination to another on a variety of public and private roads without ever having to assume control of the vehicle.
- **Level 5:** Other than setting the destination and starting the system, no human intervention is required; the automatic system can drive to any location where it is legal to drive and make its own decisions. Level 5 cars won’t even have steering wheels or acceleration/braking pedals. They will be free from geo-fencing, able to go anywhere and do anything that an experienced human driver can do. Fully autonomous cars are undergoing testing in several pockets of the world, but none are yet available to the general public.

The Figure II.12 shows the market penetration of vehicles equipped with ADAS systems. By 2045 more than 70% of all vehicles sold will integrate autonomous capabilities (Litman, 2021). This report is based on the automotive field only. We wonder what the prospects would be in terms of market penetration, sustainability, safety, and performance, if these systems were applied in other sectors such as public transport by tram.

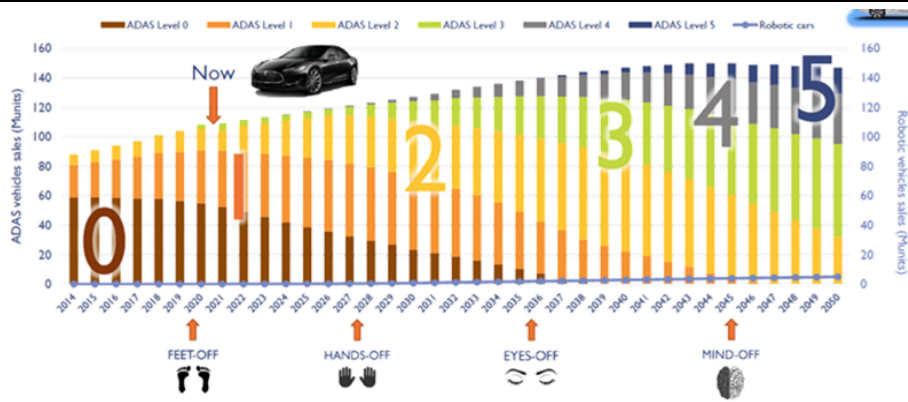


**Figure II.12** Market penetration of ADAS vehicle

#### II.4 Sensor Fusion and Perception Technology

Sensor fusion is an essential technology of AVs. The acquired data from multiple sensing modalities are integrates to reduce the number of detection uncertainties and overcome the shortcomings of individual sensors operating independently. As reported in (Lundquist, 2011), the sensor fusion helps to develop a consistent model that can perceive the surroundings accurately in various environmental conditions. For instance, camera and RADAR fusion may provide high-resolution images and the relative velocities of the detected obstacles in the perceived scene.

Starting from the previous description on environmental sensors, it is possible to qualitatively summarizes in Table II.1 the strengths and weaknesses of the commonly utilized perception-based sensors in AVs, such as camera, LiDAR, and RADAR. The “√” symbol is used for the sensor operates competently under the specific factor; the “~” symbol indicates that the sensor performs reasonably well under the specific factor, whereas the “X” symbol indicates that the sensor does not operate well under the specific factor relative to the other sensors.

In literature the research on multi-sensor fusion systems in AVs for environment perception and object detection is well-established (Yeong, 2021).

A survey conveyed by (Wang, 2019) showed that the camera-RADAR sensors combination is the most employed in the multi-sensor fusion systems for environment perception, followed by camera-LiDAR-RADAR and camera-LiDAR.

**Table II.1** Comparison of the commonly employed sensors in self-driving cars

Factors	Camera	LiDAR	Radar
Range	~	~	✓
Resolution	✓	~	✗
Distance	~	✓	✓
Accuracy	~	✓	✓
Velocity	~	✗	✓
Colour			
Perception, e.g., traffic lights	✓	✗	✗
Object Detection	~	✓	✓
Object Classification	✓	~	✗
Lane Detection	✓	✗	✗
Obstacle Edge Detection	✓	✓	✗
Illumination Conditions	✗	✓	✓
Weather Conditions	✗	~	✓

The the first pair of sensors combination offers high-resolution images while obtaining additional distance and velocity information of surrounding obstacles, as in the case of Tesla that utilizes the camera-RADAR sensors combination and other sensors, such as ultrasonic sensors, to perceive vehicle surroundings (Tesla, 2021). Similarly, the camera-LiDAR-RADAR sensors combination can provide resolution at a greater range, and precisely understands the surroundings through the LiDAR point clouds, and depth map information; it also improves the safety redundancy of the overall autonomous system, as described in (NAVYA, 2021) where a combination of these three sensors is used for environment perception in their AVs.

In (Rosique, 2019) the authors highlight the characteristics of goodness of the sensors on a larger scale of 10 points. In detail the quantification has been carried out using ten scores which reflect the general characteristics of the sensors on the market and simplify the process: 0 for none, 10 for high. Figure n shows a summary of the advantages and disadvantages of the principal sensors analysed in this section. The spider chart of features sensors show that a perfect sensor is defined as the one that obtains the best scores in all the characteristics analysed above. This means maximum values (10) for FOV, range, accuracy, processing, resolution, colour perception, and minimum values (0) for weather affections, maintenance, visibility, and price. This comparison offers a clear overview of the sensors' strengths and weaknesses.

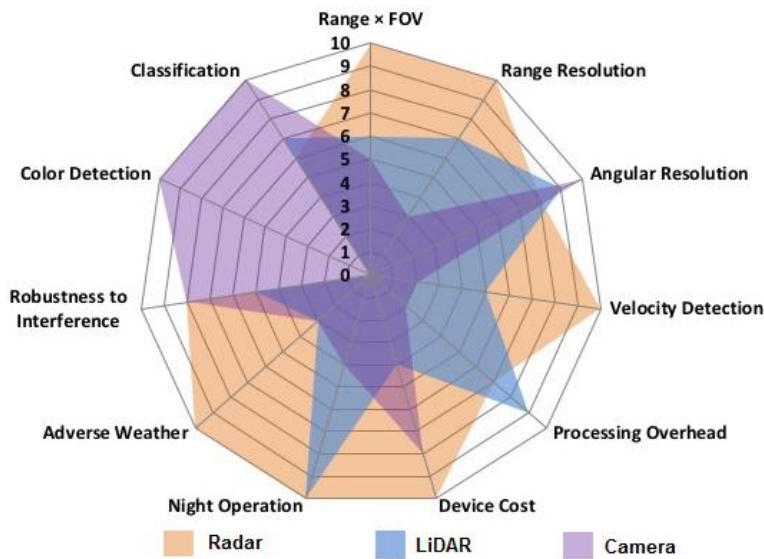


**Figure II.13** Features comparison of the principal sensors

The need for sensor fusion lies in the limitations of each sensor with respect to some characteristics.

The increase in performance obtained from the fusion of data from multiple sensors working independently and asynchronously is also due to the fact that the sensors are typically mounted in different positions of the vehicle, so their integration allows for a wider perception of the environment. In order to perform sensor fusion, the sensors require a common understanding of time and space and a standardized data interface (Steinbaeck, 2017), as shown in the block diagram of the Figure II.14.

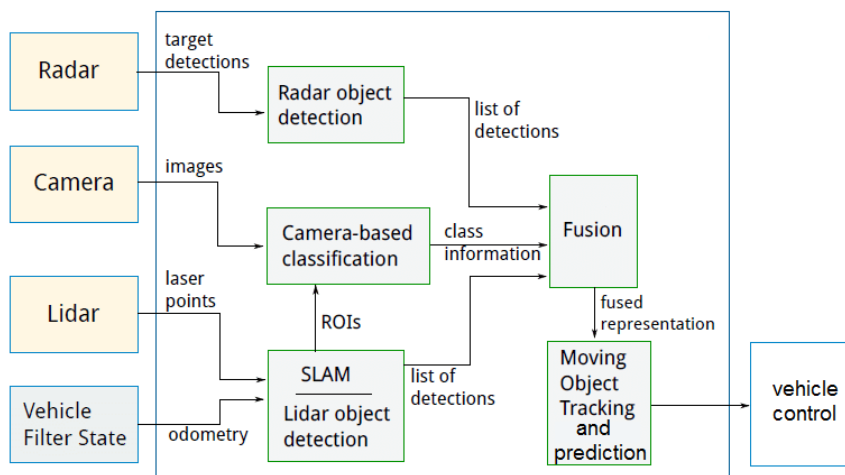


**Figure II.14** Typical sensor fusion architecture

Another key aspect in the ADAS sensor fusion and perception platform is the ability to calculate the risk by estimating the trajectories of head vehicle and the target vehicle (Rummelhard, 2017) (Wang, 2020). The risk being then estimated through a TTC approach by projecting object trajectories to the future (Baek, 2020).

# **Chapter III**

## **ADAS for trams: spread analysis and technological porting**

In 2009, the International Association of Public Transport (UITP) highlights that the number of accidents per person transported by tram compared to cars was four times lower (UITP, 2009). An update of this study in 2016 emphasizes that the tram was six times safer than the car (UITP, 2016), suggesting that to further increase safety levels driver assistance solutions would have been useful. The same conclusions are reached in (Di Palma, 2020) where it is shown how an ADAS system applied to a tram, properly programmed with environmental and travel parameters, would have helped to avoid most of the collisions analysed.

Therefore, it appears necessary to define which ADAS technologies and services to apply to the tram.

The current rail transport system is playing an essential role in driving sustainable economic growth, providing access for passengers into and between the major economic centres and fulfilling a vital position in the supply chain (TSAG, 2010). According to the published data by the UITP, LRT and trams has enjoyed a renaissance since the new millennium, with no less than 108 new cities (re)opening their first line (UITP, 2019). As Figure III.1 shows, Europe has traditionally been a leader in LRT and tram development, with 60 new systems, not including new lines in existing systems and line extensions. Europe is followed by Asia-Pacific and North America with 20 and 16 new systems respectively.

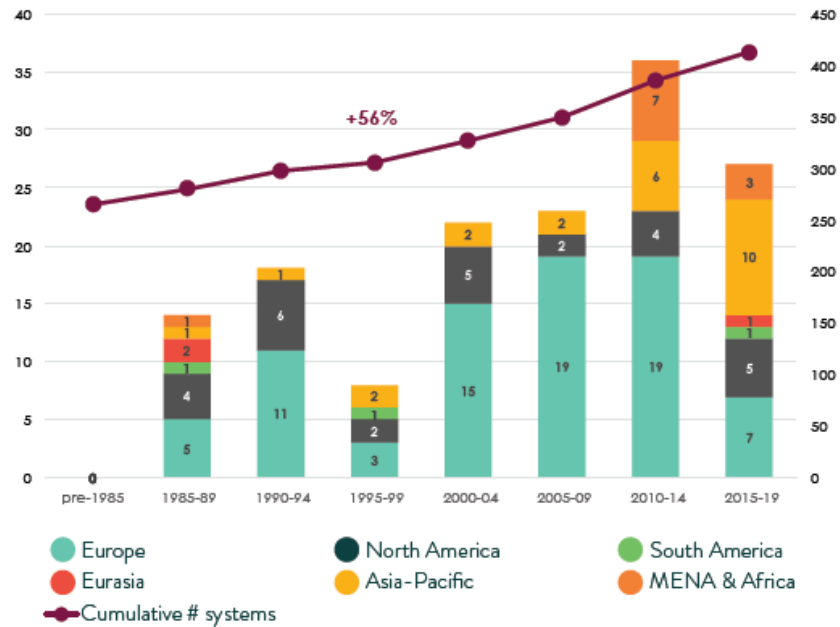


**Figure III.1** LRT and tram system opening per half-decade, 1985-2019

How to control the running of light-rail to achieve safer and more efficient operation for a tram and railway system is a long-lasting issue dating back to the birth of rail transportation. In modern metro systems this task is entrusted to the Automatic Train Control (ATC) system: an integrated signalling system that combines railway train control, supervision, and management to help drivers (or completely substituting drivers) control the train movements automatically to guarantee the safe and efficient movement of railway trains (Claudio, 2014). The target train stop for boarding and alighting aligned with the platform doors are also controlled by the ATC.

Signal boxes and decentral ATC computers protect the train through Automatic Train Protection (ATP) and the route by setting the signals. Such a rail system is separated from the other traffic areas by way of e.g. elevation, fencing or a tunnel to ensure that it does not conflict with the surrounding traffic, but it is not monitored by way of sensors. Usually, the functions of relevance to the operational safety have been integrated into the ATP system.

The driverless automatic driving is instead realized by Automatic Train Operation (ATO) systems. The operation of autonomous rail vehicles on an in-street or segregated track formation can be based on the ATO logic, but there is no signal box logic or ATP logic. Just as a tramcar operated on sight by a driver, the rail vehicle fully depends on its own perception or assessment and therefore it itself also must monitor the track and assess the situation (autonomously). To fulfil this requirement, it is equipped with either RADAR,

LiDAR or video cameras (mono or stereo), the signals/data of which are evaluated and assessed in a separate on-board computer.

This approach introduced in this chapter and referring to tramcars is called Tram Advanced Driving Assistance System (T-ADAS).

To apply ATP system in tramway sector, a theoretical studies and field tests are still being conducted to verify its feasibility and effectiveness due to the absence, in most cases, of a protected railway lane. The tram must move like other vehicles and the ATP can be developed in abstraction to the autonomous driving features and technologies that come from the automotive sector.

In this chapter, a preliminary study for technological porting by managing ADAS depending on the GoA is shown. The Grades/Levels of Automation in automotive and railway systems are presented and compared each other. Then, according to the implication level of a remote sensing system in each tram driving task, GoA for trams are proposed.

These systems are designed to help the tram driver cope with potential hazards by having a defensive driving. Therefore, the proposed GoA correlated to ADAS will be useful to understand how those automation acts on the tram driver action and the Human-Machine System safety.

### **III.1 Automatic Train Control Systems**

Automatic control systems and their affects to reduce the human error problems are more attractive in recent years to control the railway transport systems due to the growing traffic intensity and complexity of these systems. ATC system is an automatic control algorithm to protect the trains from collision (Siahvashi, 2010). In addition to collision avoidance the following items can be achieved using the ATC system:

- Improve the performance of control and signalling systems;
- Increase the safety;
- Reduce the costs;
- Reduce the energy consumption.

According to the definition, an ATC system consists of ATP, ATO and Automatic Train Supervision (ATS) (Chiusolo, 2011), as illustrated Figure III.2.

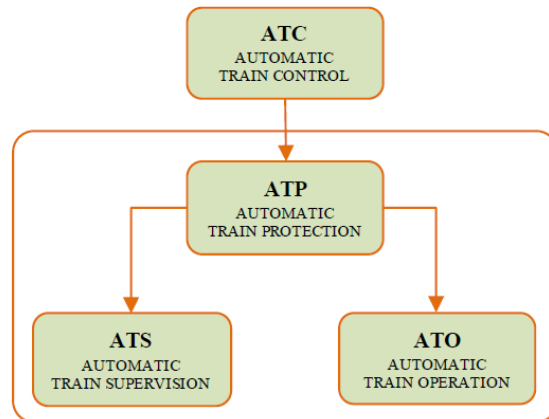


**Figure III.2** *Automatic Train Control*

In particular, the following features can be recognized for these three systems (Yin, 2017):

- ATS system is responsible for monitoring the train movement to ensure that the trains conform to an intended schedule and traffic pattern. Specifically, ATS system connects train dispatching and train operation in urban rail systems that helps to avoid or reduce damage resulting from system abnormalities and equipment malfunctions by performing the following tasks: supervision of train status, automatic routing selection, automatic schedule creation, automatic operations logging, statistics and report generation and automatic system status monitoring.
- ATP system is a fail-safe (vital) system, which is responsible for the safe movement of individual trains. ATP imposes speed limits on the moving trains, not only to maintain a safe operating distance between the trains, but also to comply with safety and speed requirements. Once the train exceeds the speed limit, ATP will automatically execute braking (or emergency braking) order to stop the train to keep safety.
- ATO system performs the on-board functions instead of a train driver to ensure a smooth acceleration of the train to the running speed, speed regulation and stopping the train at the destination platform precisely. In normal situations, ATO is responsible for all the train traction and braking control commands, and thus, it is a key to the operational efficiency and profitability of train operation systems (Dong, 2010).

In Figure III.3, the fundamental structure of a typical ATC system which contains the ATP, ATO and ATS is shown.

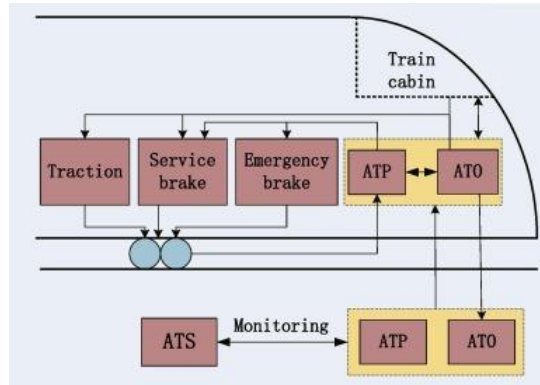


**Figure III.3** Structure of Automatic Train Control system

ATO is responsible for all the traction and braking controls, as well as parking and stopping operations, as further illustrated by Figure III.4 (Yasunobu, 1986) (Goodall, 2002).

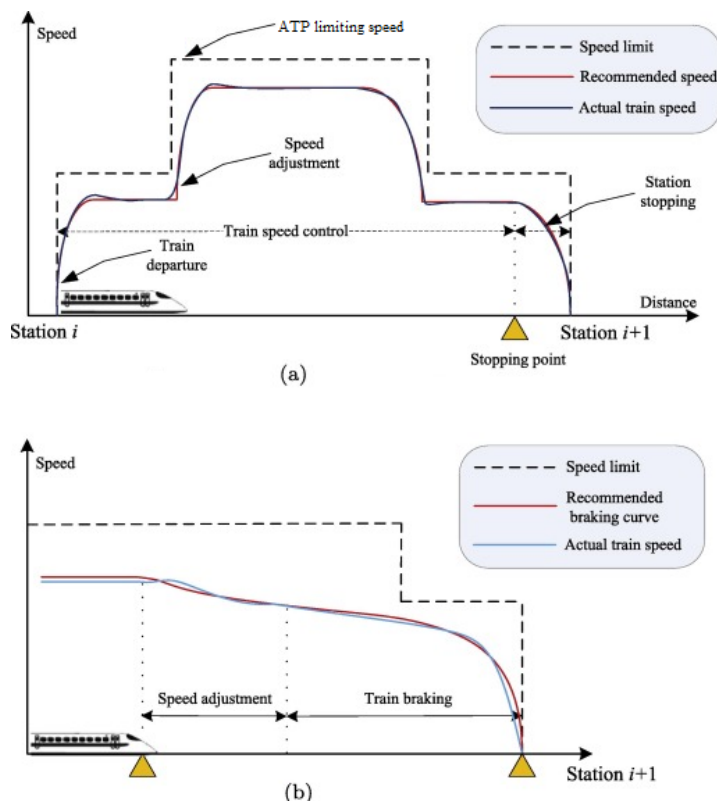


**Figure III.4** Operation of the ATO system: (a) train speed control, (b) train stopping

However, it is necessary to point out the previous description by saying that there are many kinds of ATC systems but in all of them, the ATP helps to prevent collisions through a driver's failure to observe a signal or speed restriction. The ATO provides partial or complete automatic train piloting and driverless functions and the ATS which is the basis of the train protection function and the automatic speed control devices. The ATS system, by using the block information, specifies the speed constraints and sends them to the trains by using of track circuit, loop and/or balises (Dong, 2010).

### *III.1.1 Grades of Automation (GoA)*

The notion of ATC defines the operational safety levels against functional requirements necessary to help automate train operations. The UITP defines ATO, ATC, ATP as a different level of automation in GoA paradigm. Each GoA is identified by the operational responsibilities of the train basic functions either to an automatic system or to man. In particular, UITP identify the following 5 GoA levels (Yan, 2016):

- GoA 0: is a train driver on-sight operation, similar to a tram running in street traffic, reliant entirely on train driver to manage the system safety.
- GoA 1: Non-automated Train Operation (NTO). There is a driver in the cabin and the automatic system prevents unsafe operation of drivers in respect of speed limit signals (ATP).
- GoA 2: Semi-automated Train Operation (STO). ATO system controls the train movement by the acceleration and deceleration commands. The movement of the train is supervised by the ATP system. The driver in the cabin observes the guideway and stops the train in case of a hazardous situations. The opening and closing of doors may be done automatically or performed by the driver.
- GoA 3: Driverless Train Operation (DTO). There is no driver in the cabin to observe the guideway and stop the train in case of a hazardous situation. Safe departure of the train from a station, including door closing, could be the responsibility of the operation staff on board or may be done automatically.
- GoA 4: Unattended Train Operation (UTO). There is no operation staff on board. So, the safe departure of the train from a station, including door closing, must be done automatically.

UTO is only possible for systems with GoA 4; however, in practice, not all GoA 4 systems are operated unattended. Based on the observations of automated metros, most of the GoA 4 systems are operated with attendants on-board every train, like a GoA 3 system. The difference is that in GoA 4 the attendant is not essential for the system, unlike in GoA 3, where must be always present.

The Figure III.5 shows clear classification of GoAs for urban rail transit systems.

Grade of Automation	Type of train operation	Setting train in motion	Stopping train	Door closure	Operation in event of Disruption
GoA 1 	ATP with driver	Driver	Driver	Driver	Driver
GoA 2 	ATP and ATO with driver	Automatic	Automatic	Driver	Driver
GoA 3 	Driverless	Automatic	Automatic	Train attendant	Train attendant
GoA 4 	UTO	Automatic	Automatic	Automatic	Automatic

**Figure III.5** Grade of Automation (GoA) classification

The technologies and solutions typical of the higher GoA levels, however, cannot be applied to the trams as they require the vehicle to travel on a reserved route and a continuous exchange of information through the communication systems along the rail. In fact, compared to other means of rail transit, the tram does not have a signalling system that collects and coordinates all information on the circulation and availability of an unoccupied route; its track is shared with road vehicles and pedestrians (Wang, 2018). Precisely, the absence of signalling systems that inform the tram about the possibility of moving forward without encountering obstacles makes the use of an ADAS for the tram very interesting: ADAS systems are capable of gathering the necessary information from the environment in which the vehicle is moving.

Below we will see in detail some of the main ADAS functionality used in the automotive sector potentially applicable to the tram sector.

### III.2 ADAS functionality for trams

In the previous chapter, the main functions which represent the state of the art for autonomous driving in ADAS were presented. For railway systems, on the other hand, we have introduced the meaning of automatic driving and GoA.

Unlike automated driving, the autonomous driving considers that a vehicle must be able to operate without any extraneous control and obtain all required information for safe operation from its on-board sensors. If necessary, an AV

should be able to find its way without external influences and without endangering other traffic participants (ESSER, 2016).

The reliability is one of the main requirements in the autonomous driving: the system must need an accurate detection of obstacles (vehicles, pedestrians, or bikes). In fact, false positives can distract or confuse the driver creating dangerous situations should be avoided at all (Velez, 2015). On the other hand, if the system does not alarm whenever it is necessary, its utility decreases and it can create a false feeling of safety.

To identify the characteristics of a T-ADAS it is appropriate to start from the automotive world and extend these functionalities to railway systems.

A comparison between the Levels of Automation (LoAs) in automotive, and GoAs in railway sectors is given in the Table III.1.

**Table III.1** Automation comparison for automotive and railway

AUTOMOTIVE	Railway
<i>No automation (LoA0)</i>	No automation (GoA0)
<i>Driver assistance (LoA1)</i>	Manual driving with ATP (GoA1)
<i>Partial automation (LoA2)</i>	Manual driving with ATP and ATO (GoA2)
<i>Conditional automation (LoA3)</i>	Driverless train High (GoA3)
<i>High automation (LoA4)</i>	
<i>Full automation (LoA5)</i>	Unattended train (GoA4)

The meaning of this table can be expressed as follows: The GoA 0 level is typical of the tram as it currently does not have degrees of automation, similarly to the SAE Level 0.

New technologies in railway control systems are capable of supervising, operating, and controlling the whole train operations, or even an entire fleet. A railway line equipped with ATP corresponds (at least) to a GoA 1 and allows driving assistance avoiding collisions, exceeding the red signal and the speed limits by automatically applying the brakes, which is equivalent to approximately SAE Level 1.

The GoA 2 can classify the system as semi-automatic driving, the driver only gives the starting signal and supervises the doors. In this case, in fact, the ATO system is present to carry out and control the train running dynamics.

This degree of automation can be compared to SAE Level 2 as the vehicle performs actions independently of the driver in order to perform protection and safety functions.

The GoA 3 can be compared to SAE levels 3 and 4 as the system is able to carry out all driving operations automatically.

Finally, the GoA 4 is comparable to the SAE Level 5 since in none of the cases is a driver present.

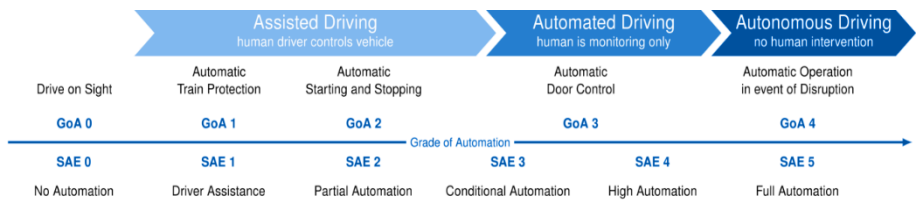


**Figure III.6** From assisted driving to autonomous driving: comparison between LoAs and GoAs

As mentioned above, the higher GoAs are already implemented in the railway sector, in driverless metro. However, they cannot be directly transposed to the control of trams, because trams operate in a less secure, more complex and dynamic road environment than that of metros and trains. The trams can therefore be the subject to various disturbances, such as the presence of other vehicles, meteorological changes, and risky obstacles on the track. Due to these limitations, today it remains impossible to automate everything and design an efficient tram system to cope with all complex needs of the dynamic road environment autonomously. Therefore, completely autonomous tram is not the purpose of this work, so the human driver will always be present in the cabin control.

The following part presents the different automotive LoAs and how to apply them for T-ADAS in order to improve driving safety.

**Table III.2** *Spread analysis for ADAS functionalities on tram*

<b>Automotive ADAS</b>	<b>Portability to T-ADAS</b>
ACC	Transfer is possible, even if it is not very significant in urban areas. Considering the tram running parameters, ACC should be used to maintain the same safety distance with the vehicle in front by continuously adjusting the speed, minimizing the risk of collisions.
FCW AEB	Transfer is possible. The tram with this system can alert the driver when an obstacle (e.g. pedestrians, bikes or cars) is located along the tram trajectory. If the driver does not react in time, taking into account the speed of the tram and the distance from the target, the system can trigger a braking mitigating the risk of collision.
LKS	Transfer is not possible. The tram keeps its lane naturally thanks to the tracks.
TSR	Transfer is possible. The system could be programmed and trained to recognize not only ordinary road signs but also tramway signs.
CTA	Transfer is not possible. The tram does not reverse gear in the normal driving path. however, the trams normally have two cabins, one for each direction of travel, so the function can be useful in the manoeuvring phases inside the depots.
PA	Transfer is not possible. In a broad sense, it can be assimilated to the stop at the target.
BSD /Blind Spot Information System (BLIS)	Transfer is possible. A warning can be produced to alert the driver when another vehicle is alongside the tram, making a blind spot evident.
Adaptive Light Control (ALC)	Transfer is possible, even if it is not very significant in urban areas. This automotive system for adjusting the light beam in dark corners can be transferred to the tram in order to offer greater visibility in curves making the road edges more visible.
Rear Collision Warning (RCW)	Transfer is possible. The driver can be warned when a vehicle arriving at high speed from the rear does not have sufficient braking distances.
DMS	Transfer is possible. This system could reduce many driving distraction accidents by monitoring the driver's attention status. For example, the last tram accident in Milan (Italy) is due to a distraction from the driver who consequently hit a car.

From the analysis conducted, we understand that there are unnecessary or non-transferable ADAS functionalities for the tram. We can conclude that for the tram the technological porting refers to two fundamental functions:

- **Longitudinal Dynamic Control:** include all the ADAS that actively pursue longitudinal safety, i.e. system's purpose is to avoid an impact with any obstacle that precedes the tram or at least reduce its speed impact.
- **Driver Warning Systems:** its purpose is to promptly warn the driver and stimulate a timely reaction in order to avoid a possible collision,

include vehicle blind spot monitoring systems, vehicle detection systems vulnerable road users (pedestrians, cyclists and motorcyclists) and systems that focus on the longitudinal and lateral safety of the vehicle.

The technical, yet generic design of the FCW-AEB system that concerning a tram, involves a threefold warning cascade, Figure III.7. Upon detection of an relevant situation, an acoustic signal alerts the driver, followed by initiating a partial braking and finally establishing the emergency braking.



**Figure III.7** Automatic emergency braking protocol for trams

The threefold warning cascade meets the EU regulations if the acoustic warning and the partial braking start at least 1.4 s and 0.8 s, respectively, before the emergency braking phase (Euro NCAP, 2021).

In soft braking the AEB will apply a light braking in order to make it more aware of the possible danger, with a deceleration request up to  $-4 \text{ m/s}^2$ . In hard autonomous braking an emergency brake is activated up to  $-10 \text{ m/s}^2$ . Taking the control of the driving actuators of the vehicle, AEB applies an emergency braking at maximum force to avoid, or at least mitigate the effects of, the imminent collision, reducing the impact speed and aiming to minimize passenger's wounds. These braking deceleration values for the AEB system are not comparable with those relating to the tram; in fact, according to the standards, the value of average service deceleration and maximum average deceleration in emergency braking (considering magnetic track brake) is respectively  $1.2 \text{ m/s}^2$  and  $2.5 \text{ m/s}^2$  (ANSF, 2019), (Directive 98/34/CE, 2015). This difference is due to the adhesion coefficient which for the rail is much lower and consequently the stopping distance is very increased compared to other road vehicles. This shows how the automotive ADAS cannot be applied to the tram unless a functional reparameterization, takes into account the different driving dynamics.

The Figure III 8 illustrates a longitudinal dynamic control, that include warning system consisting of an RCW and an FCW-AEB.

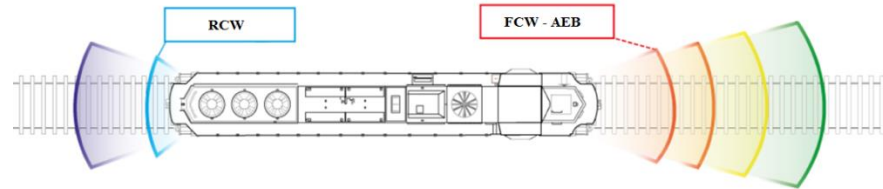


**Figure III.8** *Longitudinal dynamic control for tram*

The coloured bands from green to red indicate the different safety bands that can be defined in terms of distance from a detected obstacle. The distance between the various safety bands is among the objectives of this thesis work and will be addressed in the next chapters.

### III.3 Grades of Automation improved for trams using T-ADAS

The trams operate in a mixed traffic environment that requires a high level of situation awareness, with consistently high perceptual demands for collision avoidance. Due to the nature of the tram driving task and its relationship with the road environment, our analysis on the increase of the GoAs for the trams, taking into account the ADAS technologies and functionalities is within the limits of GoA 2. Some literature works such as (Enjalbert, 2019) (Delfa, 2016) propose eco-driving systems for the improvement of speed profiles by working on the ATP system, but still classified as GoA 1. We defined other GoAs based on the GoA 2 which take into account the various functions allowed.

#### III.3.1 Model's structure

The GoAs for conventional trams can be limitedly defined from the allocation of the following tasks: acceleration, costing, deceleration, and various types of braking between the driver and the automated system. In fact, the tram cannot acquire information from the surrounding environment and the road infrastructure, except through the driver. However, the implementation of some functionalities through the T-ADAS systems allow an increase of the GoA levels for the tram. Given the importance of the safety aspect of the tram system, which is the focus of this work, we considered the dead man's switch device to highlight that the safety of the Human-Machine System must be maintained when the dead man's switch is disabled at a high GoA (GoA-2.3). The dead man's switch or driver's safety device is commonly used in the railway domain to permanently monitor the tram driver's vigilance. The defined taxonomy of GoAs for trams is presented in Table III.3. The defined GoAs determine the functions between the driver and the T-ADAS performed by the ATP during the driving task.

**Table III.3** *GoAs improvement for trams*

<b>Dead man's switch</b>	On	On	On	On	On	Off
<b>Overspeed control</b>	Driver	T-ADAS	T-ADAS	T-ADAS	T-ADAS	T-ADAS
<b>Door side control</b>	Driver	Driver	Driver	T-ADAS	T-ADAS	T-ADAS
<b>Smart Vigilance</b>	Driver	Driver	Driver	Driver	Driver	T-ADAS
<b>ACC</b>	Driver	Driver	Driver	Driver	T-ADAS	T-ADAS
<b>FCW/AEB</b>	Driver	Driver	T-ADAS	T-ADAS	T-ADAS	T-ADAS
<b>TSR</b>	Driver	T-ADAS	T-ADAS	T-ADAS	T-ADAS	T-ADAS
<b>Manipulator</b>	Driver	Driver	Driver	Driver	Driver / T-ADAS	Driver / T-ADAS
<b>Type of train operation</b>	Driver without ADAS and ATP	Driver with ADAS and ATP	Driver with ADAS, ATP and ATO			
<b>Grade of Automation (GoA)</b>	GoA 0	GoA 1	GoA 2	GoA 2.1	GoA 2.2	GoA 2.3

The defined GoAs determine the rules for the performance of the driving task which are interposed between the driver and an automated system applied to the manipulator. We note that at each GoA, the driver controls the tram manipulator, and the action is prevalent on the automated system.

The GoA 0 is equivalent to the GoA 0 of the rail stock taxonomy, where the driver is the only responsible for driving the tram. The GoA 1 is equivalent to the GoA 1 of the rail stock taxonomy, where the driver controls the acceleration/deceleration task with an automated system that grants the respect of the speed limits and the recognition of road signs to show them in the Train Operator Display (TOD).

The GoA 2, GoA 2.1, GoA 2.2, GoA 2.3 are equivalent to the GoA 2 of the rail-stock taxonomy. However, from GoA 0 to GoA 2.1, the driver is responsible for all driving phases except for the intervention, where provided,

of the AEB. Furthermore, at each GoA the dead man’s switch remains activated except for GoA 2.3. In the latter case, in fact, the tram could drive autonomously: it manages to maintain a safe distance from the vehicles in front, brake in an emergency, recognize road signs, etc., and therefore the driver's attention is not required.

In order to perform all the above-mentioned driving tasks of the tram it is necessary to choose the sensors and set appropriately the ADAS functions.

### III.4 ADAS sensors for the tram

Environment perception is fundamental to enable autonomous tram, providing to the vehicle crucial information on the driving environment, especially in free areas and surrounding obstacles’ locations, velocities, and even predictions of their future states. Based on the sensors to be implemented, the environment perception task can be tackled by using of automotive sensors: LiDARs, cameras, short/long-range RADARs and ultrasonic sensors or a fusion between these four kinds of devices. Although porting can be done with the same sensor technologies, an adjustment of the algorithms that manage the ADAS functions starting from the data provided by the sensors must occur. In this way a Common Perception Platform (Vu, 2014) is designed and done, allowing an easy and flexible adaptation for the different sets of sensors that from the car can be installed on the tram.

Table III.4 shows the porting of technologies and sensors capable of fulfilling it, so that the level of automation and driving assistance rises to GoA 2.3 degree. The tram by its conception does not have the possibility to take information from the railway infrastructure, it must be considered for this purpose similar to a car.

**Table III.4** *Porting of sensors on tram to achieve the GoA 2.3 level*

T-ADAS	Sensor for GoA 2.3				
	Lidar	Radar	IR	Camera	Ultrasound
ACC		X			
FCW		X			
AEB	X	X	X	X	
TSR	X			X	
BLIS		X	X		X
ALC			X		
RCW		X			
DMS				X	

■ Good      ■ Fair

It is worth to note that none of these sensors can cover all types of T-ADAS; therefore, it is necessary to operate a sensor fusion to provide redundancy to the autonomous functions (Ziebinski, 2016). Figure III.9 proposes the technology spread and the determination of the sensor setup. Different sensors have different observation capabilities and various detection properties.

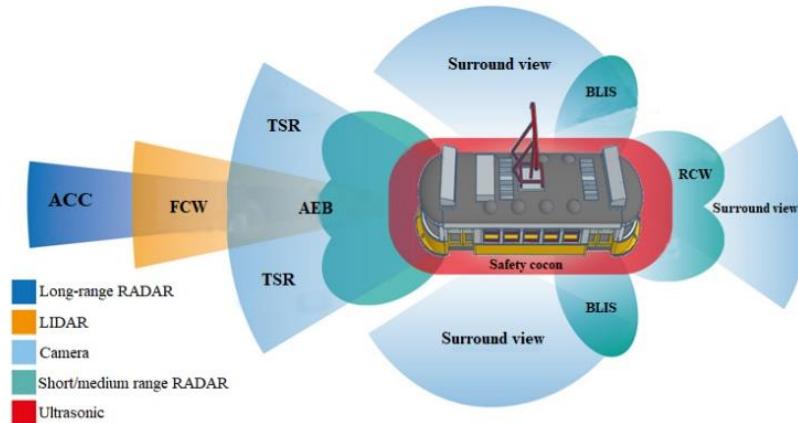


**Figure III.9** ADAS spread to tram: T-ADAS

This technology could integrate many railway operations, different potential applications arise for different degrees of automation. It should be noted, however, that the tram does not reverse the direction of travel, but once it reaches the end of the line, the driver passes to the other head cabin. Therefore, the sensor system presented must be installed on the two driving cabs and can be used alternatively to control the front or rear of the tram.

Taking into account the increasing availability of the ADAS technologies in the automotive sector, the proposed approach can be effectively adopted by public transport companies to upgrade their tram systems. Since the goal of the automotive industry is to develop connected self-driving cars capable of handling even critical urban traffic situations, the logical development will be to integrate the trams into that ecosystem, too.

#### ***III.4.1 The remote sensing requirements for the tram***

As of today, a single sensor does not have the capability to simultaneously provide reliable, precise detection, classification, measurement, and robustness to adverse conditions. To ensure a comprehensive detectability, a multimodal approach is required to cover detectability of all relevant entities.

In the case of the tram where the maximum speed is set at 70 km/h (Hitachi, 2021), the camera is not excessively affected by the poor velocity resolution, however given the very often presence of underpasses and tunnels that the

trams travel through the problems related to the darkness/ambient light disturbance they can be more pronounced.

Another example related to the need to have a sensor fusion is shown in Figure III.10.

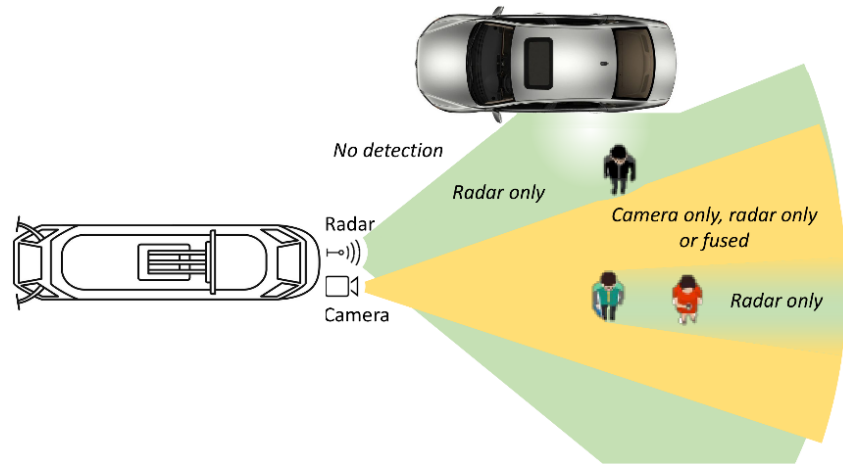


**Figure III.10** Layout of camera-radar sensor pair

One typical camera-RADAR sensor pair layout designed for environmental perception in front of a vehicle is presented. Due to the various sensor FoV, different regions of the environment are covered by no one, one or both sensors. Moreover, it can be expected that the characteristics of sensor operation change locally depending on the scene layout. For the camera, every occluding object creates blind spots where misdetection is likely. On the example layout, the person in red cannot be detected by the camera because of occlusion.

However, this occluded region in the camera, although attenuated, is still visible by radar. Additional problems for radar detection come from the effect of multipath propagation caused by reflections from flat surfaces (walls, particular positions of vehicle sides, etc.). On the diagram on Figure III.10 this is visualized as a hole in the radar frustum near the flat surface of a truck. In such areas, the RADAR signal fades significantly, and detection rates reduce accordingly.

Therefore, fusion of different sensors will lead to an overall excellent result for a large range of all environment conditions.

The FoV of the various sensors are of great importance, it shows how the collision estimation algorithms can measure on the basis of the point dynamics, the trajectories of the host vehicle with respect to the remote object to understand if a collision will occur. In the Figure III.11 and Figure III.12 we have simulated a driving scenario to show the substantial differences between a car that houses these systems and the tram that should house them.

We used the most common parameters of conventional ADAS sensors also reported in (Baek, 2020) by considering one Long Range Radar (LRR), one LIDAR and one camera.

In the first case we are considering a car traveling at 13 m/s (50 km/h) in a straight direction and equipped with ADAS. From another direction comes a generic vehicle at a speed of 10 m/s. The scenario is dangerous, and the two vehicles could be on a collision course or touch each other.

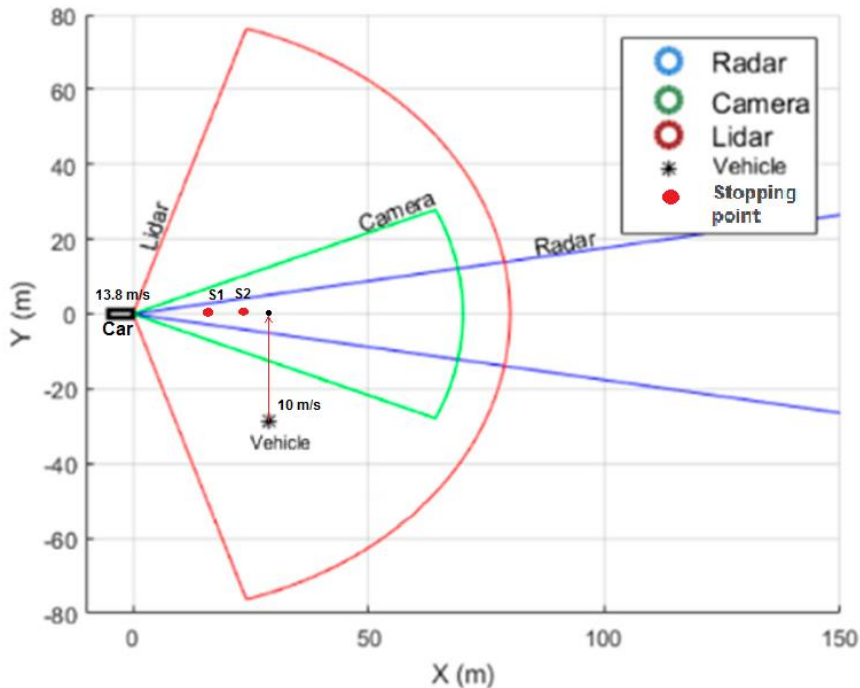


**Figure III.11** Car-vehicle dangerous simulation scenario

In accordance with the laws of motion, with (Chae, 2017), and with the standard (EN 13452-1, 2003), assuming a light emergency braking as dictated by (Euro NCAP, 2021), for the AEB system the car in fig will stop after 24.1 m, in S2 on the figure. In the case of critical emergency braking, instead, it will stop after 19.2 m, i.e. in S1.

In the case of the tram, by imposing a braking in accordance with the regulations, the tram for the first level emergency railroad will take 80 m to stop, in S4 on the figure. With an emergency braking at maximum level, it will take 40 m to stop, i.e. in S3. For the stopping point is far from the point where the generic vehicle crosses the trajectory, the FCW-AEB system was able to avoid the accident and/or mitigate the dangerous situation.

Vice versa for the tram in both cases we are beyond the crossing point of the trajectory, also considering its length (on average about 20 m) the probability of impact in these cases are very high.

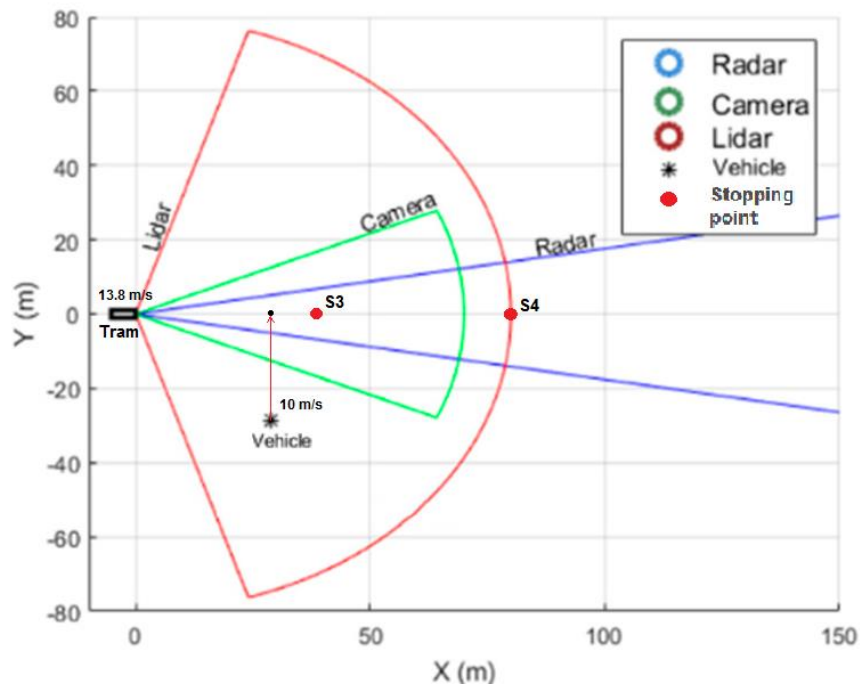


**Figure III.12** Tram-vehicle dangerous simulation scenario

Ultimately, the detection of obstacles in the case of the tram must come in advance, risking that these come out of the range of some sensors such as the camera or SRR. Furthermore, the FOVs for the tram must be wider in order for potential obstacles to be intercepted laterally in advance.

In Figure III.13 we have summarized the sensors performances that can be installed on the tram. The table is populated with coloured arrows indicating relative performance.

The various sensors have different sensitivities towards different environment conditions. By using a combination of sensors that work together, the limitations of any given sensor are potentially supplemented by the strengths of another, thereby allowing enhanced functionality even in conditions that may be challenging for any given sensor.



Figure III.13 T-ADAS sensors performances

### III.5 T-ADAS: between future and revamping

In recent years, the tendency to restore old trams has grown enormously. The companies that manage mobility in large cities and that enjoy a fleet of historic and disused trams have sensed the potential expressed by the recovery operations in terms of aesthetic impact and incentives for public mobility. A restored historic tram is very fascinating and can offer new sensations in everyday mobility. However, more than a restoration in most cases it is, in jargon, a revamping: engines, interiors, new regulatory adjustments, and diagnostic and infotainment systems are installed. In Table III.5 we report among the main companies that have operated on the revamping of historic trams.

Table III.5 Main revamping trams

COMPANY	TRAM MODEL	REVAMPING TRAM UNIT	CONSTRUCTION YEARS	CITY
ANM	CTK Series	15	1938	Neaples
ATM	1500 Series	125	1927-1930	Milan
	4700 Series	51	1955-1960	
	4900 Series	20	1976-1978	
CARRIS	Remodelados	45	1936-1947	Lisbon
	500 Series	8		
	Ligeiros 700 Series			

These vehicles are a strong tourist attraction and are often preferred to the more modern ones, making them particularly crowded. This suggests the importance of being able to equip these vehicles with driver assistance technologies. The T-ADAS systems conceived with the technologies just introduced could interface with the revamped or new on-board systems of the trams that are based on Ethernet bus and provide information to the TCMS and to both vital and non-vital systems on board, contributing significantly to the further safety increase of the tram system.

# **Chapter IV**

## **Distance to Collision Estimation (DCE) model for T-ADAS**

The previous chapter has outlined the context and the scope of this thesis, which is further explored below.

The goal of this chapter is to describe a model to estimate the stopping distance for the tram in order to define quantitative requirements for design and validation of FCW-AEB system, taking into account the dynamics of the tram. The need for such a model is evident: although the solutions for assisted or automatic braking in the automotive sector are well established, the braking dynamic of trams is profoundly different from that of the cars.

The proposed Distance to Collision Estimation (DCE) algorithm will utilize the tram speed, tram weight, weather condition, slope of the tramway, bend radius, and etc. to figure out the safety braking distance.

### **IV.1 Forward vehicle collision warning systems**

Forward Collision Warning systems target a major accident type, the rear-end collisions, warning the driver of an imminent collision, such that he can take appropriate corrective actions in order to mitigate or to completely avoid the collision. The first modern forward collision avoidance system was patented in 1990 by William L Kelley. Since its introduction, several FCW systems have been developed with warning algorithms generally time-based (Ćosić, 2019), but also distance-based (Liu, 2016), deceleration-based (HIRAOKA, 2009) and probability-based. These algorithms are briefly summarized below in accordance of Standard ISO 15623.

### Vehicle stopping distance

Collision warning algorithms generally issue an alert when the distance to an object (the headway)  $x_{head}$  is less than a critical warning distance  $s_{cwd}$ , so that the driver can stop or approach a maximum of a designated distance  $s_{dd}$ .

Taking into account two vehicles: a host vehicle and a target one, each with state:

$$x_i = [x_i \ v_i \ a_i]^T$$

where  $x_i$  is the position,  $v_i$  the velocity and  $a_i$  the acceleration. With a vehicle length  $L_i$ , it is possible to define the headway as:

$$x_{head,i} = x_{t,i} - x_{host,i} - L_i$$

and its velocity as:

$$v_{head,i} = v_{t,i} - v_{host,i}$$

Assuming constant values for the host vehicle maximum braking capability  $a_{host,max}$ , and for the accelerations  $a_t$  and  $a_{host}$ , for the acceleration discontinuity that occurs at standstill, three possible scenarios should be distinguished:

- an initially moving target vehicle stops prior to the host vehicle;
- the target is still in motion when a potential collision would occur;
- the target is initially stopped.

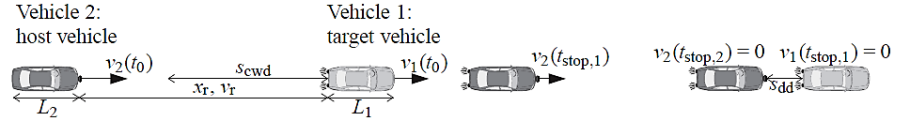


**Figure IV.1** Schematic of the forward collision process

To determine which case applies, the target vehicle stopping time  $t_{t,stop}$  and host vehicle stopping time  $t_{host,stop}$  are calculated:

$$t_{t,stop} = -\frac{v_t}{a_t} \quad (IV.1)$$

$$t_{host,stop} = t_{man} - \frac{v_{host} + a_{host}t_{man}}{a_{host,max}} \quad (IV.2)$$

where  $t_{man}$  is the driver reaction time.

For each of these cases the critical warning distance  $s_{cwd}$  can be calculated:

$$s_{cwd} = \begin{cases} v_{host}t_{man} + \frac{1}{2} a_{host}t_{man}^2 - \frac{(v_{host} + a_{host}t_{man})^2}{2 a_{host,max}} + \frac{v_t^2}{2 a_t} + s_{dd} \\ \quad \text{if } t_{t,stop} \leq t_{host,stop} \text{ and } t_{t,stop} \neq 0 \\ -v_{head}t_{man} - \frac{1}{2} a_{head}t_{man}^2 + \frac{(v_{head} + a_{head}t_{man})^2}{2(a_t - a_{host,max})} + s_{dd} \\ \quad \text{if } t_{t,stop} > t_{host,stop} \text{ or } t_{t,stop} = 0 \end{cases} \quad (IV.3)$$

with  $a_{head} = a_t - a_{host}$  the relative acceleration.

Unfortunately, this type of algorithm will also warn drivers when they intend to perform a late lane-change maneuver, since the algorithm only considers longitudinal vehicle motion.

### **Required deceleration**

A collision with a safety margin  $s_{dd}$  can be avoided considering a required deceleration  $a_{dec}$  given by:

$$a_{dec} = \begin{cases} \frac{a_t v_{host}^2}{2 a_t (t_{man} v_{host} - x_{head} + s_{dd}) + v_t^2} \\ \quad \text{if } t_{t,stop} \leq t_{host,stop} \text{ and } t_{t,stop} \neq 0 \\ \frac{a_t (x_{head} - s_{dd}) - \frac{1}{2} v_{head}^2}{t_{man} \left( \frac{1}{2} t_{man} a_t + v_{head} \right) + x_{head} - s_{dd}} \\ \quad \text{if } t_{t,stop} > t_{host,stop} \text{ or } t_{t,stop} = 0 \end{cases} \quad (IV.4)$$

### **Time-To-Collision**

An interesting algorithm can be obtained using the time-to-collision  $t_{collision}$  that refers to the time it takes for a collision starting. Considering a constant velocity, the  $t_{TTC}$  is given by:

$$t_{TTC} = -\frac{x_{head}}{v_{head}} \quad (IV.5)$$

The previous formula can be modified considering the acceleration of both vehicles:

$$t_{TTC} = \frac{-v_{head}(t) \pm \sqrt{v(t)_{head}^2 - 2x_{head}(t)a_{head}(t)}}{a_{head}(t)}, \quad (IV.6)$$

but this method introduces a lot of uncertainty due to the unexpected changing of the target vehicle acceleration.

When the  $t_{TTC}$  is less than the driver's time to reaction  $t_{man}$ , a warning is issued and, at the same time, the system may activate automatic emergency braking. So, the critical braking distance  $s_{cbd}$  is:

$$s_{cbd} = v_{head}t_{man} + \frac{1}{2} a_{host}t_{man}^2 \quad (IV.7)$$

### **Probabilistic approach**

The deterministic nature of the above algorithms based on a fixed structure highlights a disagreement between the human drivers and the system response. Deterministic algorithms may therefore be too conservative in some, or not responsive enough in other scenarios. Instead, a probabilistic approach can be used, where sensor data is provided to a Kalman filter (Sharma, 2014). This allows to estimate the probability for a preventive maneuver and issue a warning at a certain collision probability.

Alternatively, the collision probability can be estimated by an on-line Monte Carlo simulation of possible scenarios (Khan, 2011).

## **IV.2 Railway braking models**

The braking curves are derived starting from a braking model, that calculates train deceleration considering some parameters (time, braking weight percentage, speed, etc.). The deceleration used for the definition of the braking curves must be 'safe', in other terms it must assure that the actual braking performance of the train will be sufficient to guarantee the respect of the objective speed. The main literature railway braking models are discussed below.

### **Pedeluq braking model**

Among the models present in the literature, the Pedeluq formula is certainly the most used to calculate the stopping distance of a railway vehicle. As in (Augusto, 2003), (Vicuna, 1986) or (Stagni, 1980), the stopping distance calculated with the Pedeluq formula is:

$$S_c = \frac{v_0^2}{\frac{1.09375\lambda_c}{\varphi(v_0)} + \frac{0.127}{\varphi(v_0)} \pm 0.235i_{\%00}} \quad (IV.7)$$

where  $i_{\%00}$  is the slope in permilles,  $\lambda_c$  is the conventional braking mass percentage, the coefficient  $\varphi(v_0)$  depends on the initial braking speed only.

Furthermore, the model already considers the mechanical intervention time of the brake, therefore it does not take into account the reaction time of the driver and the braking system. The value of the coefficient  $\varphi(v_0)$  is expressed in Table IV.1.

**Table IV.1** Coefficient  $\varphi(v_0)$  as a function of speed for Pedelucq formula

$v_0$ (km/h)	70	80	90	100	110	120	130	140	150	160	170	180	190	200
$\varphi$	0.0611	0.0676	0.0681	0.0686	0.0691	0.0696	0.0714	0.0731	0.0742	0.0755	0.0763	0.0771	0.0779	0.0787

In the case of the tram, we consider the value of the coefficient  $\varphi$  interpolated for lower speed values suitable. Given a set of velocity values we have the following graph.

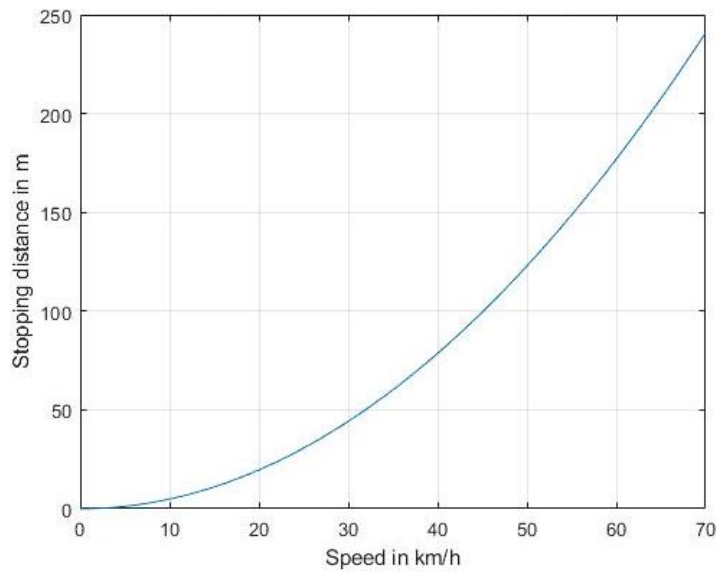


**Figure IV.2** Stopping distance for Pedelucq formula

**The RFI braking model**

The Rete Ferroviaria Italiana (RFI) braking model was created for the ATP systems of the System of Train Running Control (SCMT) type. Like any ATP system consists of two distinct subsystems:

- the SST (Sub Ground System);
- the SSB (Sub System of Board)

which cooperate to ensure the control of the gear. In particular, the SSB of an SCMT processes the braking curve up to the next target speed and check that the train always remains within this curve.

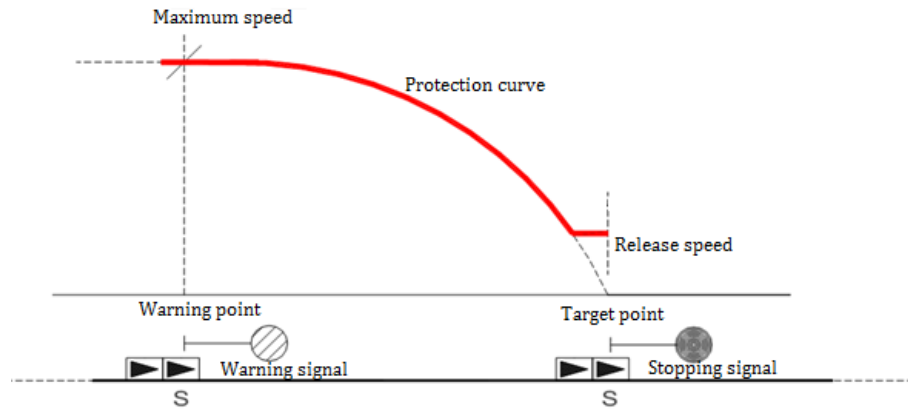


**Figure IV.3 SCMT protection curve**

The SCMT is the national ATP system developed in Italy for non-high-speed networks, but which lends itself to being easily transformed into a Level 1 of the European Train Control System (ETCS).

This model does not contemplate the information transmission times, that is the time required for the different ground technologies used in the SCMT to transmit the appearance of the line signal to the cabin, but it limits itself to considering the information processing times; in other words, the times necessary for the SSB to pick up the signal coming from the buoy, process it and translate it into the appropriate commands (e.g. traction release and/or brake actuation).

The analytical model is based on the integration of the fundamental kinematic quantities (acceleration, speed, and space) which vary at each instant of the braking phase.

The braking distance  $S_c$  is obtained as the sum of the covered space for each step of the integration, considering the speed and acceleration variations. For the generic instant  $t$ , the braking distance is calculated considering the constant speed during the initial waster time and assuming the uniformly decelerated motion in the braking phase:

$$S_c = (h + t_f)V_i + \frac{(V_i - V_0)^2}{2(d_p + d_i)} \quad (IV.8)$$

For each instant  $t$  of the braking phase, the mathematical model provides the speed values implemented from the vehicle and the space traveled. The model input variables are:

- $V_i$ , initial speed;
- $V_0$ , target speed;
- $h$ , SSB delay time;
- $t_f$ , driver reaction time;
- $d_p$  deceleration due to the action of the brakes;
- $d_i$  acceleration or deceleration due to the slope.

The value of the slope of the track is provided to the SSB by the fixed buoys of the land subsystem. The braking model for SCMT provides the stopping distance assuming a single slope value for the whole section of the line between the head of the vehicle and the target point. The acceleration or deceleration  $d_i$  due to the slope of the track is obtained from the slope  $i$  of the line as:

$$d_i = K_i \cdot g \cdot i \quad (IV.9)$$

where:

- $g$  is the acceleration of gravity [ $m/s^2$ ];
- $i$  is the slope of the path expressed as a pure number [-];
- $K_i$  is a coefficient that depends on the inertia force and is a function of the slope of the path [-].

The value of deceleration  $d_p$  due to the action of the brakes, which is considered constant by the model in the braking phase at full speed, is a correct value of the nominal deceleration through a series of protection coefficients:

$$d_p = K_r \cdot K_v \cdot K_L \cdot K_{v0} \cdot d_r \quad (IV.10)$$

where:

- $K_r$  takes into account the dispersion of the braking performance around the average value;
- $K_v$  used for high speeds;
- $K_L$  takes into account the different levels of protection to be offered as the speed varies and the integration with the legislation;
- $K_{v0}$  depends on the target velocity and the initial speed;
- $d_r$  is the nominal deceleration and is a function of the percentage of braked weight.

These parameters are not easy to determine and depend on many other factors. In particular, the nominal deceleration is obtained as specified in the Fiche UIC 544-1.

**Semi-empirical braking model**

Another model for calculating the stopping distance, reported in (Perticaroli, 2001) and here called the semiempirical model, takes into account only the adhesion coefficient  $f_a$  and acceleration of gravity  $g$ :

$$S_c = (h + t_f)V_i + \frac{(V_i - V_0)^2}{2f_a g} \quad (\text{IV.11})$$

The input variables of the model are:

- $V_i$ , initial speed;
- $V_0$ , target speed;
- $h$ , brake system delay time;
- $t_f$ , driver reaction time;
- $g$ , gravity acceleration

Many studies have been conducted on measurements and determinations of the adhesion coefficient within railway systems in different conditions. In particular, as can be easily understood, the value of the adhesion coefficient strongly depends on the vehicle speed as well as on the conditions of the contact area between wheels and rails, e.g. if the surfaces are wet (due to rain, snow, etc.) or dry. For example, Curtius and Kniffler (1943) defined a model that is still among the most used today and which expresses the adhesion coefficient as a function of speed, for dry and wet rails:

$$f_a = \frac{7.5}{v + 44} + 0.161 \quad (\text{IV.12})$$

or, Muller's experimental equation:

$$f_a = \frac{f_a^*}{1 + 0.01v} \quad (\text{IV.13})$$

where  $f_a^*$  is adhesion coefficient when  $v = 0$  (with  $v$  in km/h) and assumes different values in the case of dry rail ( $f_a^* = 0.33$ ) or wet rail ( $f_a^* = 0.25$ ).

The coefficient of adhesion considered is calculated according to the Muller experimental expression. Figure IV.4 shows the trend of the adhesion coefficient as a function of speed.

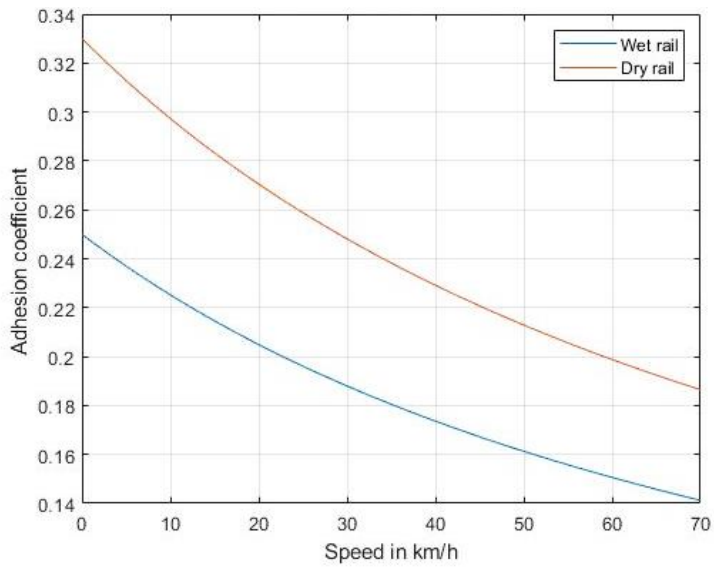


**Figure IV.4** Coefficient of adhesion as a function of speed

We also calculate for this model the different values of  $S_c$  in the plain, distinguishing the case of dry and wet rail.

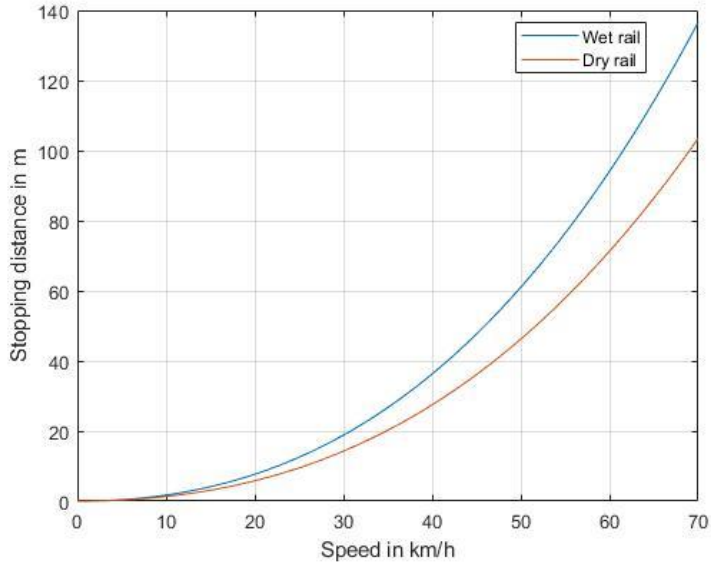


**Figure IV.5** Stopping distance for Semi-empirical braking model for wet and dry rail

### ***IV.2.1 Requirements for trams and light rail vehicles***

At this time, no European rules/regulations exist giving requirements and performances for braking of guided vehicles for urban transport systems (EN 13452-1, 2003). There are some national rules which cover certain types of rolling stock. Regarding the Europe-wide competition required now, this European Standard allows all prospective bidders to propose or offer rolling stock meeting specified minimum requirements for braking performances.

This European Standard (EN 13452-1) specifies the minimum and maximum limiting requirements and performances for braking systems and performance of vehicles for urban transport systems, running on steel or rubber-tyred wheels and guided by steel rails or other equivalent means. The Transport Authority defines the particular parameters, where required in this European Standard, and specifies any additional braking requirements to the vehicle builder/braking system supplier.

The brake system must meet some fundamental requirements:

- Vehicles can be stopped without risk to passengers and third parties;
- Excessive or unrealistic levels of adhesion are not demanded;
- The brake system's rating is consistent with the prevailing gradients and specific operating conditions.

In order to meet these specifications different types of braking can be defined:

- ***Service braking*** occurs by the driver or by means of automatic speed and braking adjustment to reach the desired speed or until the train comes to a complete stop without any danger to passengers. It is a type of braking used with high frequency and for this reason, it is necessary to minimize the environmental effects (e.g. noise, dust generation).
- The various ***emergency braking*** modes are defined about initiation as follows:
  - ***Emergency 1*** is available on vehicles for passenger transport with driver, equipped with surveillance devices which, if the driver fails, applies automatic braking until the vehicle stops. The main aim of this braking system is to maximize the safety of passengers, staff and non-user of the railway.
  - ***Emergency 2*** can be activated by passengers using of special devices and which determines a direct or indirect stop of the train.
  - ***Emergency 3*** is activated when a hazard is detected by the driver. This type of braking involves high decelerations and jolts. Any resulting risk to passengers is accepted in

consideration of the overall danger. The vehicle does not necessarily have to be braked to a complete stop, as if the hazard disappears during braking, the braking process can be interrupted without the vehicle coming to a stop.

- **Emergency 4** refers to driverless UTO and is activated by authorized personnel using a control device, regardless of the start/brake switch.

**Table IV.2** *Types of emergency braking*

<b>EMERGENCY BRAKING TYPE</b>	<b>PRINCIPAL MEANS OF INITIATION</b>
<i>Emergency 1</i>	Driver vigilance, or ATO
<i>Emergency 2</i>	Passenger alarm
<i>Emergency 3</i>	Driver, via dedicated position on brake controller, or ATP system
<i>Emergency 4</i>	Authorised person via control separate from brake controller

We can observe that in the specific case of the tram, the operating, and emergency braking with the aid of a magnetic track brake (Emergency 3) must be considered. In fact, due to the absence of a surveillance device or ATO, absence of the passenger brake lever and driverless capacity it is not possible to consider supervisory braking, (Emergency 1), passenger emergency braking (Emergency 2), emergency braking in the event of automatic driving (Emergency 4).

It should be noted that onboard trams and light rail, the emergency lever, located near the emergency intercom, commands the opening of the doors in the event of an emergency. If the speed is zero the door opens, instead if the tram is moving the door loosens and the driver is warned by a signal in the TOD, once the tram is stopped the doors will open completely and autonomously.

- **Security braking** has a higher level of functionality (availability) than service braking, passenger-emergency braking, and emergency braking. The braking capacity may be lower than in service braking or passenger-emergency braking.
- **Holding brake**  is braking to prevent the movement of the stationary vehicle
- **Parking brake**  is used while the train is stabled. It shall be capable of holding a defined load, on a defined gradient for an indefinite period of time. The parking brake effort shall not degrade, with time, below that required to meet the specified performance.

The following performances are defined as minimum requirements. Different criteria may be defined by the Transport Authority to satisfy particular requirements.

The maximum stopping distances under normal conditions, i.e., all brakes available, shall be those calculated with the following criteria.

**Table IV.3** *Theoretical operational performances*

Parameter	Service	Em. 1	Em. 2	Em. 3	Em. 4	Security
<b>Minimum deceleration <math>a_e</math></b>	0 ÷ 1.2	1.2	1.2	2.8	2.8	1
<b>Maximum equivalent response time <math>t_e</math></b>	1.5	1.5	1.5	0.85	0.87	2

Using these values, for any initial speed the nominal stopping distance can be predicted as defined below:

$$S_f = v_0 t_e + \frac{v_0^2}{2a_e} \quad (IV.14)$$

where  $S_f$  is the stopping distance in  $m$ ,  $a_e$  is the nominal allowable deceleration in  $m/s^2$  (values in Table IV.3),  $v_0$  initial speed in  $m/s$ ,  $t_e$  equivalent response time in  $s$ . Both the values of  $a_e$  and  $t_e$  are from the table Table IV.3.

Similarly, reasoning in terms of acceleration:

$$a_e = \frac{v_0^2}{2(S_f - v_0 t_e)} \quad (IV.15)$$

The braking characteristic in Figure IV.6 shows the application of theoretical operating braking with an applied average deceleration of  $1.2 m/s^2$  over the entire stopping distance. The response time corresponds to the addition of the delay time and the build-up time for the braking action, hence the deceleration, to reach 90%.

The reaction time is the elapsed time from the moment the driver decides to brake to the moment in which the vehicle actually start braking; this dead time is a potentially reducible element with the application of ADAS systems (Kim, 2021). The reaction time multiplied by the speed establishes the distance traveled while there is the intention of braking, without vehicle deceleration.

Figure IV.6 also shows the jerk value with its typical step trend concerning deceleration.

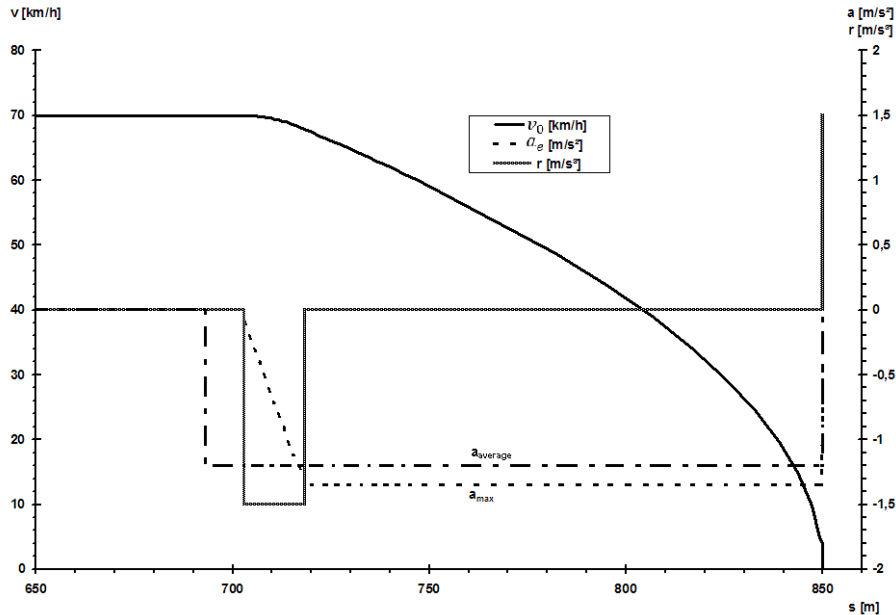


**Figure IV.6** *Braking process detail*

### IV.3 Proposed braking model

As previously introduced, assisted braking is provided with the principal objective of maximizing the safety of passengers, staff, and non-users of the railway; moreover, we have shown the models that regulate the FCW and railway braking systems respectively. However, the actual braking performance of a tram is different from the nominal one due to several physical parameters. In this paragraph, a new model for Distance to Collision Estimation for trams is proposed and described for FCW-AEB system implementation which will be calibrated on this distance.

Unlike the approaches followed in the literature, which consider a small number of variables to adapt to most railway applications, the proposed model calculates the distance to collision considering the input parameters of the tram and of the tramway, like the distance between the tram ahead and the obstacle, tram weight, tram speed, tramway slope, condition of tramway surface, tramway bend radius, etc. The proposed algorithm compares the distance of obstacle and safety braking distance to determine if moving tram's safety conditions are enough or not. The reaction time of the driver and pressure build-up time of the braking system are all considered. These input parameters allow a more accurate stopping distance estimation.

### ***IV.3.1 Proposed methodology***

As mentioned before, an accurate estimation of the stopping distance is important to plan the overall braking action in case of danger starting from warning the driver to the stop of the tram.

In the preceding paragraph, we have shown some of the models on which FCW systems are based and how stopping distances are calculated for wheeled and rail vehicles. The basis of the proposed procedure starts from the general model of motion and, taking into account the characteristics of the tram and of the tramway, it is able to achieve better tracking accuracy than the legislation model introducing only a moderate increase of calculus complexity.

The model output will allow the calibration of the T-ADAS system with the various warning levels. We remind that the tram has no driving support and in road emergency situations, safety depends upon the visual interpretation of the dynamics of the onward obstacle from the tram driver.

The average reaction time for a driver is 1.5 sec, that includes the time for the driver to evaluate the situation and apply brakes. If a certain situation arises where the control of the driver decreases due to certain distractions, the driver may not be aware of the obstacles in front. Hence to prevent, the vehicle from collisions, it issues a warning of the obstacle. If the danger is still not dealt with, then the T-ADAS performs an action in place of the manipulator to avoid the collision.

The input parameters to the model differ in several categories. We have the intrinsic fixed ones of the tram and tramway such as the total mass, the weight per axle, the coefficient of adhesion, and those that, despite being fixed values, vary according to the position. In fact, knowing a priori the characteristics of the line, it is possible to link the GPS position of the tram to the model, updating dynamically the resistance to the motion with additional ones due to the curves and slope variations. Moreover, for the coefficient of adhesion, it is possible to consider rain information provided by the Sensor Fusion System (SFS), as previously described in Chapter II.

A two-dimensional plane of the circular sector (FOV of sensors) where all potential obstacles have a  $x$ - $y$  coordinate with respect to the tram is considered: each circular sector is divided into safety bands starting from the distance to the collision calculated by the model. For each band, the T-ADAS can act if the driver does not react or reacts badly (costing, a percentage braking, emergency braking), according to the most conservative logic in terms of safety.

The T-ADAS sensors are fixed in the front of the tram (in the bumper, behind the windshield, and on the roof); these installation points offer greater reliability in the coverage area than cars. The boundaries of safety bands (or warning as we will call them later) zones vary according to the speed of the tram. In the event that an obstacle or the crossing point of the trajectories is

detected by the sensors entering into this zone, a warning is issued in a dashboard gauge, as the target vehicle approaches the host vehicle a graduated light display indicates the proximity of the target vehicle.

This enables safe driving and mitigates any distractions by drivers it can also be of support to beginner drivers.

### ***IV.3.2 Model's structure***

The first phase of the DCE model's building process, as described in the flow chart of Figure IV.7, is the acquisition of the estimated collision point with the potential targets for the tram (pedestrians, cyclists, motorcyclists, cars, etc.) provided by SFS. Subsequently, this distance is compared with the distance to collision provided by the model, unless than a margin divided into four safety bands (Figure IV.7). Please note that the distance to the collision is intended as the maximum stopping distance in service conditions (maximum value of the service braking), without the aid of an emergency brake. This is mainly to prevent the system from assisting the driver in the region where there is only emergency braking, where a sharp deceleration would create a significant reduction in comfort and problems for passengers. When the distance of the obstacle from the tram becomes close to the distance to collision, T-ADAS will communicate the information to the vehicle logic that undertakes the foreseen emergency braking.

The warning distance is the sum of the stopping distance calculated by the model and the length of the safety bands.

For the purposes of the calculation, the model receives as input all the variables and parameters required, some of these are initialization (mass, slope, etc), others are acquired in real-time (position, speed, etc). Then the estimated collision point in the defined safety bands is evaluated to take the most conservative action. The simple action of the driver is not enough to get the system out of the cycle, his braking curve is compared in real-time with the theoretical one. If the discrepancy exceeds the guard level, the system will intervene again.

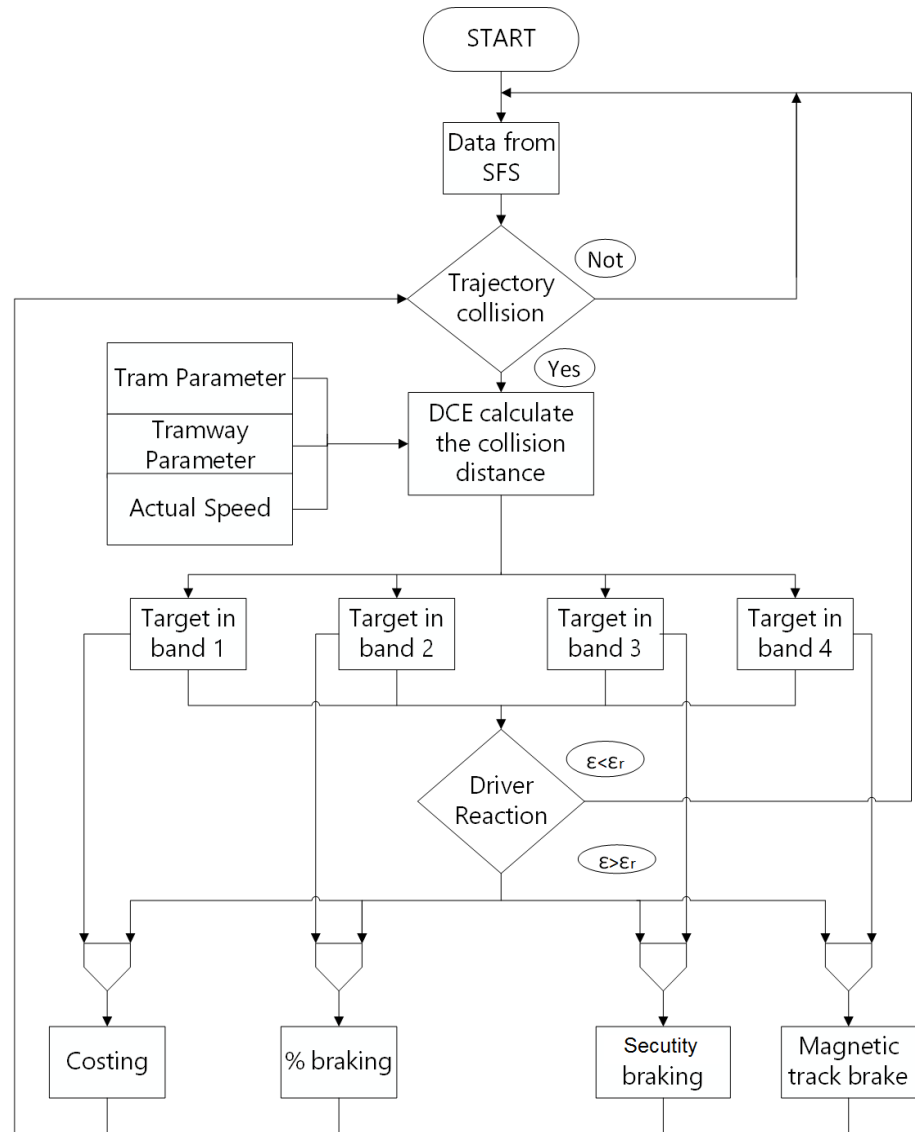


**Figure IV.7** Flowchart of the proposed model

### IV.3.3 DCE model formulation

The model has been developed starting from the general equation of motion in which both technical and physical parameters were considered. Once the contribution of every single parameter has been analyzed, the unimportant ones have been discarded.

Considering that during the braking the traction is disconnected, in the general motion equation a braking distance must be considered which is added to the total resistances:

$$-F_f - R = m_e \frac{dv}{dt} \quad (IV.16)$$

The equivalent mass  $m_e$ , higher than the simple (static) mass  $m$ , takes into account the rotating masses (wheels, motors, etc.) connected with the translational motion, phenomena that determine increases in energy effects in the various motion phases. It is given by the following expression:

$$m_e = m \cdot (1 + \beta) \quad (IV.17)$$

where the static mass is:

$$m = \frac{P}{g} \quad (IV.18)$$

that is the ratio between the total weight  $P$  and the gravity  $g$  acceleration, and where  $\beta$  is the inertia factor, which considers the variations in motion due to the rotating masses (Vicuna, 1986).

We specify a variation of the space  $ds$  corresponding to a variation of the speed during braking:

$$-F_f - R = m_e \frac{dv}{dt} \frac{ds}{dv} \quad (IV.19)$$

From which the variation of space results:

$$ds = -m_e \frac{v}{F_f + R} dv \quad (IV.20)$$

We obtain the general formula for the braking distance:

$$S_f = \int_0^{v_0} ds = -m_e \int_{v_0}^0 \frac{v}{F_f + R} dv = m_e \int_0^{v_0} \frac{v}{F_f + R} dv \quad (IV.21)$$

Explaining all the motion resistance  $R$  we will have:

$$S_f = (1 + \beta) \frac{P}{g} \int_0^{v_0} \frac{v}{F_f + R_p + R_c + R_{ae} + R_{rr} + R_{bp} + R_{wg}} dv \quad (IV.22)$$

where:

- $R_p$  is the ramp resistance
- $R_c$  is the cornering resistance
- $R_{ae}$  is the aerodynamic resistance
- $R_{rr}$  is the rolling resistance
- $R_{bp}$  is the bearing-pin torque (negligible)
- $R_{wg}$  is the wheel-ground resistance (negligible)

The coefficient of the rotating masses  $\beta$  can assume very variable values depending on the type of convoy. One of the empirical formulas that can be used is the following:

$$\beta = 0.04 + (0.7 \div 0.8) \frac{N}{M} m^2 \quad (\text{IV.23})$$

where  $N$  is the engine power in  $kW$  of the motor,  $M$  is the vehicle mass in  $t$ , and  $m$  is the transmission ratio.

In the railway sector, the slopes take on very small values, so the uphill resistance takes on values:

$$R_p = m \cdot g \cdot \tan(\alpha) = m \cdot g \cdot i \quad (\text{IV.24})$$

Below curve radii of 1000 meters or less, cornering resistance cannot be neglected. Since this is work dissipated by friction, it can be considered proportional to the weight of the convoy, therefore it can be expressed in terms of unit weight  $R_c$  [kW/kN], furthermore, the sliding will be greater as the track gauge and the rigid wheelbase of the vehicle increase and the radius of curvature decreases. Considering the difficulty of theoretical evaluation  $R_c$  reference is made to experimental formulas such as the one shown below (Von Rockl):

$$R_c = \frac{a}{\mathcal{R} - b} \quad (\text{IV.25})$$

where the values of the constants  $a$  and  $b$  are functions of track gauge and radius of curvature  $\mathcal{R}$  as shown in the Table IV.4.

**Table IV.4** Gauge values and radius of curvature

Gauge Railway (mm)	Radius of curvature (m)	$a$	$b$
1435	$\geq 850$	600	55
1435	250÷350	600	65
1435	150÷250	600	30
1000	$\geq 60$	500	30
900	$\geq 60$	380	17
750	$\geq 40$	350	10

The aerodynamic resistance  $R_{ae}$  is due to the friction caused by the vehicle sliding in the air (Vicuna, 1986). It is determined by a multitude of factors, such as the overpressure on the front surface of the vehicle, the lateral friction between the air currents and the convoy walls (vehicle extension, shape irregularities, running gear) and the rear depression due to vortices of the air. This resistance is expressed through the "Eiffel" relationship for aerodynamics and is traditionally applied for the evaluation of the forces due to the wind on

buildings. It can be used for vehicles moving at speeds slower than 100 km/h (Table IV.5) and in any case for low speeds, as it only takes into account the shape of the solid moving at speed  $v$  (or symmetrically hit by a current of air at speed  $v$ ) and the consequent trend of the pressures and depressions relating to the shape itself.

$$R_{ae} = kSv^2 \quad (IV.26)$$

**Table IV.5** Values of the coefficient  $k$  for surface vehicles

TYPE	SPEED	
	m/s	km/h
Very elongated rectangular plate	0.10	0.0077
Circular plate	0.07	0.0054
Sphere	0.018	0.0014
Cylindrical solid, transverse axis to motion	0.065	0.0050
Convex hemisphere	0.02	0.0015
Concave hemisphere	0.08	0.0062
Fusiform solid with great penetration	0.0035	0.00027
Steam locomotive (indicative value)	0.06	0.0046
Bad profiling motor vehicles, trucks	0.05	0.0039
Moder type ordinary cars, bus, self-propelled, max values	0.04	0.003
Moder type ordinary cars, bus, self-propelled, min values	0.02	0.0015

Note – the conversion from m/sec values to km/h is done dividing by 3.6<sup>2</sup>

Starting from equation IV.22, specialized to the railway parameter with the introduction of all the appropriate coefficients, we arrive at the expression for the determination of the stopping spaces.

$$S_f = (1 + \beta) \frac{P}{g} \int_0^{v_0} \frac{v}{F_f + P \left( \frac{R_{rr}}{10^3} + \frac{R_c}{10^3} + \frac{kSv^2}{P} \pm \frac{i_{0/00}}{10^3} \right)} dv \quad (IV.27)$$

Another important parameter underlying the braking model, already introduced previously, is the delay associated with the start of actual braking. This parameter, therefore, constitutes the period of time during which the vehicle runs in a so-called "drift" regime, i.e., in the absence of traction and braking forces, subjected to the action of gravity which can act for or against the forward motion (generating an acceleration or deceleration).

The calculation of the initial delay relating to the activation of the brakes is obtained as the sum of two rates:

$$t_s = t_r + t_0 \quad (\text{IV.28})$$

where:

- $t_r$  is the delay related to the on-board devices to command the traction disconnection and brake operation. It is a characteristic parameter of the tram's on-board apparatus;
- $t_0$  is the delay due to the driver's reaction from the moment he perceives the danger he performs the braking action.

Adding time  $t_s$  as the time of perception and reaction of the driver and of the mechanical intervention of the brake, the stopping distance of the tram is obtained as:

$$S_{DCE} = S_r + S_f \quad (\text{IV.29})$$

where  $S_r$  is the space covered in the reaction time. So:

$$S_{DCE} = v_0 t_s + \frac{(1 + \beta)}{g} \int_0^{v_0} \frac{v}{\frac{F_f}{P} + \left(\frac{R_{rr}}{10^3} + \frac{R_c}{10^3} + \frac{kSv^2}{P} \pm \frac{i_{\theta/60}}{10^3}\right)} dv \quad (\text{IV.30})$$

Considering the braking action:

$$f'Q \leq f_a P \Rightarrow \frac{Q}{P} \leq \frac{f_a}{f'} \quad (\text{IV.31})$$

where  $f'$  is the friction coefficient between the mechanical element in charge of the brake (shoe or pincer) and wheel rim,  $f_a$  is the adhesion coefficient of Muller formula,  $Q$  is the braking or radial effort applied through the block or pincer. The coefficients  $f'$  and  $f_a$  change with the speed according to the law in Figure IV.8.

Therefore, the grip is proportional to the weight that is unloaded on the wheel and depends on various factors, including speed  $v$ , the nature of the wheel-rail contact, and the conditions of humidity and cleanliness of the surfaces in contact.

In the railway case, the adhesion coefficient does not depend on the characteristics of the two surfaces in contact (which are both metallic and almost perfectly smooth), but on the type of traction (internal combustion engine, electric motor), on the state of the surfaces in contact (presence of water and impurities) and the speed of rotation of the wheel.

Wheel blocking must be avoided because there would no longer be the grip force, but the sliding friction force (wheel-rail) which is lower. With a brake that can exert a single value of  $Q$ , if you want to avoid wheel blocking at all speeds, you must consider the most binding situation: this occurs in the

vicinity of  $v = 0$ , where  $f' > f_a$ . From the graph, we can see that for zero speed the ratio  $f_a/f' = 0.7$

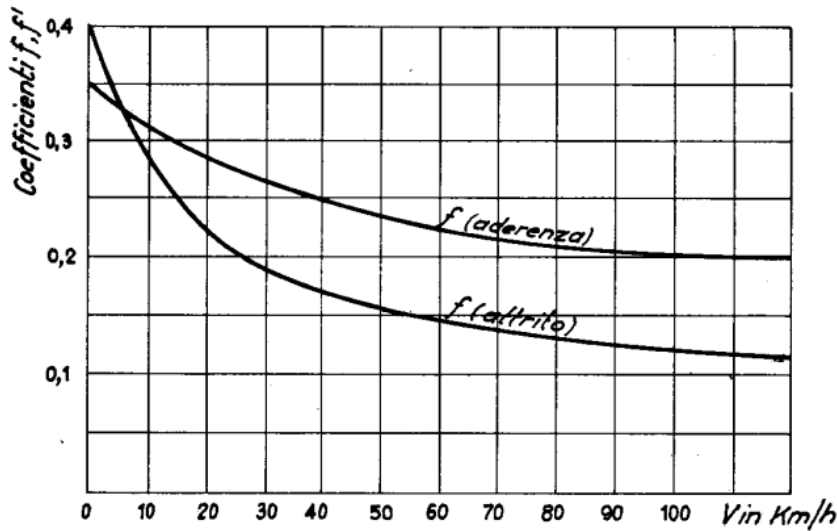


Figure IV.8 Adhesion and friction coefficients

So, an allowable maximum  $Q$  value is  $0.7P$ :

$$\frac{Q}{P} = \lambda_r \leq 0.7 \quad (IV.32)$$

where  $\lambda_r$  represents the actual braked weight percentage.

However, a tram is made up of many axles, so consider a total braking effort  $F_f$  given by the sum of the braking forces for each individual wheel.

$$\frac{F_f}{P} = \frac{\sum_i f' Q_i}{P} \quad (IV.33)$$

In this way, a percentage of braked weight has been introduced  $\lambda_c$  called conventional which is equal to 1 when  $\lambda_r = 0.7$ :

$$\frac{F_f}{P} = f' 0.7 \lambda_c = f_a \lambda_c \quad (IV.34)$$

The formula for calculating the stopping space will become:

$$S_f = S_r + \frac{(1 + \beta)}{g} \int_0^{v_0} \frac{v}{f_a \lambda_c + \left( \frac{R_{rr}}{10^3} + \frac{R_c}{10^3} + \frac{kSv^2}{P} \pm \frac{i_{\%00}}{10^3} \right)} dv \quad (IV.35)$$

The rolling resistance  $R_{rr}$  for a railway vehicle, takes the following empirical expression:

$$R_{rr} = 0.65 \div 0.70 + \frac{120 \div 130}{P_a} + 0.009v \quad (IV.36)$$

with  $P_a$  the weight in kN for each shaft.

The formula explaining all the parameters is:

$$S_f = v_0(t_r + t_0) + \frac{(1+\beta)}{g} \cdot \int_0^{v_0} \frac{v}{f'0.7\lambda_c + \left( \frac{0.675 + \frac{125}{P_a} + 0.009v}{10^3} + \frac{a}{10^3} + \frac{kSv^2}{P} \pm \frac{i_{\%00}}{10^3} \right)} dv \quad (IV.37)$$

The  $\beta$  and  $\lambda_c$  values have been calculated with reference to Sirio tram manufactured by Hitachi Rail STS S.p.A., managed by the Azienda Napoletana Mobilità and in circulation in Naples:  $\beta = 1$  e  $\lambda_c = 1.3$ .

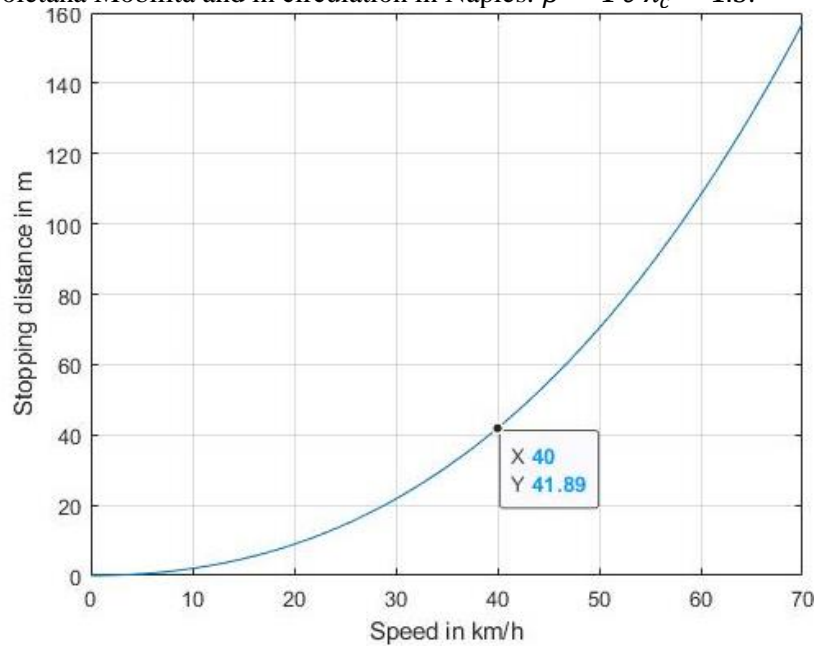


**Figure IV.9** Braking distance in the proposed model

The figure shows the stopping distance as a function of speed considering the straight case, on the plain and with a reaction time equal to zero. We will also consider this last assumption in the evaluation and comparison of the model's performance. In fact, this parameter is common to all models, and we will omit it to compare them better.

It should be noted that within this model there is the possibility to modify or adequately insert parameters concerning the tramway and the specific vehicle. This makes it particularly flexible and adaptable to different environmental and technical scenarios.

**Warning distance definition**

Starting from the stopping distance calculated by the DCE model, it is possible to define an operability zone of the T-ADAS system for the tram in order to obtain a warning distance in which the system will perform braking actions in the driving task.

The Figure IV.10 shows the FOV of the sensors divided according to four safety bands  $S_{bn}$ . These represent the area within which the system will perform the braking actions according to the flow chart of Figure IV.7.

The width of each safety band depends on the instantaneous speed with a linear law, and which considers a minimum threshold when the tram is stopped.

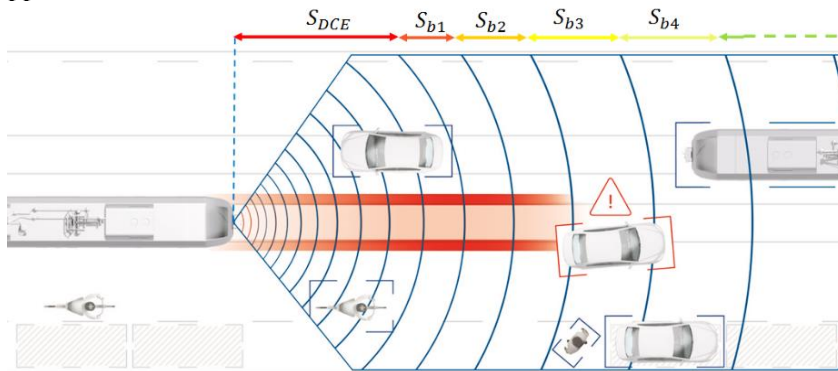


**Figure IV.10** Safety band definition in driving task

This is essential to prevent accidental departures where there may be a potential obstacle in the vicinity of the tram. As we know, trams have usually commercial speeds very lower than the maximum project speed. By virtue of this we assume that a tram travels at a speed of 50 km/h and we consider, as reported in (Dimitrakopoulos, 2020), an ADAS system that covers with RADAR and LiDAR sensors a FOV at least 150 m long.

The stopping distance according to the DCE model is  $S_{DCE} = 92\text{ m}$  in which we considered 20 m relative to a reaction time of 1.5 s. The usable space up to the end of the sensor range is therefore 58 m. By dividing the 4 bands equally, we obtain that each of these has a maximum size of 14.5 m. So, the law that defines the length of each band as a function of speed is the following:

$$S_{bn} = nv + c \tag{IV.38}$$

where  $c$  is a constant that guarantees the system operability at zero speed, and  $n$  is a multiplicative coefficient. When the tram is stopped for example at a platform many pedestrians cross the street,  $c$  can be chosen considering the situation of a tram which, coming from the opposite direction, screens a part of the FOV. In this case, a pedestrian could come out from the rear and not be seen in time in the starting phase. For  $c$ , a value is chosen which form the entire warning distance at zero speed is comparable to the length of a tram. The coefficient  $n$  is calculated as:

$$n = \frac{S_{bmax} - S_{bmin}}{v} \quad (IV.39)$$

So, if the tram at zero speed, the system keeps a 24 m long FOV area under control ( $c$  is about 6 m per band). In this area, any obstacle on the tram's trajectory inhibits departure.

This logic could prevent the approach to the terminus usually created with a concrete block. In this case, through the TSR functionality of T-ADAS, a stop signal can be recognized so as not to be interpreted as a false positive target. Then the driver will be able to approach the terminus without interference from the system.

#### ***IV.3.4 Theoretical performance of the model***

In order to investigate the effectiveness of the proposed model, the stopping distances calculated from the literature models and seen previously are compared.

The analysis of the model's performance and the comparison with other models demonstrate that the proposed model calculates the stopping distance, in the same boundary conditions, in a more similar way to the normative reference, unlike the Pedelucq formula which overestimates this distance. Conversely, the semi-empirical model, intended as an extraction of the RFI model, underestimates the stopping distance.

Furthermore, the model provided interesting answers by introducing slope and radius of curvature. In fact, there is an appreciable action of these forces which are not considered before on tramway, and which allow a more accurate determination of the stopping distance.

The complexity of execution of a model increases with the number of parameters to be estimated. Consequently, in the standard modelling framework, the number of free parameters is typically used as a simple but fair complexity metrics. An increase in the complexity of the model naturally leads to an increase of estimation goodness, and the choice of a model is necessarily a trade-off.

The trade-off between simplicity and accuracy can then be readily addressed in this form: select the simpler model that reaches the required accuracy for the considered application. The DCE model has comparable complexity to the models in the literature because we have considered only the significant parameters in the dynamic analysis of the tram.

Obviously, modelling accuracy can be further improved by considering additional phenomena, at the price of a higher complexity, but this would lead to an increase in processing time and consequently poor effectiveness in assisting the driver on time.

The accuracy-simplicity trade-off is a fundamental question in model formulation. The best model depends on the target application and should be as simple as possible while still capturing the relevant phenomena, as in the case of the proposed model.

#### **Comparison on dry and wet rail in the plains**

A first analysis of the effectiveness of the model is carried out by comparing the various braking curve introduced. The evaluation of the performances in the different conditions of the rail suggests the first a good reliability of the model. In fact, it is noted that in dry rail conditions DCE is the model closest to the standard, while the Pedelucq formula overestimates the stopping distance, and the semi-empirical model underestimates it. In wet rail conditions, DCE is more prudent than the standard and semi-empirical model. The goodness of the estimate of this distance is postponed to the comparison with the experimental data.

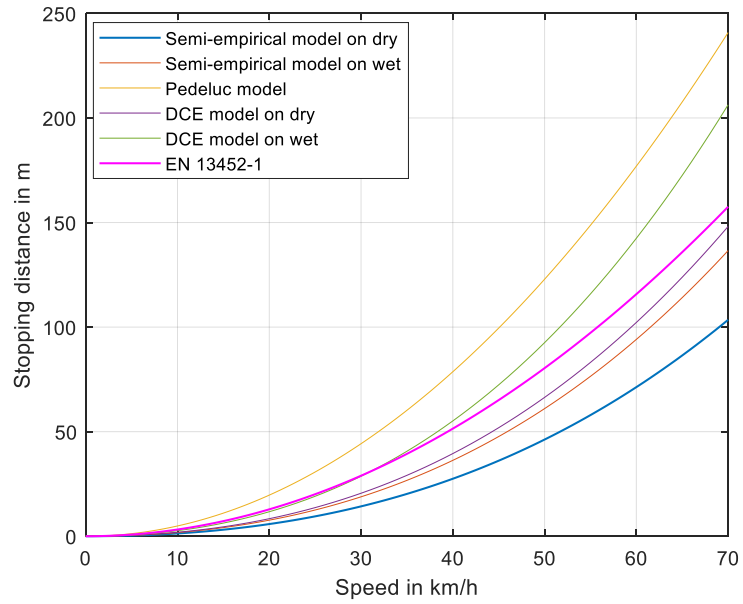


**Figure IV.11** *Theoretical braking performance comparison on dry and wet tramways in the plains*

**Comparison on slope and dry tramways**

In this case, the comparison was performed in dry rail conditions, but on an inclined plane with both positive and negative slopes of  $\pm 5\%$  and  $\pm 10\%$  respectively.

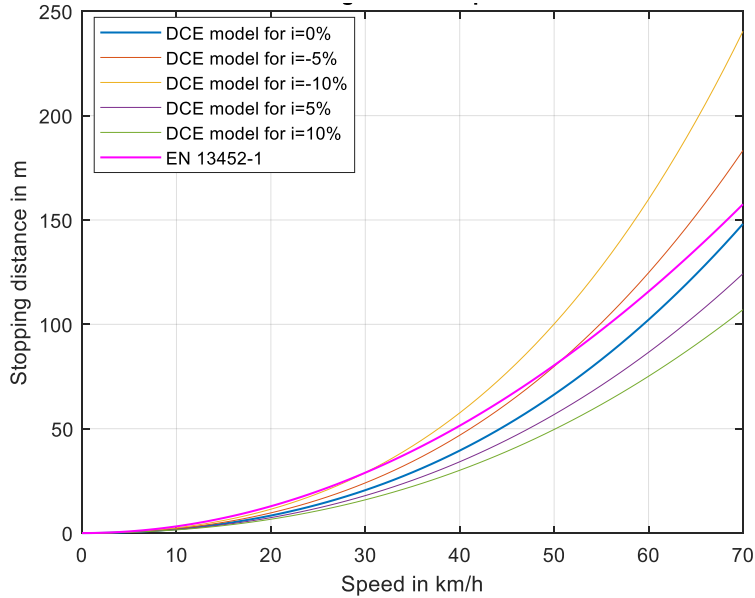


**Figure IV.12** *Theoretical braking performance comparison on slope and dry tramways*

A slope value of  $\pm 10\%$  can be considered high in railways and unworkable, but in the case of the tramway this is a usual value, just think that in Lisbon some sections have a 14.5% slope (Dario, n.d.).

**Comparison on curve and dry tramways**

Here the comparison is made with a path that includes several radii of curvature. The effect of the resistances due to the curvature of the tramway is more contained than the slope, but it is not negligible.

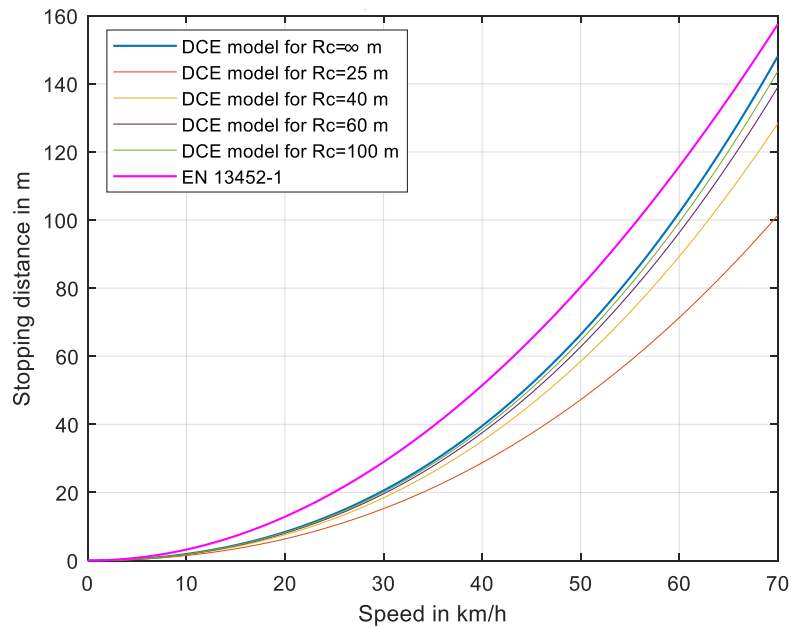


**Figure IV.13** Theoretical braking performance comparison on curve and dry tramways

#### IV.4 Case study

The implemented DCE model is used to calculate the braking distance on a tramway line of Napoli. The parameters of these tramway and of the Sirio tram model (vehicle with internal serial number 1101) were taken as a reference for the model. An experimental part followed in which trip data (acceleration, instantaneous speed, deceleration under braking, stopping distance from the start of braking, etc.) were taken from the RS485 serial port of the tram and a specific software tool, as shown in the following pictures.



**Figure IV.14** Connection to the RS485 data line in the valance.

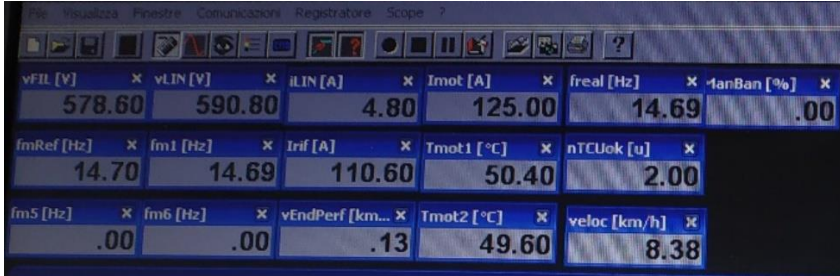


**Figure IV.15** Monitoring of parameters in real time

The acquired data are owned by ANM and therefore no further views are possible as they are covered by NDA (Nondisclosure agreement).

These data allowed us to graph the real braking of the tram and study its course. Here, we will analyze the comparison between some benchmark braking in dry and wet rail conditions with service braking. Available data on emergency braking even with the use of magnetic track brake have been acquired but are not subject to comparison.

### Features of tramway line

Originally built with an ordinary gauge, the Neapolitan tram network is equipped with electric traction initially at 550 V/600 V, raised to the new standard value of 750 V in conjunction with the start of the services of the new trams delivered by Hitachi Rail STS SpA.

**Table IV.6** Main features of Naples tram network

PHYSICAL CHARACTERISTICS	VALUE
Opening	1875
Last extension	2013
Network operator	ANM
Rolling stock	Sirio
Track gauge in straight	1.435 mm
Track gauge in curve	1.445 mm
Traction	Electrical – 750 V DC
Stations	31
Length	11.8km
Mean distance between stations	380 m
Minimum radius of curvature	13 m
Feed height	5000 mm – 5500 mm

The Naples tram network offers a structured service on three lines for a total length of 11.8 km:

- line 1 from via Stadera (Hemicycle of Poggioreale) to via Cristoforo Colombo (Maritime Station);
- line 2 from Piazza Nazionale to San Giovanni a Teduccio (ANM depot);
- line 4 from San Giovanni a Teduccio (ANM depot) to via Cristoforo Colombo (Maritime Station).

### **Features of rolling stocks**

The SIRIO tram for the city of Naples is a bidirectional vehicle with 3 boxes and 2 trolleys with a gauge of 1435 mm.

Enclosure takes place via 3 internal roto-translating doors per side. The doors located near the driving cabs are of the single-leaf type.

The traction system uses two independent units located on the roof of the MA and MB boxes. The motor trolley is equipped with two self-ventilated three-phase asynchronous motors.

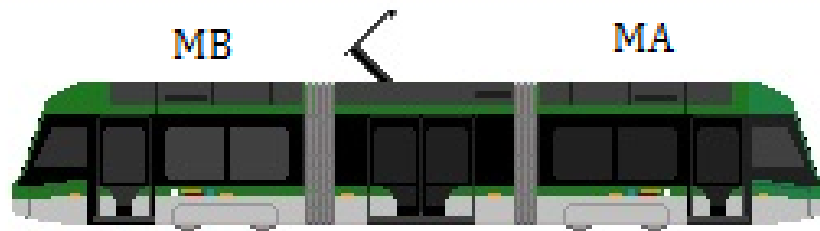


**Figure IV.16** Layout of Sirio tram Napoli

The motor carriage is equipped with 2-disc brake units with electro-hydraulic actuator and the supporting carriage (central) is equipped with 4-disc units. The mechanical brake is used only as a parking brake and to intervene when the electric brake is no longer able on its own to provide the required performance.

**Table IV.7** *Technical information of SIRIO tram Napoli*

<b>PHYSICAL CHARACTERISTICS</b>	<b>VALUE</b>
Power supply	750 Vdc (-33% ÷ +20%)
Power socket	Pantograph
Operation	Bidirectional
Running gear	B02
Maximum height without pantograph	3300 mm
Length (with energy absorbers)	19800 mm
External width	2300 mm
Number of passenger doors (per side)	3
Seats	31
Standing passenger area	380 m
Standing spaces at 6 passengers/m <sup>2</sup>	124
Unladen weight	21.6 t
Loaded weight (155 passengers)	32 t
Maximum speed	70 km/h
Average acceleration (0-40km / h)	1 m/s <sup>2</sup>
Service deceleration	1.2 m/s <sup>2</sup>
Emergency deceleration	2.2 m/s <sup>2</sup>
Jerk in traction and service braking	1.2 m/s <sup>3</sup>
Mechanical brake	Two discs on the internal axis
Motors	Two, 106 kW each
Magnetic track brake	Two, 58 kN each

#### ***IV.4.1 Real acquisition of braking distance***

Along line 2, a campaign of real measurements on wet tramway (rainy day) and dry tramway (sunny day) was carried out in collaboration with the ANM. The comparison with the DCE is reported below. It is noted that concerning the legislation this follows the real case with greater accuracy.

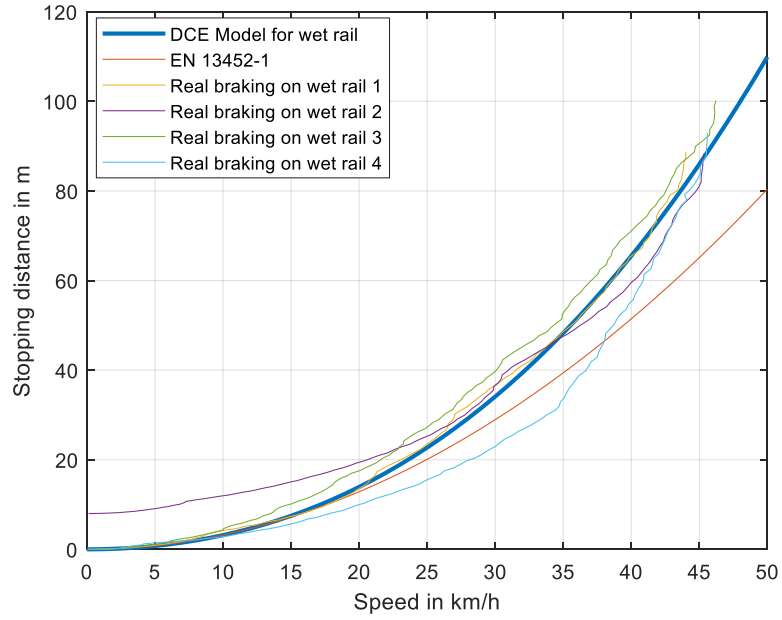


**Figure IV.17** Real braking performance comparison on wet tramways

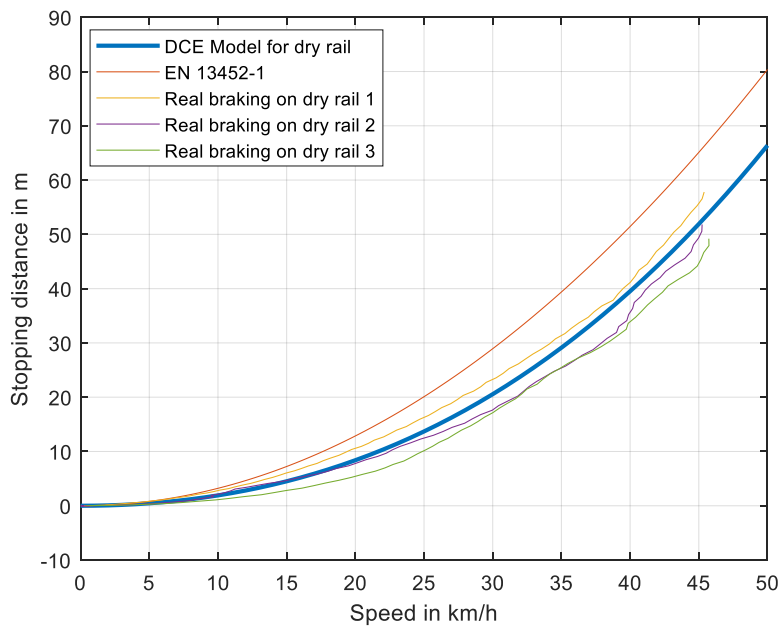


**Figure IV.18** Real braking performance comparison on dry tramways

A quantitative analysis is reported in the next paragraph.

#### IV.5 Analysis of braking distance results

In order to investigate the effectiveness of the proposed model, the figure of merit RMSE is evaluated for the distance braking obtained in the DCE.

The analysis of the model's performance and the comparison with the legislation model demonstrate, as shown in Table IV.8, that the proposed model calculates braking distance with a lower error than the EN 13452-1.

**Table IV.8** *Evaluation metrics of the DCE and the EN 13452-1*

BRAKING DISTANCE	MODEL	
	DCE	EN 13452-1
	RMSE	RMSE
REAL BRAKING 1	2.08	5.59
REAL BRAKING 2	2.32	10.02
REAL BRAKING 3	3.9	12.41

In particular, the DCE and normative models were fed with real speed data acquired during the measurement campaign. The stopping distance for these two models is compared with the real stopping distance. On three reference braking runs, covering the same line section and the same boundary conditions, the RMSE for the two models is done.

The model's performance analysis reveals that the proposed approach presents lower values for the figure of merit than the reference model.

##### *IV.5.1 Driver reaction error definition*

Since the proposed DCE model manages to minimize the error with respect to real braking both dry and wet, it is considered appropriate to choose this model as a reference in order to establish the driver's reaction error. As reported in (RAIB, 2016), most of the accidents in the railway environment can be attributed to human error. The driver of a tram can be distracted by the smartphone (Il Mattino, 2019) or lost in thought and therefore not see road signs or foresee an approaching obstacle.

Let's consider the case of real braking during service in which the driver notices an obstacle at a certain distance while at a travel speed of approximately 45 km/h. Figure IV.17 shows the comparison between the real braking and the theoretical one generated by the DCE model after the potential warning phases.

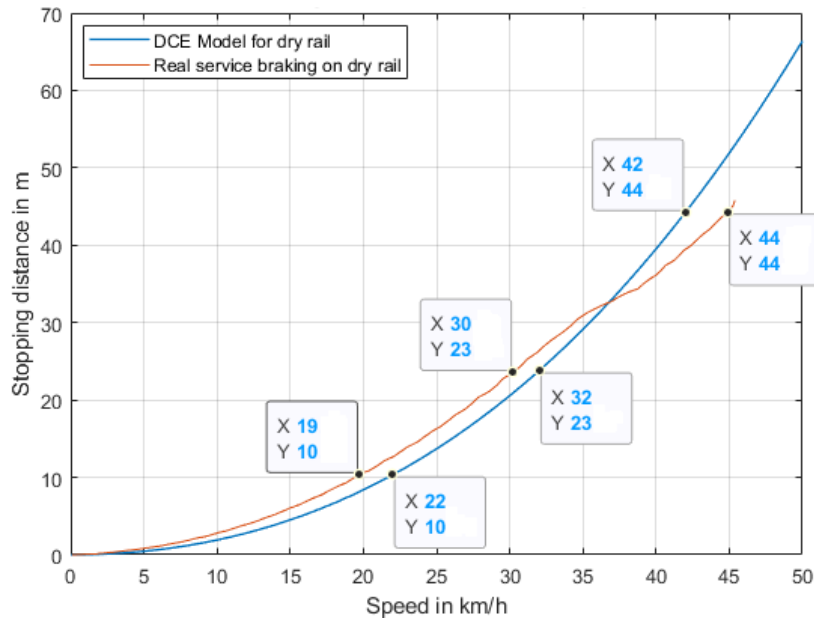


**Figure IV.19** Misjudgement in real braking, comparison with DCE

The obstacle is clearly visible, but the driver approaches the action with an inappropriate braking percentage level. The tram loses speed, but this is not enough, and the obstacle is still present. The driver brakes further until the tram is brought to a stop in useful space and without the aid of safety braking and therefore with skates. This was however perceived by us passengers with a further tug while we were already pulling force on the bridle.

This test shows how in situations of distraction or imminent danger the system can make a fundamental contribution.

In this single measurement campaign, no events were recorded in which the driver braked too much and then weakened the braking with respect to the reference curve. Therefore, we have not reported this case which will be the subject of future developments, also to understand if the T-ADAS system should intervene or be silent.

As shown previously,  $S_{DCE}$  is the stopping distance of the tram calculated with the DCE model as a function of speed. The driver braking error definition can be made by calculating the difference between the distance measured by the SFS and  $S_{DCE}$  obtained with the instantaneous speed value. A negative value of this difference determines how far the driver is missing the stopping point at any one time. The error  $\varepsilon_d$  in term of distance is:

$$\varepsilon_d = (S_T - S_{DCE}) \tag{IV.40}$$

where  $S_T$  is the distance to target.

The system will apply a percentage braking value to make the error null and void less than a safety margin.

Vice versa, the error can be evaluated in terms of speed: knowing the distance from the target, the theoretical speed that the tram should be calculated using the DCE curve. The latter will be compared with the real instantaneous one and must always have a lower value. The error  $\varepsilon_v$  in term of speed is:

$$\varepsilon_v = (v_{dce} + v_i) \quad (IV.41)$$

where  $v_i$  is the instantaneous tram speed.

The manipulator stroke is linearly proportional to the set deceleration value. Therefore, a percentage braking is considered as a function of deceleration  $a_e$  reported in Table IV.3 for which 100% braking correspond to  $a_e = 1.2 \text{ m/s}^2$ .



# Chapter V

## T-ADAS implementation: a holistic approach for a next generation Tram

This chapter describes the implementation of the T-ADAS system on the tram communication network. The chapter starts with the description of the technologies, general requirements, and architecture of the communication network.

The word “train” or “tram” will be used indiscriminately in the first part of the chapter: this is due as at this functional level also the legislation does not make particular distinctions.

### V.1 In-vehicle networking infrastructure

A Train Communication Network (TCN) is the infrastructure enabling the exchange of information throughout the railway vehicle (IEC, 2017). It usually consists of a vehicle bus for intra-vehicle communications and a train bus for train-wide information exchange.

The general architecture of the TCN, is made up of two basic networks:

- Train Backbones (TB) with different characteristics for interconnecting vehicles in close or open trains.
- Consist Networks (CN) with different characteristics for connecting standard on-board equipment.

TCN architecture, in accordance with international standard EN 61375-1, is defined as a hierarchy of CN and TB, as shown in Figure V.1.

The network technologies can be used either solely or in combination to set up the train communication network.

These network technologies can be classified in two technology classes:

- Bus technology class that includes the Wire Train Bus (WTB), Multifunction Vehicle Bus (MVB), Controller Area Network open (CANopen).
- Switched technology class which refers to the Ethernet Train Backbone (ETB) and the Ethernet Consist Network (ECN).

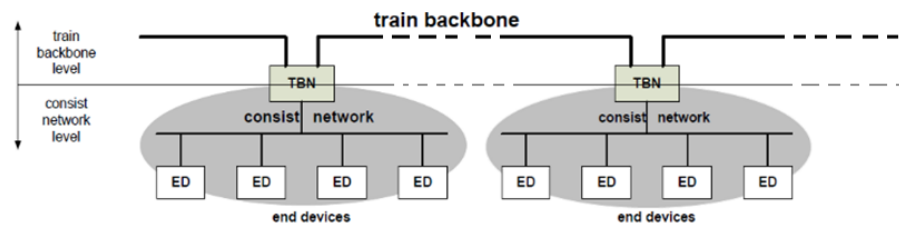


**Figure V.1** *TCN architecture: Train Backbone and Consist Network*

The bus technology class is characterized by having multiple end devices connected to the same data transmission media, forming one broadcast and one collision domain. In the switched technology, class is one end device connected to a switch, which is responsible for actively forwarding user data inside the network. A switched technology-based network has the possibility to restrict broadcast and collision domains.

The TCN is set up by two types of communication devices: Network Devices (ND) and End Devices (ED). ND are all those devices whose primary use is to transport and forward user data. Examples of ND are passive components, like cables and connectors, or active components, like repeaters, bridges, switches, routers, or application layer gateways. ED on the other hand provide typically the sources and sinks of user data. Examples of ED are controllers, displays, or sub-systems.

The communication between consist networks is only possible over the train backbone. This two-level architecture has been selected for the following reasons:

- The communication network which is set up by the CN is a static, preconfigured network. In opposite to that is the communication network, which is set up by the TB, a dynamic network, which changes its topology each time there is a change in the train composition. Communication between TB nodes may be interrupted if a reconfiguration of the TB happens. During times of the unavailability of the TB communication the CN communication is not affected;
- A breakdown of a CN does not (e.g. due to power loss in the consist) compromise the communication between other consists of the same train;

- The train backbone cannot be loaded with all the data traffic in a train, therefore intra-consist data will be kept local to the consist. Only data traffic directed to other consists will be transported over the train backbone.

### V.1.1 Network standard requirements

As we observed, the TB interconnects the backbone nodes which are located in the consists constituting the train. Each consist could have 0, or 1, or more train backbone nodes.

In modern train, ETB bus technology is the most used technology, enabling a cost-effective set up with a large bandwidth (up to 100 Mbit/s vs 1 Mbit/s for WTB). It can replace or be used together with WTB and other train buses. ETB uses physical lines along the train to connect the active network devices together (ETB nodes, Repeater, etc.). These lines are also called physical segments and shall use passive components such as cables and connectors, dedicated to ethernet.

In order to highlight the advantages of ethernet technology compared to other network technologies used up to now, we have focused on comparing transmission speeds according to the minimum regulatory requirements.

**Table V.1** Comparison for train bus technology

Feature	WTB	ETB	MVB	ECN
<b>Bandwidth</b>	1 Mbit/s	100 Mbit/s	1.5 Mbit/s	100 Mbit/s
<b>Maximum nodes and network length</b>	32 nodes, 860 meters for shielded, twisted pair,	63 nodes, 100 m between nodes	- 20 m, 32 devices for twisted wire pair, biased RS485; - 200 m, 32 devices for shielded twisted wire pair isolated by transformer; - 2000 m, 2 devices - star coupler for optical glass fibre.	63 nodes, 100 m between nodes
<b>Standard</b>	IEC 61375-2-1	IEC 61375-2-5	IEC 61375-3-1	IEC 61375-3-4

For the ethernet network technology the 1 Gbit/s network is not standardized, but technically available by most suppliers of railway technology (EKE, 2021). The general requirements of the network allow to establish the amount of traffic that can circulate and the maximum capacity in

terms of bandwidth of the communication system. Just think of the traffic generated by the video surveillance system which often integrates the passenger counter system which in turn exchanges the data with the diagnostic network (Lawrence, 2003). The integration of a T-ADAS system that generates an important amount of dates could pursue a distributed integration logic only in the case of sufficient bandwidth as we will see later.

### V.1.2 TCMS functional zone

Train Control & Management System (TCMS) is a train-borne distributed control system. It comprises computer devices and software, human-machine interfaces, digital and analog input/output (I/O) capability, and the data networks to connect all these together in a secure and fault-resistant manner.

Typically, TCMS provides data communications interfaces to other train-borne systems, and telecommunications to supporting systems operating remotely on the wayside also.

The functional structure of these communications lets prevent non-safety functions from having an impact on the TCMS network security process. A concrete solution is to introduce the concepts of functional zones (EuroSpec, 2019), gateway and TCMS Data Service. The Data Service can allow for the exchange of information inside one given functional zone or between two functional zones. The following figure shown the concept of functional zones.

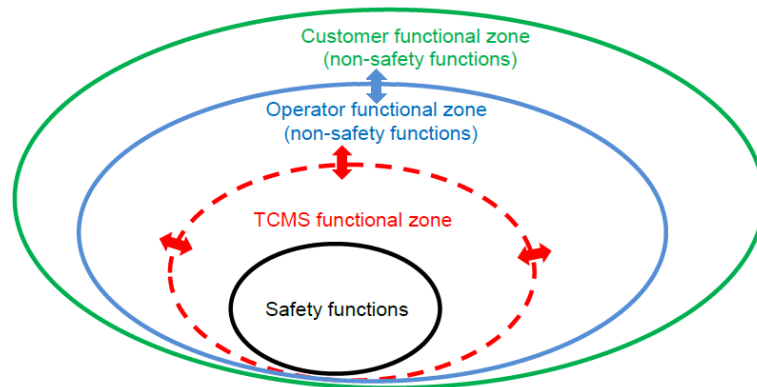


**Figure V.2** *Concept of functional zones*

Note that in the Figure V.2 does neither imply that the TCMS is a subset of operator functions nor that the operator functions are a subset of customer functions. Therefore, in the process of exchanging information between the different consistent networks it is important that non-security functions have an impact on the TCMS network. A concrete solution to optimise the functional design of this communication is to introduce redundant Application Layer Gateway (ALG) devices between the consist networks.

Figure V.3 shows an example of an architecture using these concepts.

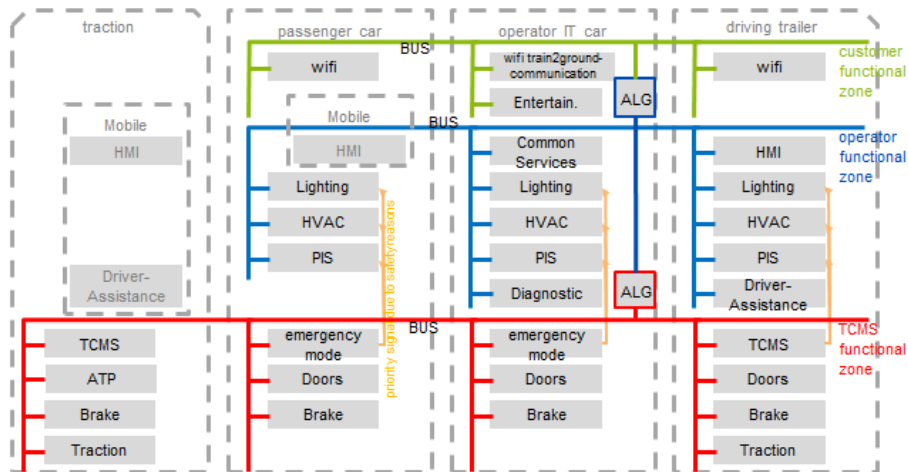


**Figure V.3** Functional zone implementation example

It is noted that an ALG has been inserted between the Passenger Information System (PIS) network and of the TCMS network.

Any of the consist network technologies MVB, CAN or ECN may be used in a consist. Each functional zone must take care of its own information needs (e.g., if PIS and TCMS need the speed signal, then it has to be appropriately exchanged between the networks).

Below we propose an approach to the implementation of the T-ADAS system based on the two fundamental network technologies MVB and ECN.

## V.2 Proposed implementation approach for ECN

The integration of T-ADAS systems into railway next-generation switching networks certainly represents the ideal case. Suffice it to say that modern trams, subways, and trains have network infrastructures with ethernet standards and the end devices such as the CCTV system, intercoms, passenger counting systems, etc., have an RJ45 connection and Power on Ethernet (PoE) connector for power supply. Thanks to the large amount of data, also related to infotainment, these networks request more and more efficient, and the producers of railway technologies are concentrating on providing systems with data transmission speeds higher than 1 Gbps. Furthermore, ADAS systems are also becoming increasingly commercial, and many applications see automotive ethernet networks interconnecting them (Agarwal, 2021). This solution is the one adopted by the author for the experiments and future developments starting from this work. In fact, let's consider the sensors being

tested with the characteristics shown in the Table V.2. These sensors can be integrated at ECN according to a concentrated or distributed logic.

**Table V.2** *Sensor’s characteristics of the T-ADAS system*

Sensor	Data rate required
Mono Camera	50 Mbps
Stereo Camera	145 Mbps
Livox Lidar	100 Mbps
Ouster 360° Lidar	254 Mbps

The first case is shown in Figure V.4 where we have created two ECNs for the PIS and the TCMS respectively, by way of example. The T-ADAS system consisting of the group of sensors and the SFS exchanges to the TCMS only the information useful for diagnostic purposes and therefore the drives. The feature of this implementation is that everything takes place at the PIS network level and only enabled flows can enter the TCMS network. This is possible thanks to the ALGs which provide a barrier (firewall) to protect the diagnostic network.

The Ethernet interface between TCMS and PIS has the task of:

- Communicate the status of the tram and its components to the Communication System by means of the Train Real Time Data Protocol (TRDP) protocol for the implementation of its specific functions (e.g. state of braking, state of the doors, etc.);
- Communicate the monitoring and diagnostic data of the PIS to the TCMS;
- Allow access from PIS to the TOD of the TCMS for real-time viewing of the images of the ADAS sensors, as is already the case for the video surveillance system.

The devices involved in the communication between TCMS and PIS, TCMS side are:

- Ethernet Network Administrator (ENA), periodically stimulates the Monitoring and Diagnostic Control Unit (MDCU) and Central Control Unit (CCU) of the TCMS to send data on the TRDP protocol;
- The CCU, sends commands and statuses to various onboard subsystems, including the PIS;

- The MDCU, sends general information on the status of the vehicle;
- TOD, driver's monitor on which real-time images of the video surveillance system are displayed.

The devices involved in the communication between TCMS and PIS, on the communications network side are:

- PIS Control Unit (PIS CU), represents the front-end of the Communications System in the TRDP communication with the TCMS. It collects data from the PIS devices and sends them to the TCMS and, vice versa forwards the TCMS data to the PIS devices that request them;
- CCTV and T-ADAS that send the images in real-time to the TOD.

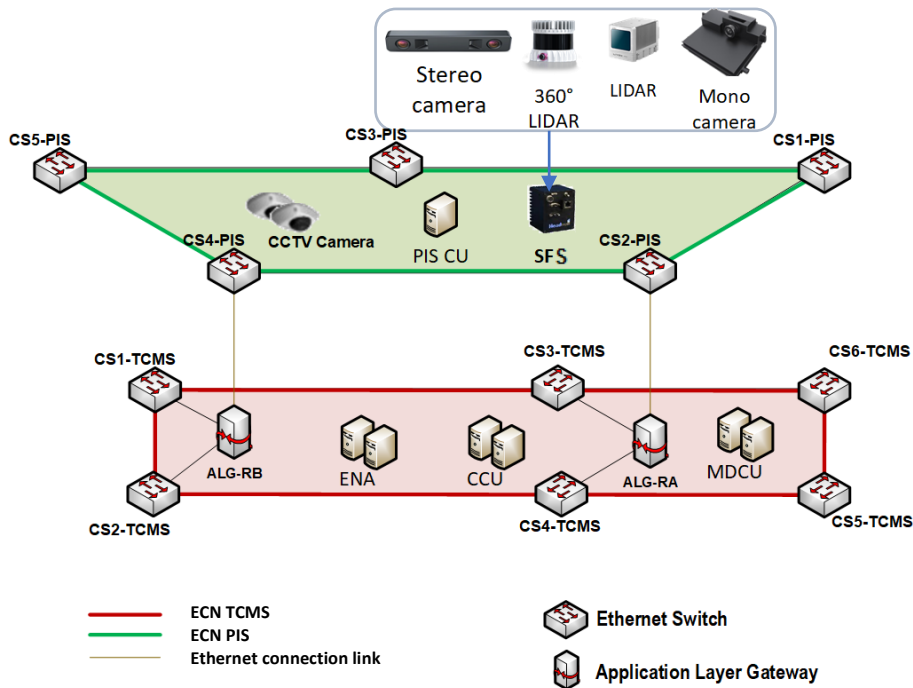


**Figure V.4** ECN architecture for T-ASAS concentrate integration

It should be emphasized that the tram has two driver's cab and therefore a T-ADAS system should be considered for each of them. However, from a conceptual point of view, only the system on the cabin enabled to travel will work, unless additional functions such as the Backward Collision Warning (BCW), which are not the subject of this thesis, are foreseen.

Considering, instead, a distributed logic of the T-ADAS system, the sensors can be connected to the various Consist Switches (CS) installed along the ECN, as in Figure V.5. This solution can be advantageous in terms of resources used since, in the case of the tram that has two driver's cabs, it would

be possible to use only one SFS to which the switches direct the transmission. The various sensors would work on the network like those of the CCTV system, for example.

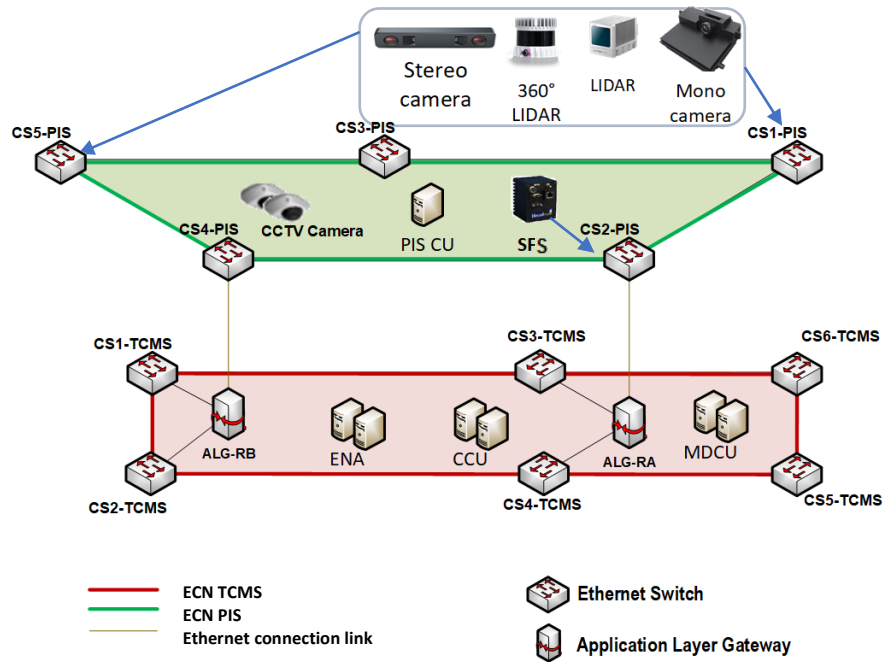


**Figure V.5** ECN architecture for T-ADAS concentrate integration

However, for this solution, there is a problem related to the residual band of the ECN that can be destined to the T-ADAS system. Equipping the system with additional sensors such as RADAR, ultrasound and other side or rear sensors would saturate the band of the most commercially popular systems. As reported in (Brown, 2021) the automotive ADAS sector is moving on a high-speed data network solution based on ethernet standards and therefore the overall bandwidth is expected at 10 Gbps due to the large amount of data generated by the sensors. The rail sector would have an advantage as it already uses this network technology.

### V.3 Proposed implementation approach for MVB

As mentioned, the MVB is a serial communication bus for railway vehicles. It is used to connect programmable devices to each other and can connect directly to simple sensors and actuators such as the manipulator for controlling the running of the tram.

The TCMS architecture is represented in Figure V.6 and it is based on the use of communications via Bus MVB and Bus WTB through which the CCU

acquires information from the bench. The Decentralized Units (UD) acquire the local information with the task of acting as an intermediary between the module systems and the CCU, while the Centralized Vehicle Diagnostics (CVD) is informed about the operating status of the main sub-assemblies/systems of the vehicle.

The TCMS implements the following functions on the MVB bus:

- Vehicle Logic by CCU and UD governs the entire vehicle in relation to all operating functions, by monitoring the logic functions for the correct supervision of the electromechanical equipment and for the control and command of the main tram states (traction, coasting, and braking);
- Centralized diagnostics via CVD carries out the monitoring action which is not limited only to the electrical traction/braking equipment but extends also to those onboard systems whose operation is in any case decisive for the purposes of vehicle operation.
- WTB interface via MVB-WTB Gateway (GTW) manages the exchange of control and diagnostic information between two coupled vehicles.

The MVB Bus as well as the WTB Bus is redundant, generally on two lines capable of operating separately.

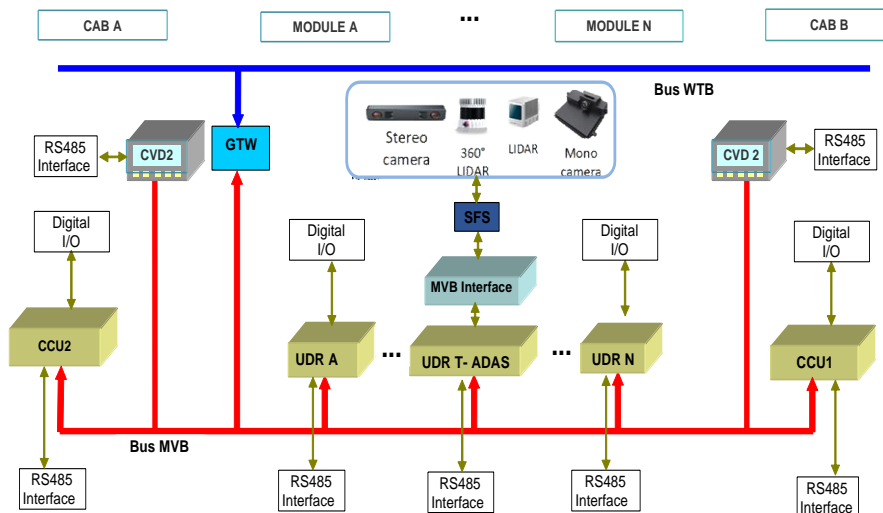


**Figure V.6** MVB architecture for T-ASAS concentrate integration

The integration of the T-ADAS system can, therefore, take place at the level of the UDRs as the CCU has the task of acquiring local information from them and the bench controls in order to manage the vehicle logic by governing all the operating functions. The T-ADAS system simulates, by means of the MVB interface, the decisions of the SFS as if they were given by the driver through the operator. The CCU, by means of the vehicle logic, transmits the

information imparted by the simulated operator via MVB to the drives, supervises the logic functions for the correct management of the electromechanical equipment, for the control and command of the main traction, coasting, percentage braking, safety braking, emergency braking by means of magnetic track brake, coordinating the mechanical brake with the electrodynamic one.

The diagram shows also how redundancy has been created for the CCUs. In fact, under normal operating conditions, one of the two CCUs, upon enabling the system, assumes the function of master of the MVB bus and therefore of system control.

In case of failure of the CCU that temporarily plays the role of master, control of the system passes to the other CCU.

It should be emphasized that most of the trams in circulation are equipped with MVB technology for the communication of the drives. The development of T-ADAS system that can be implemented according to the proposed logic would allow its stable diffusion over time as these means have a very slow obsolescence.

Also, in Chapter III many historical trams have been reported that have been the subject of restoration and revamping and which are currently in circulation. These means consist of electromechanical devices for the drives and poor control logics. Thanks to the new network infrastructures such as ethernet, the installation of a T-ADAS is easy to implement, low costs, simple wiring, bandwidth requirements, minimum latency compatible with the application and standardized interfaces.

Therefore, if it is true that the tram has a long life, certainly the T-ADAS represents the innovative key that still slows down its disposal.

# Conclusions

The ever-increasing societal cost of road traffic in terms of safety, accessibility, and environmental sustainability, has stimulated the study presents in this Ph.D. dissertation on Advanced Driver Assistance Systems for trams (T-ADAS), inspired by the automotive ADAS. While there are numerous advanced studies and prototypes of autonomous driving vehicles, even driverless, and many solutions with intermediate levels of automation are already available on the market, in the tram sector the problem is only in its starting phase, with first pilot realizations, as in Potsdam or Vitry-sur-Seine, and very few studies published on the topic.

In the development of sustainable and increasingly smart public mobility, it is unthinkable to neglect an ecological means of transport par excellence and with a high capacity to penetrate the urban fabric such as the tram. Chapter I aims to strengthen this thesis by focusing on the ever-increasing demand for mobility, emissions, and road safety.

Under this reference context, the main contributions of this dissertation are:

- Analysis of the technological porting of the automotive ADAS systems towards the tram and increase of its automation levels. The analysis begins with the description of the main parameters of all the elements that make up an automotive ADAS system, as reported in Chapter II. The ADAS functionalities that can be transferred to the tram allowed us to establish the degree of automation for the tram from GoA 0 to GoA 2.3, as well as to ascertain that for the different driving dynamics the tram needs specific algorithms to best implement fundamental ADAS functionalities such as FCW and the AEB in case of obstacles. The studies have shown the strong capabilities of the approach and provide insights into the impacts of deepening penetration of ADAS in the tramway sector.
- A specific algorithm for the tram to calculate the collision distance and the safety distance to accurately implement the FCW and AEB functions. The contribution is described in Chapter IV. In accordance with the Standard ISO 15623 and Euro NCAPs Test Protocol, that define the reference parameters for the FCW and AEB systems available exclusively for the automotive sector, we have built a model that also starts from the reference equation of motion but takes into account

---

different physical parameters of the tram and tramway in order to calculate the stopping distance. The algorithm has been shown to provide results that are closer to the experimental data, in terms of RMSE, than the sector and literature models.

- Implementation approach of the T-ADAS system in the on-board tram network. The contribution is described in Chapter V where the two currently most widespread network technologies are highlighted. The first concerns the integration on the newest ECN networks. Here a preliminary analysis is made on the available bandwidth to keep the entire communication and diagnostic system efficient, presenting two integration logics: concentrated and distributed. The second concerns the existing trams equipped with MVB network on which it is possible to implement T-ADAS in a revamping logic as an aftermarket system. In this case, given the limited bandwidth capacity of the bus and the need to adapt the communication protocol, the SFS and the MVB interface are respectively required.

The good performance of the proposed approach may open new development scenarios for the scientific community and for applications of safety systems aimed at a better integration of ADAS for tramway, which can lead to further improving or extending the methodology presented in this thesis.

The proposed approach highlights the key role of the tram in modern and classic cities, enhancing its characteristics, the increase in safety, making it possible for the tram to experience a new spring together with other research branches such as the study of hydrogen trams, catenary free trams, etc. This study would also facilitate eco driving applications as the ability to activate ACC functions would require moderate effort.

# References

- Abboud, K., 2016. Interworking of DSRC and cellular network technologies for V2X communications: A survey. *IEEE Trans. Vehicular Technologies*, 65(12), pp. 9457-9470.
- ACI - Istat, 2020. *Incidenti stradali 2019*, Roma: s.n.
- Adomat, R., 2003. Advanced driver assistance systems for increased comfort and safety - current developments and an outlook to the future on the road. *Advanced Microsystems for Automotive*, Volume 3, p. 431-446.
- Agarwal, Y., 2021. Automotive Ethernet Physical Optimization and IEEE 1588 Implementation. *Proceeding of Fifth International Conference on Microelectronics, Computing and Communication Systems*, Volume 748, pp. 489-500.
- Ajanovic, A., 2021. On the Historical Development and Future Prospects of Various Types of Electric Mobility. *Energies*, Volume 1070, pp. 1-25.
- Alturbeh, H., 2018. Modelling and simulation of the train brake system in low adhesion conditions. *SAGE Journals*, 234(3), pp. 301-320.
- Ammoun, 2009. *Real Time Trajectory Prediction for Collision Risk Estimation between Vehicles*. Romania, IEEE, p. 417-422.
- ANSF, 2019. *Norme tecniche e standard di sicurezza applicabili alle reti funzionalmente isolate dal resto del sistema ferroviario, nonché ai gestori del servizio che operano su tali reti*, Firenze: s.n.
- Augusto, C., 2003. *Meccanica dei Trasporti Ferroviari Tecnica delle Locomotive*. 3 a cura di Torino: Levrotto & Bella.
- Baek, M., 2020. Vehicle Trajectory Prediction and Collision Warning via Fusion of Multisensors and Wireless Vehicular Communications. *MDPI*, 20(1), pp. 1-26.
- Bhatia, 2003. *Vehicle Technologies to Improve Performance and Safety*, Berkeley: California Digital Library.
- Bishop, R., 2005. *Intelligent vehicle technology and trends*. Norwood: s.n.
- Brown, C., 2021. *EETimes ASIA*. [Online] Available at: <https://www.eetasia.com/looking-ahead-high-speed-in-vehicle-display-and-sensor-connections/> [Accessed 27 12 2021].

- Cao, J., 2019. Improved Traffic Sign Detection and Recognition Algorithm for Intelligent Vehicles. *Intelligent Sensors*, 9(18).
- Chae, H., 2017. *Autonomous Braking System via Deep Reinforcement Learning*. Yokohama, IEEE .
- Chen, G., 2017. Global Urban Passenger Travel Demand and CO2 Emissions to 2050: New Model. *SAGE Journals*, 2471(1), pp. 71-79.
- Chiusolo, S., 2011. *Automation of high density metro lines: Rome line A case study*. Paris, ReserchGate.
- Choi, S., 2016. *Advanced driver-assistance systems: Challenges and opportunities ahead*, s.l.: McKinsey & Company.
- Cicchino, 2018. "Effects of lane departure warning on police-reported crash rates. *Journal of Safety Research* , Volume 66, pp. 61-70.
- Cicchino, J. B., 2017. Effectiveness of forward collision warning and autonomous emergency braking systems in reducing front-to-rear crash rates. *ELSEVIER*, Volume 99, pp. 142-152.
- Cioran, A., 2015. *System Integration Testing of Advanced Driver Assistance*, Stockholm: Kth Royal Institute of Technology.
- Claudio, M. D., 2014. *Model-based development of an Automatic Train Operation component for Communication Based Train Control*. Qingdao, China, IEEE.
- Ćosić, L., 2019. *Time to collision estimation for vehicles coming from behind using in-vehicle camera*. Novi Sad, IEEE.
- COST , 2015. *Operation and safety of tramways in interaction with public space. Report. September 2015*, France: s.n.
- Dario, b., n.d. *Mondo Tram*. [Online] Available at: <http://www.mondotram.it/lisbona-dario/> [Accessed 03 11 2021].
- Delfa, S. L., 2016. Eco-driving command for tram-driver system. *ELSEVIER*, 49(19), p. 444–449.
- Di Palma, C., 2020. *Driver Assistance System for Trams: Smart Tram in Smart Cities*. Madrid, IEEE.
- Dimitrakopoulos, G., 2020. *The Future of Intelligent Transport Systems*. 1 a cura di Amsterdam: ELSEVIER.
- Directive 98/34/CE, 2015. *Technical Rules for Trams Dimensioning and Testing Vehicle Brakes*, Berlin: s.n.
- Dong, H., 2010. Automatic Train Control System Development and Simulation for High-Speed Railways. *IEEE Circuits and Systems Magazine*, 10(2), pp. 6 - 18.
- EKE, 2021. *Technology for smarter trains*, Espoo: IRIS.
- EN 13452-1, 2003. *Railway applications – Braking – Mass transit brake systems – Part 1: Performance requirements*, Charlottenlund : Dansk standard.
- Enjalbert, S., 2019. On the Eco-driving Trajectory for Tramway System. *ELSEVIR*, 59(19), pp. 115-120.

- ESSER, F., 2016. *Assisted, automated and autonomous driving (“triple a”) for railway traffic*. Serbia, s.n.
- Euro NCAP, 2021. *TEST PROTOCOL – AEB SYSTEMS*, Bruxelles: Euro NCAP.
- EuroSpec, 2019. *Specification TCMS Data Service*, Paris: EuroSpec.
- Földes, D., 2016. *Conception of future integrated smart mobility*. Prague , IEEE.
- Garbey, 2007. Contact-free measurement of cardiac pulse based on the analysis of thermal imagery. *IEEE Transactions on Biomedical Engineering*, 54(8), pp. 1418-1426.
- Gietelink, O., 2007. *Design and Validation of Advanced Driver Assistance System*, s.l.: Netherlands TRAIL Research School.
- Goodall, R.-M., 2002. Mechatronic developments for railway vehicles of the future. *Control Eng, Volume Pract.*, p. 887–898.
- Gorner, M., 2018. *Decarbonising urban transport*, Paris: s.n.
- Greiner, 1997. Radar sensing of heartbeat and respiration at a distance with applications of the technology Radar, vol. 97, no. 449, pp. 150-154, 1997.. *Radar Sensor Technology II*, 97(449), pp. 150-154.
- Guo, 2018. Traffic-Sign Spotting in the Wild via Deep Features. *IEEE Intelligent Vehicles Symposium* , p. 120–125.
- HAN, 2016. VEHICLE DISTANCE ESTIMATION USING A MONO-CAMERA FOR FCW/AEB SYSTEMS. *International Journal of Automotive Technology*, 17(3), p. 483–491.
- Hechri, 2015. Robust road lanes and traffic signs recognition for driver assistance system. *International Journal of Computational Science and Engineering*, Volume 10, p. 202–209.
- HengirmenTercan, Ş., 2021. Second-hand renovated trams as a novel decision strategy for public transport investment. *Transport Policy*, Volume 114, pp. 364-371.
- HIRAOKA, T., 2009. Collision Risk Evaluation Index Based on Deceleration for Collision Avoidance. *ReserchGate*, 30(4), pp. 429-437.
- Hitachi, 2021. *Prodotti e soluzioni*. [Online] Available at: <https://www.hitachirail.com/it/prodotti-e-soluzioni/i-nostri-treni/tram/> [Accessed 11 10 2021].
- IEC, 2017. *Electronic railway equipment – Train communication network*, Germany: Dansk Standard.
- Il Mattino, 2019. *Il Mattino*. [Online] Available at: [https://www.ilmattino.it/video/societa/impressionante\\_incidente\\_tram\\_russia\\_autista\\_distratta\\_dallo\\_smartphone-4816209.html](https://www.ilmattino.it/video/societa/impressionante_incidente_tram_russia_autista_distratta_dallo_smartphone-4816209.html) [Accessed 15 11 2021].

- Inagaki, T., 2018. A critique of the SAE conditional driving automation definition, and analyses of options for improvement. *Cognition, Technology & Work*, Volume 21, p. 569–578.
- Istat, 2019. *Incidenti stradali 2018*, Roma: s.n.
- ITF, 2019. *Road Safety Annual Report 2019*, Paris: s.n.
- Kavurucu, Y., 2017. *Predictive Cruise Control*. Istanbul, IEEE.
- Khan, A. M., 2011. *Bayesian-Monte Carlo Model for Collision Avoidance System Design of Cognitive Connected Vehicle*. Orlando Florida, ResearchGate.
- Kim, H., 2021. Effect Evaluation of Forward Collision Warning System Using IoT Log and Virtual Driving Simulation Data. *MDPI Applied Sciences*, Volume 11, pp. 1-15.
- Kim, J., 2016. *Performance Test of Autonomous Emergency Braking System Based on Commercial Radar*. Kumamoto, IEEE.
- Kim, W., 2019. Lightweight Driver Monitoring System Based on Multi-Task Mobilenets. *Deep Learning-Based Image Sensors*, 19(14).
- Kong, 2015. Investigating driver fatigue versus alertness using the granger causality network. *Sensors in New Road Vehicles*, 15(8), p. 19181–19198.
- Land Rover, 2018. *Adaptive cruise control*, Whitley: Land Rover.
- Lawrence, 2003. *Passenger Counting and Service Monitoring*, Brooklyn: MTA New York City Transit.
- Litman, T., 2021. *Autonomous Vehicle Implementation Predictions*, Victoria : Victoria Transport Policy Institute.
- Litman, T., 2021. *Land Use Impacts on Transport*, Victoria: s.n.
- Liu, 2008. *Development of a Vision-Based Driver Assistance System with Lane Departure Warning and Forward Collision Warning Functions*. Canberra, IEEE, pp. 480-485.
- Liu, L. C., 2016. A Novel Distance Estimation Method Leading a Forward Collision Avoidance Assist System for Vehicles on Highways. *IEEE*, 18(4), pp. 937-949.
- Li, Z., 2017. Online Detection of Driver Fatigue Using Steering Wheel Angles for Real Driving Conditions. *Sensors for Transportation*, 14(3), pp. 1-12.
- Llaneras, 2013. Human factors issues associated with limited ability autonomous driving systems: Drivers' allocation of visual attention to the forward roadway. *Driving Symp. Hum. Factors Driving Assessment Training Veh*, pp. 92-98.
- Lundquist, C., 2011. *Sensor Fusion for Automotive Applications*. Linköping: Linköping University.
- Moghaddam, D. K., 2017. *Transport Networks, Land Use and Travel Behaviour: a Long Term Investigation*. 1 a cura di Nederlandse : Springer.
- NAVYA, 2021. *Self-Driving Made Real*. [Online] Available at: <https://navya.tech/fr/> [Accessed 21 12 2021].
- OECD, 2017. *ITF Transport Outlook 2017*, Paris: s.n.

- Perticaroli, F., 2001. *Sistemi elettrici per i trasporti - Trazione elettrica*. 2 a cura di Milano: Zanichelli.
- Qian, 2015. *Robust Chinese traffic sign detection and recognition with deep convolutional neural network*. Zhangjiajie, IEEE.
- RAIB, 2016. *Rail Accident Report*, Derby: s.n.
- Rendon, E., 2010. *Classification and overview of Advanced Driver Assistance Systems according to the driving process*. Montreal, ASME.
- Rendon, E., 2010. *CLASSIFICATION AND OVERVIEW OF ADVANCED DRIVER ASSISTANCE SYSTEMS ACCORDING TO THE DRIVING PROCESS*. Montreal,, ASME.
- Rosique, F., 2019. A Systematic Review of Perception System and Simulators for Autonomous Vehicles Research" Cartagena, Spain, 5 February 2019. *Sensors, Perception Sensors for Road Applications*, 19(3).
- Rummelhard, L., 2017. *Perception and Automation for Intelligent Mobility in Dynamic Environments*. Singapore, HAL Id.
- Saito, 2016. Driver assistance system with a dual control scheme: Effectiveness of identifying driver drowsiness and preventing lane departure accidents. *IEEE Trans. Human-Mach. Syst*, 46(5), pp. 660-671.
- Scanlon, J., 2016. Lane Departure Warning and Prevention Systems in the U.S. Vehicle Fleet: Influence of Roadway Characteristics on Potential Safety Benefits. *Transportation Research Record*, 2559(1), pp. 17-23.
- Sharma, R., 2014. *Sensor fusion for prediction of orientation and position from obstacle using multiple IR sensors an approach based on Kalman filter*. Pilsen, IEEE.
- Siahvashi, A., 2010. Automatic Train Control based on the Multi-Agent Control of Cooperative Systems. *The Journal of Mathematics and Computer Science*, Vol .1 (No.4), pp. 247-257.
- Son, 2015. Robust multirate control scheme with predictive virtual lanes for lane-keeping system of autonomous highway driving. *IEEE Trans. Veh. Technol*, 64(8), pp. 3378-3391.
- Stagni, E., 1980. *Meccanica della Locomozione*. Bologna : Pàtron.
- Steinbaeck, J., 2017. *Next generation radar sensors in automotive sensor fusion systems*. Bonn, IEEE, pp. 205-209.
- Sun, 2014. Application of BW-ELM model on traffic sign recognition. *Neurocomputing* , Volume 128, p. 153–159.
- Sun, Y., 2019. *Traffic Sign Detection and Recognition Based on Convolutional Neural Network*. Hangzhou, China, IEEE.
- Teoh, E. R., 2020. Effectiveness of front crash prevention systems in reducing large truck realworld crash rates. *ResearchGate*, 22(4), pp. 284-289.
- Tesla, 2021. *Future of Driving*. [Online] Available at: [https://www.tesla.com/en\\_IE/autopilot](https://www.tesla.com/en_IE/autopilot) [Accessed 21 12 2021].
- TSAG, 2010. *Shaping the 30 year Rail Technical Strategy*. London, The Royal Academy of Engineering.

- UITP, 2009. *Light Rail transit, a safe means of transport*, Belgium: MYLIBRARY.
- UITP, 2016. *Light Rail: knowledge brief a tool to serve customers and cities*, Belgium: MYLIBRARY.
- UITP, 2019. *The global tram and light rail landscape*. Belgium, MYLIBRARY.
- Ulyanov, 1993. Pulse-wave monitoring by means of focused laser beams scattered by skin surface and membranes Nossal. *Static and Dynamic Light Scattering in Medicine and Biology*, pp. 160-167.
- Velez, G., 2015. *Embedded platforms for computer vision-based advanced driver assistance systems: a survey*. Spain, ReserchGate.
- Vicuna, G., 1986. *Organizzazione e Tecnica Ferroviaria*. Roma: CIFI.
- Vivek, N., 2014. "On field performance analysis of IEEE 802.11 P and WAVE protocol stack for V2V & V2I communication", *Proc. IEEE Int. Conf. Information Communication Embedded Systems (ICICES)*, pp. 1-6, 2014. Chennai, India, IEEE.
- Volvo, 2021. *Lane Keeping Aid (LKA)*. [Online] Available at: <https://www.volvocars.com/uk/support/manuals/xc60/2016w17/driver-support/lane-assistance/lane-keeping-aid-lka> [Accessed 20 12 2021].
- Vu, T.-D., 2014. *Object Perception for Intelligent Vehicle Applications: A Multi-Sensor Fusion Approach*. Dearborn, IEEE.
- Wallner, J., 2014. *Development of an Emergency Braking System for Teleoperated Vehicles Based on Lidar Sensor Data*. Wien, IEEE.
- Wang, 2014. Hole-based traffic sign detection method for traffic signs with red rim. *Computer Science*, Volume 30, p. 539–551.
- Wang, 2019. Multi-Sensor Fusion in Automated Driving: A Survey. 2847 - 2868, Volume 8, pp. 2847 - 2868.
- Wang, 2020. *Accurate Perception for Autonomous Driving: Application of Kalman Filter for Sensor Fusion*. Kuala Lumpur, IEEE.
- Wang, G., 2018. Research on Modern Tram Auxiliary Safety Protection Technology Based on Obstacles Detection. *International Symposium for Intelligent Transportation and Smart City*, Volume 62, pp. 37-50.
- Williams, B., 2021. Automated Driving Levels. In: *Automated Vehicles and MaaS: Removing the Barriers*. s.l.: John Wiley & Sons Ltd.
- Xiang, X., 2014. Research on a DSRC-Based Rear-End Collision Warning Model. *IEEE*, 15(3), pp. 1054 - 1065.
- Xie, F., 2011. *Evolving Transportation Networks*. 1 a cura di New York: Springer.
- Yan, F., 2016. *Scenario Based STPA Analysis in Automated Urban Guided Transport System*. China, IEEE.

- 
- Yasunobu, S., 1986. Evaluation of an automatic container crane operation system based on predictive fuzzy control. *Control Theory Adv. Technol*, 2(3), p. 419–432.
- Yeong, D. J., 2021. Sensor and Sensor Fusion Technology in Autonomous Vehicles: A Review. *State-of-the-Art Sensors Technologies in Ireland 2020*, 21(6), pp. 1-12.
- Ye, W., 2021. Investigation of Bus Drivers' Reaction to ADAS Warning System: Application of the Gaussian Mixed Model. *Sustainability*, 13(16), p. 20.
- Yin, J., 2017. Research and development of automatic train operation for railway transportation systems: A survey. *Transportation Research Part C: Emerging Technologies*, C(85), p. 548–572.
- Ziebinski, A., 2016. A Survey of ADAS Technologies for the Future Perspective of Sensor Fusion. *Lecture Notes in Computer Science*, Volume 9876, p. 135–146.



# List of Acronyms

The table below contains an explanation of frequently used abbreviations. They are not introduced in every chapter, to keep the reading of each chapter self-contained can be found here. Very common abbreviations, project acronyms, software packages, and names of organizations and companies are always explained.

ADAS	Advanced Driver Assistance Systems
ABS	Anti-lock Braking System
ACC	Adaptive Cruise Control
AEB	Autonomous Emergency Braking
AI	Artificial Intelligence
ALG	Application Layer Gateway
ANM	Azienda Napoletana Mobilità
ATC	Automatic Train Control
ATO	Automatic Train Operation
ATP	Automatic Train Protection
ATP	Automatic Train Protection
ATS	Automatic Train Supervision
AV	Autonomous vehicle
BCW	Backward Collision Warning
BSD	Blind Spot Detection
CACC	Cooperative Adaptive Cruise Control
CAN	Controller Area Network
CCD	Charge Coupled Device

CCU	Central Control Unit
CMOS	Complementary Metal Oxide Semiconductor
CN	Consist Networks
CNN	Convolutional Neural Network
CS	Consist Switches
CVD	Centralized Vehicle Diagnostics
DAS	Driver Assistance Systems
DCE	Distance to Collision Estimation
DSM	Driver Status Monitoring
DSRC	Dedicated Short-Range Communications
DTO	Driverless Train Operation
EB	Emergency Brake
ECN	Ethernet Consist Network
ED	End Devices
ENA	Ethernet Network Administrator
ESC	Electronic Stability Control
ETB	Ethernet Train Backbone
ETCS	European Train Control System
FC	Forward Collision
FCTA	Forward Cross Traffic Alert
FCW	Forward Collision Warning
FMCW	Frequency Modulated Continuous Wave
FOV	Field of View
GDP	Gross Domestic Product
GhG	Greenhouse Gas
GoA	Grade of Automation
IoT	Internet of Things
IPPG	Imaging Photoplethysmography

IR	InfraRed
LCA	Lane Change Assistant
LDW	Lane Departure Warning
LiDAR	Light Detection and Ranging
LKA	Lane-Keeping Assistance
LU	Land Use
LUT	Integrated Land Use and Transport Planning
MDCU	Monitoring and Diagnostic Control Unit
MMW	Millimetre Wave
MVB	Multifunction Vehicle Bus
ND	Network Devices
NTO	Non-automated Train Operation
OECD	Organization for Economic Co-operation and Development
PA	Parking Assistance
PCC	Predictive Cruise Control
PIS	Passenger Information System
PoE	Power on Ethernet
RADAR	RAdio Detection And Ranging
RCTA	Rear Cross Traffic Alert
RFI	Rete Ferroviaria Italiana
ROG	Robust Governance
RoI	Region of Interest
SAE	Society of Automotive Engineers
SCMT	System of Train Running Control
SFS	Sensor Fusion System
SSB	Sub System of Board
SST	Sub Ground System

STO	Semi-automated Train Operation
T-ADAS	Tram - Advanced Driver Assistance System
TB	Train Backbones
TCMS	Train Control Management System
TCN	Train Communication Network
TIN	Transport Infrastructure Network
TOD	Train Operator Display
TRDP	Train Real Time Data Protocol
TSDR	Traffic Sign Detection and Recognition
UCS	Union of Concerned Scientists
UD	Decentralized Units
UITP	International Association of Public Transport
UTO	Unattended Train Operation
V2I	Vehicle to Infrastructure
V2V	Vehicle to Vehicle
V2X	Vehicle to Everything
VIS	VISible
WTB	Wire Train Bus

# List of Symbols

$v_0$	Initial speed
$R_f$	Risk estimation function
$a_e$	Minimum deceleration
$h_i$	Hazard indexes
$\Delta$	Extra margin distance
$t_{TTC}$	Time to collision
$t_0$	Driver reaction time
$s_{cbd}$	Critical braking distance
$i_{\%0}$	Slope
$\lambda_c$	Braking mass percentage
$\varphi$	Coefficients of Pedelucq
$g$	Acceleration of gravity
$f_a$	Adhesion coefficient
$S_f$	Stopping distance
$a_e$	Nominal deceleration
$m_e$	Equivalent mass
$m$	Static mass
$P$	Total weight
$\beta$	Inertia factor
$R$	Total resistance
$\alpha$	Ramp angle

$f'$	Friction coefficient
$f_a$	Adhesion coefficient
$Q$	Braking effort
$t_s$	Initial braking delay
$t_r$	Delay braking device
$k$	Aerodynamic coefficient
$S_{DCE}$	Stopping distance for DCE model
$S_r$	Space in reaction time
$S_f$	Stopping distance
$\mathcal{R}$	Radius of curvature
$n$	Multiplicative coefficient
$c$	Constant at zero speed
$S_{bn}$	Length of safety band